

SUPPORTING INFORMATION FOR

Pushing the Boundaries of BODIPY Chemistry: 2-(Dimethylamino)methyl BODIPYs as Enablers of Diversification with Nucleophiles

Sergio Serrano-Buitrago,^a Carla Marcos,^a Natalia Casado,^b Andrea Aranda,^a
Florencio Moreno,^a Jorge Bañuelos,^b David Valdivieso González,^c
Iván López-Montero,^{c,d,e} Beatriz L. Maroto*^a and Santiago de la Moya*^a

^a Departamento de Química Orgánica, Facultad de Ciencias Químicas, Universidad Complutense de Madrid, Ciudad Universitaria s/n, Madrid 28040, Spain. E-mail: santmoya@ucm.es

^b Departamento de Química-Física, Facultad de Ciencia y Tecnología, Universidad del País Vasco-EHU, Bilbao 48080, Spain.

^c Departamento de Química Física, Facultad de Ciencias Químicas, Universidad Complutense de Madrid, Ciudad Universitaria s/n, 28040 Madrid, Spain.

^d Instituto de Investigación Biomédica Hospital Doce de Octubre (imas12), Avda. de Córdoba s/n, 28041, Madrid, Spain.

^e Instituto Pluridisciplinar, Universidad Complutense de Madrid, Pº Juan XXIII 1, 28040, Madrid, Spain.

TABLE OF CONTENTS

1. General methods and equipment	S2
2. Synthetic procedures and characterization data	S6
3. NMR spectra of new compounds	S15
4. Additional (photo)physical data	S81
5. Additional biophotonic data	S85
6. References	S86

1. General methods and equipment

1.1. Synthesis and structural characterization

Anhydrous solvents were prepared by distillation over standard drying agents according to common methods. All other solvents were of HPLC grade and were used as provided. Starting organic substrates and chemical reagents were used as commercially provided unless otherwise indicated. Thin-layer chromatography (TLC) was performed on alumina plates (aluminum oxide 60, F254 neutral, supported on aluminum) or silica gel plates (silica gel 60 F254 supported on aluminum) and the chromatograms were visualized by using UV light ($\lambda = 254$ or 365 nm). Column chromatography was performed using activated neutral alumina (activity degree 1, 70-290 mesh ASTM) or silica gel. When silica gel (230-400 mesh) was used, the separation typically performed as flash column chromatography or using deactivated silica gel. Deactivated silica gel was prepared by slurring with a 10% (v/v) triethylamine (Et_3N) solution in hexanes, stirring briefly, then concentrating to dryness using a rotary evaporator. ^1H and ^{13}C NMR spectra were recorded in CDCl_3 , MeOD or CD_3CN solution at 20°C unless otherwise indicated. NMR chemical shifts are expressed in parts per million (δ scale) and are referenced to the residual signals of CDCl_3 ($\delta = 7.260$ and 77.16 ppm, respectively), MeOD ($\delta = 3.310$ and 49.00 ppm, respectively) or CD_3CN ($\delta = 1.940$ and 1.32 ppm, respectively) unless otherwise indicated. ^{19}F NMR spectra are referenced to trifluorotoluene ($\delta = -63.72$ ppm) as external standard. Multiplicity is indicated as follows: s = singlet, d = doublet, t = triplet, m = multiplet and/or multiple resonances, br = broad. Coupling constants (J) are dated in hertz (Hz). The type of carbon (CH_3 , CH_2 , CH or C) was assigned by DEPT-135 experiments. Further assignments of proton and carbon chemical shifts, particularly for those carbons not visible in the one-dimensional ^{13}C NMR spectrum, were confirmed by 2D NMR experiments such as HMQC and HMBC. Low intensity carbon resonances not observed in the 1D ^{13}C NMR spectra were identified through 2D HMQC and HMBC experiments. Complex spin-system signals were simulated by using MestRe-C¹ FTIR spectra were obtained from neat samples using the attenuated total reflection (ATR) technique. High-resolution mass spectrometry (HRMS) was performed using electrospray ionization (ESI) and hybrid quadrupole time-of-flight mass analyzer (QTOF; positive-ion mode is indicated as ESI^+).

1.2. Photophysical characterization

The ultraviolet-visible (UV-vis) absorption and fluorescence spectra were recorded on a CARY 7000 spectrophotometer (Agilent Technologies) and an Edinburgh Instruments spectrofluorometer (model FLSP920), respectively. The ground photophysical properties were registered from diluted solutions (around 2×10^{-6} M and using quartz cuvettes with path length of 1 cm), prepared by adding the corresponding solvent (spectroscopic grade or milliQ grade

water) to the residue from the adequate amount of a concentrated stock solution (ca. 10^{-3} M) in acetone, after vacuum evaporation of this solvent. For the studies at high concentrations (around 2×10^{-4} M), the optical density was adjusted to be similar to diluted solution choosing a narrow pathlength quartz cuvette (0.01 cm) and avoid inner filter effects. Furthermore, the fluorescence signatures of these concentrated solutions were recorded in the front-face configuration, instead of the right-angle configuration for the diluted solutions, to reduce the effects of the reabsorption and reemission phenomena. For the measurements in acid conditions, *p*-toluenesulfonic acid dissolved in ethanol was used as acidifying agent. Fluorescence quantum yields (ϕ) were determined from corrected spectra (detector sensibility to the wavelength) of diluted solutions (ca. 10^{-6} M) by the optically dilute relative method using as reference the commercial *F*-BODIPY dye PM567 ($\phi = 0.81$ in ethanol), except for dyes **11** and **14**, which emit beyond 600 nm, where cresyl violet ($\phi = 0.54$ in methanol) was used as reference. The radiative decay curves were registered with the time correlated single-photon counting technique, as implemented in the aforementioned spectrofluorometer. Fluorescence emission was monitored at the maximum emission wavelength, by means a microchannel plate detector of picosecond time-resolution (20 ps), after excitation with a Fianium pulsed laser (time resolution of around 150 ps). The fluorescence lifetime (τ) was obtained after the deconvolution of the instrumental response signal from the recorded decay curves by means of an iterative method. The goodness of the exponential fit was controlled by statistical parameters (chi-square) and the analysis of the residuals.

1.3. Electrochemistry

Electrochemical properties were measured by cyclic voltammetry (Metrohm Autolab) using a three-electrode set up with a platinum disk (diameter 3 mm) or layer (surface 8 mm \times 7.5 mm) working electrode, platinum wire as counter electrode and Ag/AgCl as reference electrode. A 0.1 M solution of tetrabutylammonium hexafluorophosphate (TBAPF₆) in dry acetonitrile was used as the electrolyte solvent in which the compounds were dissolved to achieve a concentration of 0.5-1.0 mM. All redox potentials were reported *vs.* ferrocene as internal standard. The solutions were purged with argon and all the measurements were performed under an inert atmosphere.

1.4. Computational calculations

Ground-state (S_0) geometries were optimized using a hybrid exchange-correlation functional with the Coulomb-attenuating method (CAM-B3LYP), within Density Functional Theory (DFT), and a triple valence basis set with a polarization function (6-311g*). The absorption transition was simulated as a vertical Franck-Condon transition from the S_0 optimized geometry using the Time Dependent (TD) method at the aforementioned calculation level and basis set. All the calculations were done without any geometrical constraint, and the geometries were considered to be at minimum energy when the corresponding frequency analysis did not give any negative value. All

calculations were run on the Gaussian 16 software implemented in the “Arina” informatics cluster of the UPV/EHU. Pharmacokinetics parameters, including skin permeation parameter (K_p) were predicted with the free web tool SwissADME.²

1.5. Dye lasing

Laser spectra and efficiencies were measured from aqueous solutions of dyes, with dye concentration 1×10^{-3} M, contained in 1 cm optical-path rectangular quartz cells carefully sealed to avoid solvent evaporation during experiments. The solutions were transversely pumped with a wavelength tunable optical parametric oscillator (OPO) coupled to the third harmonic (355 nm) of a Q-switched Nd:YAG laser (Lotis TII 2134) at a repetition rate of 1 Hz. The exciting pulses were line-focused onto the cell using a combination of positive and negative cylindrical lenses ($f = 15$ cm and $f = -15$ cm, respectively) perpendicularly arranged. The plane parallel oscillation cavity (2 cm length) consisted of a 90% reflectivity aluminum mirror acting as back reflector, and the lateral face of the cell acting as output coupler (4% reflectivity). The pump and output energies were detected by an Ophir power meter, whereas the laser spectra was collected by an optical fiber and imaged onto a spectrometer (USB2000+ from Ocean Optics).

1.6. Live-cell imaging

Cell culture. Mouse embryonic fibroblasts (MEFs) were obtained from the American Type Culture Collection (ATCC CRL-2991). MEFs were cultured in Dulbecco modified Eagle medium high glucose (DMEM 25 mM glucose) supplemented with 10% premium fetal bovine serum (FBS, South Africa S1300; Biowest, Nuallé, France), 1% non-essential amino acids (MEM-NEA) and 1% penicillin/streptomycin (final concentration of 100 U/mL penicillin and 100 μ g/mL streptomycin), from S3 Gibco. Cells were grown in a humidified incubator (Thermo Fisher Steri-Cycle Shape with HEPA filter, 5% CO₂) at 37 °C and maintained at 80% confluence in Flask T75 (Nunc). For confocal microscopy imaging, cells were collected and seeded in an 8-chamber LabTek™ slide (Thermofisher) and incubated at 37 °C to a final concentration of 10⁵ cells/well. MEFs were incubated with the various dyes at a final concentration of 100 nM and imaged after 30 minutes. For colocalization studies, MEFs were co-stained with LysoTracker™ Red (100 nM) prior to confocal fluorescence imaging. For fluorescence brightness comparisons, MEFs were stained independently with BODIPY dyes and LysoTracker™ Green (100 nM) and imaged at different power settings (4%, 10%, 20%, 30%, and 40%).

Confocal scanning laser microscopy. Fluorescence micrographs by confocal scanning laser microscopy (CSLM) were collected using a Nikon Ti-E inverted microscope equipped with a Nikon C2 confocal scanning confocal module, 488-nm and 561-nm continuous lasers, emission band-pass filters (525/ 50 and dichroic 561LP for the green and red channel, respectively) and a

Nikon Plan Apo λ 100 \times 1.45 oil ∞ /0.17 WD 0.13 immersion objective (Nikon ref. CFI Plan Apo DM Lambda 100X Oil).

2. Synthetic procedures and structural characterization data

2.1. Synthesis of **1**

Based on the general method described by Peng,³ a solution of 4-methylbenzaldehyde (1.00 g, 8.3 mmol, 1.0 mol equiv.) and 2,4-dimethylpyrrole (1.58 g, 16.6 mmol, 2.0 mol equiv.) in anhydrous dichloromethane (DCM, 60 mL) was treated with trifluoroacetic acid (TFA, 150 μ L), and the mixture was stirred at room temperature (r.t.) for 16 h. After this time, 2,3,5,6-tetrachloro-1,4-benzoquinone (*p*-chloranil, 2.05 g, 8.3 mmol, 1.0 mol equiv.) was added, and stirring was continued for 1 h at r.t.. The reaction mixture was placed under an argon atmosphere and cooled to 0 °C, and Et₃N (4.24 g, 41.6 mmol, 5.0 mol equiv.) was added dropwise. After stirring for 15 min at 0 °C, BF₃·OEt₂ (11.8 g, 83.2 mmol, 10.0 mol equiv.) was added dropwise while maintaining the temperature at 0 °C. The mixture was then allowed to warm gradually to r.t., and stirred for an additional 90 min. The solvent was removed under reduced pressure, and the crude residue dissolved in AcOEt (50 mL). The organic solution was washed with saturated NaHCO₃ solution (2 \times 50 mL) and water (2 \times 50 mL). The combined aqueous phases were extracted with AcOEt (2 \times 50 mL). The combined organic phases were dried over Na₂SO₄, filtered, and the solvent was evaporated under reduced pressure. The crude product was purified by flash chromatography (silica gel, hexane/DCM 9:1 \rightarrow 7:3) to afford **1** as an orange solid (1.63 g, 58%). ¹H NMR (300 MHz, CDCl₃) δ 7.28 (d, *J* = 7.8 Hz, 2H), 7.14 (d, *J* = 8.1 Hz, 2H), 5.97 (s, 2H), 2.55 (s, 6H), 2.43 (s, 3H), 1.40 (s, 6H) ppm. ¹³C NMR (75 MHz, CDCl₃) δ 155.4 (C), 143.3 (C), 142.3 (C), 139.0 (C), 132.1 (C), 131.7 (C), 129.9 (CH), 127.89 (CH), 121.2 (CH), 21.5 (CH₃), 14.7 (CH₃) ppm. The spectroscopic data agree with those reported previously.³

2.2. Synthesis of **2**

To a flame-dried flask under an argon atmosphere, a solution of **1** (50.0 mg, 0.148 mmol, 1.0 mol equiv.), *N,N*-dimethylmethaniminium iodide (Eschenmoser's salt, 82.1 mg, 0.444 mmol, 3.0 mol equiv.) and K₂CO₃ (122.6 mg, 0.887 mmol, 6.0 mol equiv.) in anhydrous 1,2-dichloroethane (DCE, 7.4 mL) was refluxed for 2.5 h. The mixture was cooled to r.t. and filtered through a fritted funnel. The filtered solid was thoroughly washed with DCM (4 \times 5 mL). The combined organic phases were washed with distilled water (2 \times 30 mL) and brine (2 \times 30 mL), dried over Na₂SO₄, filtered, and the solvent was removed under reduced pressure. The crude product was purified by flash chromatography (deactivated silica gel, hexane/DCM 9:1 \rightarrow 4:6) to afford **2** as an orange solid (46.8 mg, 80%). ¹H NMR (CDCl₃, 300 MHz) δ 7.28 (d, *J* = 8.0 Hz, 2H), 7.14 (d, *J* = 8.0 Hz, 2H), 5.96 (s, 1H), 3.15 (s, 2H), 2.58 (s, 3H), 2.55 (s, 3H), 2.43 (s, 3H), 2.19 (s, 6H), 1.38 (s, 6H) ppm. ¹³C NMR (CDCl₃, 75 MHz) δ 155.8 (C), 155.2 (C), 143.2 (C), 142.2 (C), 141.8 (C), 139.0 (C), 132.3 (C), 131.8 (C), 131.2 (C), 129.9 (CH), 128.0 (CH), 121.2 (CH), 52.6 (CH₂), 45.1

(CH₃), 21.6 (CH₃), 14.7 (br s, CH₃), 14.6 (CH₃), 12.9 (CH₃), 12.3 (br s, CH₃) ppm. **FTIR** ν 2927, 2856, 1712, 1541, 1517, 1478, 1406, 1354, 1312, 1265, 1198, 1163, 1112, 1067, 1033, 1020, 943 cm⁻¹. **HRMS** (ESI⁺) m/z [M + H]⁺ Calcd. for C₂₃H₂₉BF₂N₃ 396.2417; Found 396.2428.

2.3. Synthesis of 3

Under an argon atmosphere, MeI (736.1 mg, 5.186 mmol, 20.5 mol equiv.) was added over a solution of **2** (100.0 mg, 0.253 mmol, 1.0 mol equiv.) in 4.0 mL of anhydrous DCM, and the mixture was stirred at r.t. for 15 min. Solvent and MeI were then removed under reduced pressure, and the crude product was purified by chromatography (neutral alumina, DCM→DCM/MeOH 9.5:0.5) to afford **3** as an orange solid (135.3 mg, 100%). **¹H NMR** (CDCl₃, 300 MHz) δ 7.29 (d, J = 8.0 Hz, 2H), 7.09 (d, J = 8.0 Hz, 2H), 6.08 (s, 1H), 4.67 (s, 2H), 3.29 (s, 9H), 2.66 (s, 3H), 2.55 (s, 3H), 2.41 (s, 3H), 1.56 (s, 3H), 1.42 (s, 3H) ppm. **¹³C NMR** (CDCl₃, 75 MHz) δ 160.6 (C), 152.7 (C), 147.2 (C), 143.5 (C), 142.2 (C), 139.7 (C), 133.7 (C), 131.3 (C), 130.6 (C), 130.4 (CH), 127.4 (CH), 123.5 (CH), 116.3 (C), 59.9 (CH₂), 52.5 (CH₃), 21.5 (CH₃), 15.1 (br s, CH₃), 15.0 (CH₃), 14.2 (CH₃), 14.0 (br s, CH₃) ppm. **FTIR** ν 3406, 2958, 2924, 2853, 1540, 1520, 1480, 1312, 1196, 1167, 1067, 984 cm⁻¹. **HRMS** (ESI⁺) m/z [M]⁺ 410.2574 Calcd. for C₂₄H₃₁BF₂N₃; Found 410.2581.

2.4. Synthesis of 5a

Under argon atmosphere, a solution of **2** (30.0 mg, 0.076 mmol, 1.0 mol equiv.), tosyl chloride (TsCl, 18.8 mg, 0.099 mmol, 1.3 mol equiv.) and K₂CO₃ (2.4 mg, 0.379 mmol, 5.0 mol equiv.) in anhydrous acetonitrile (ACN, 4.5 mL) was stirred at r.t. for 5 min. Then, benzyl alcohol (BnOH, 12.3, mg, 12 μ L 1.5 mol equiv.) was added, and the mixture was stirred at r.t. for an addition 5 min. The mixture was filtered through a fritted funnel. The filtered solid was thoroughly washed with DCM (4 \times 5 mL). The combined organic phases were washed with distilled water (2 \times 30 mL), dried over Na₂SO₄, filtered, and the solvent was removed under reduced pressure. The crude product was purified by flash chromatography (deactivated silica gel, hexane/Et₂O 9:1) to afford **5a** as an orange solid (27.2 mg, 78%). **¹H NMR** (CDCl₃, 300 MHz) δ 7.37-7.25 (m, 5H), 7.29 (d, J = 7.6 Hz, 2H), 7.13 (d, J = 8.1 Hz, 2H), 5.98 (s, 1H), 4.48 (s, 2H), 4.26 (s, 2H), 2.56 (s, 6H), 2.44 (s, 3H), 1.39 (s, 6H) ppm. **¹³C NMR** (CDCl₃, 75 MHz) δ 155.9 (C), 155.2 (C), 143.7 (C), 142.5 (C), 141.8 (C), 139.0 (C), 138.4 (C), 132.2 (C), 130.0 (CH), 128.5 (CH), 128.0 (CH), 127.9 (CH), 127.8 (CH), 127.0 (C), 121.5 (CH), 72.1 (CH₂), 61.7 (CH₂), 21.6 (CH₃), 14.8 (t, J = 2.2 Hz, CH₃), 14.7 (CH₃), 12.7 (t, J = 2.3 Hz, CH₃), 12.1 (CH₃) ppm. **FTIR** ν 3030, 2924, 2855, 1714, 1540, 1516, 1479, 1354, 1310, 1195, 1161, 1113, 1063, 1043, 980, 963 cm⁻¹. **HRMS** (ESI⁺) m/z [M + H]⁺ Calcd. for C₂₈H₃₀BF₂N₂O 459.2414; Found 459.2424.

2.5. Synthesis of 5b

According to the above-described procedure for the synthesis of **5a, 2** (30.0 mg, 0.076 mmol) was reacted with BnOH (14.2 mg, 0.114 mmol.) to obtain **5b** as an orange solid (15.9 mg, 44% chemical yield) upon flash chromatography purification (deactivated silica gel, hexane/Et₂O 9:1). ¹H NMR (CDCl₃, 300 MHz) δ 7.29 (d, *J* = 7.8 Hz, 2H), 7.13 (d, *J* = 8.0 Hz, 2H), 5.99 (s, 1H), 4.31 (s, 2H), 3.72 (t, *J* = 6.1 Hz, 2H), 3.44 (t, *J* = 6.1 Hz, 2H), 2.60 (s, 3H), 2.56 (s, 3H), 2.44 (s, 3H), 1.42 (s, 3H), 1.39 (s, 3H) ppm. ¹³C NMR (CDCl₃, 75 MHz) δ 156.3 (C), 154.7 (C), 144.0 (C), 142.7 (C), 141.6 (C), 139.1 (C), 132.1 (C), 132.1 (C), 130.0 (CH), 127.9 (CH), 126.3 (C), 121.7 (CH), 69.7 (CH₂), 62.8 (CH₂), 30.6 (CH₂), 21.6 (CH₃), 14.8 (br s, CH₃), 14.7 (CH₃), 12.7 (br s, CH₃), 12.1 (CH₃) ppm. FTIR ν 2960, 2924, 2858, 1713, 1539, 1516, 1479, 1437, 1406, 1351, 1310, 1267, 1196, 1161, 1104, 1068, 1042, 1020, 979, 963 cm⁻¹. HRMS (ESI⁺) *m/z* [M + H]⁺ Calcd. for C₂₃H₂₇BBrF₂N₂O 475.1362; Found 475.1365.

2.6. Synthesis of 5c

According to the above-described procedure for the synthesis of **5a, 2** (30.0 mg, 0.076 mmol) was reacted with 4-hydroxybenzaldehyde (13.9 mg, 0.114 mmol) to obtain **5c** as an orange solid (16.2 mg, 45%) upon flash chromatography purification (deactivated silica gel, hexane/Et₂O 9.5:0.5 → 8.5:1.5). ¹H NMR (CDCl₃, 300 MHz) δ 9.89 (s, 1H), 7.84 (d, *J* = 8.8 Hz, 2H), 7.30 (d, *J* = 7.8 Hz, 2H), 7.15 (d, *J* = 8.0 Hz, 2H), 7.04 (d, *J* = 8.6 Hz, 2H), 6.03 (s, 1H), 4.83 (s, 2H), 2.60 (s, 3H), 2.58 (s, 3H), 2.44 (s, 3H), 1.42 (s, 6H) ppm. ¹³C NMR (CDCl₃, 75 MHz) δ 190.9 (CH), 164.0 (C), 157.4 (C), 153.8 (C), 144.8 (C), 143.0 (C), 141.2 (C), 139.2 (C), 132.1 (CH), 131.9 (C), 130.2 (C), 130.1 (CH), 127.9 (CH), 124.2 (C), 122.2 (CH), 115.1 (CH), 60.8 (CH₂), 21.6 (CH₃), 14.9 (br s, CH₃), 14.8 (CH₃), 12.7 (br s, CH₃), 12.1 (CH₃) ppm. FTIR ν 2920, 2849, 2734, 1692, 1599, 1541, 1519, 1506, 1484, 1311, 1197, 1159, 1113, 1077, 1044 cm⁻¹. HRMS (ESI⁺) *m/z* [M + Na]⁺ Calcd. for C₂₈H₂₇BF₂N₂O₂Na 495.2026; Found 495.2036.

2.7. Synthesis of 5d

According to the above-described procedure for the synthesis of **5a, 2** (30.0 mg, 0.076 mmol) was reacted with benzoic acid (13.9 mg, 0.114 mmol) to obtain **5d** as an orange solid (17.1 mg, 48%) upon flash chromatography purification (deactivated silica gel, hexane/Et₂O 9:1→7:3). ¹H NMR (CD₃CN, 300 MHz) δ 7.97-7.92 (m, 2H), 7.59 (tt, *J* = 7.4, 1.4 Hz, 1H), 7.45 (m, 2H), 7.35 (d, *J* = 7.7 Hz, 2H), 7.21 (d, *J* = 8.1 Hz, 2H), 6.12 (s, 1H), 5.13 (s, 2H), 2.59 (s, 3H), 2.50 (s, 3H), 2.41 (s, 3H), 1.47 (s, 3H), 1.40 (s, 3H) ppm. ¹³C NMR (CD₃CN, 75 MHz) δ 167.0 (C), 157.8 (C), 155.1 (C), 145.8 (C), 144.3 (C), 142.9 (C), 140.4 (C), 134.1 (CH), 132.5 (C, two signals by HMBC), 132.5 (C), 131.2 (C), 130.8 (CH), 130.2 (CH), 129.6 (CH), 128.8 (CH), 126.1 (C), 122.9 (CH), 57.7 (CH₂), 21.4 (CH₃), 14.85 (br s, CH₃), 14.81 (CH₃), 12.9 (br s, CH₃), 12.3 (CH₃) ppm.

FTIR ν 2959, 2926, 2857, 1715, 1542, 1519, 1483, 1312, 1266, 1197, 1164, 1104, 1069, 1043, 1024, 982, 948 cm^{-1} . **HRMS** (ESI⁺) m/z [M + Na]⁺ Calcd. for C₂₈H₂₇BF₂N₂O₂Na 495.2026; Found 495.2035.

2.8. Synthesis of 5e

According to the above-described procedure for the synthesis of **5a, 2** (30.0 mg, 0.076 mmol) was reacted with methoxyacetic acid (10.3 mg, 0.114 mmol) to obtain **5e** as an orange solid (16.4 mg, 49%) upon flash chromatography purification (deactivated silica gel, hexane/Et₂O 9.5:0.5→8:2). **¹H NMR** (CDCl₃, 300 MHz) δ 7.29 (d, J = 7.7 Hz, 2H), 7.13 (d, J = 8.1 Hz, 2H), 6.01 (s, 1H), 4.98 (s, 2H), 3.99 (s, 2H), 3.42 (s, 3H), 2.59 (s, 3H), 2.56 (s, 3H), 2.44 (s, 3H), 1.40 (s, 6H) ppm. **¹³C NMR** (CDCl₃, 75 MHz) δ 170.2 (C), 157.1 (C), 154.0 (C), 144.6 (C), 142.8 (C), 141.5 (C), 139.1 (C), 132.3 (C), 131.8 (C), 129.9 (CH), 127.7 (CH), 124.0 (C), 121.9 (CH), 69.7 (CH₂), 59.4 (CH₃), 56.7 (CH₂), 21.5 (CH₃), 14.7 (br s, CH₃), 14.6 (CH₃), 12.5 (br s, CH₃), 11.9 (CH₃) ppm. **FTIR** ν 2961, 2923, 1752, 1337, 1311, 1184, 1157, 1117, 1088, 948 cm^{-1} . **HRMS** (ESI⁺) m/z [M + Na]⁺ Calcd. for C₂₄H₂₇BF₂N₂O₃Na 463.1975; Found 463.1990.

2.9. Synthesis of 5f

According to the above-described procedure for the synthesis of **5a, 2** (30.0 mg, 0.076 mmol) was reacted with piperidine (9.7 mg, 0.114 mmol) to obtain **5f** as an orange solid (25.5 mg, 77%) upon chromatography purification (neutral alumina, DCM/AcOEt 9:1). **¹H NMR** (CDCl₃, 500 MHz) δ 7.28 (d, J = 7.9 Hz, 2H), 7.14 (d, J = 8.0 Hz, 2H), 5.96 (s, 1H), 3.20 (br s, 2H), 2.58 (s, 3H), 2.55 (s, 3H), 2.43 (s, 3H), 2.33 (br s, 4H), 1.53 (br s, 4H), 1.40 (br s, 2H), 1.38 (s, 3H), 1.37 (s, 3H) ppm. **¹³C NMR** (CDCl₃, 126 MHz) δ 156.5 (C), 154.7 (C), 142.9 (C), 142.0 (C), 138.9 (C), 132.3 (C), 131.6 (C), 131.3 (C), 130.3 (C), 129.9 (CH), 128.0 (CH), 127.7 (C), 121.1 (CH), 54.2 (CH₂), 52.1 (CH₂), 25.9 (CH₂), 24.3 (CH₂), 21.6 (CH₃), 14.7 (CH₃), 14.6 (CH₃), 13.1 (CH₃), 12.4 (CH₃) ppm. **FTIR** ν 2929, 2853, 1714, 1540, 1515, 1476, 1361, 1311, 1193, 1161, 1114, 1063, 1039, 1020, 981, 962 cm^{-1} . **HRMS** (ESI⁺) m/z [M + Na]⁺ Calcd. for C₂₆H₃₂BF₂N₃Na 458.2550; Found 458.2554.

2.10. Synthesis of 5g

According to the above-described procedure for the synthesis of **5a, 2** (30.0 mg, 0.076 mmol) was reacted with propargylamine (6.3 mg, 0.114 mmol) to obtain **5g** as an orange solid (26.0 mg, 84%) upon flash chromatography purification (deactivated silica gel, hexane/Et₂O 8:2→6:4). **¹H NMR** (CDCl₃, 300 MHz) δ 7.28 (d, J = 8.0 Hz, 2H), 7.13 (d, J = 7.9 Hz, 2H), 5.97 (s, 1H), 3.60 (s, 2H), 3.37 (d, J = 2.4 Hz, 2H), 2.61 (s, 3H), 2.55 (s, 3H), 2.44 (s, 3H), 2.23 (t, J = 2.2 Hz, 1H), 1.50 (br s, 1H), 1.41 (s, 3H), 1.39 (s, 3H) ppm. **¹³C NMR** (CDCl₃, 75 MHz) δ 155.4 (C), 155.2

(C), 143.3 (C), 142.2 (C), 141.3 (C), 139.0 (C), 132.2 (C), 131.8 (C), 131.2 (C), 129.9 (CH), 128.2 (C), 127.9 (CH), 121.3 (CH), 82.3 (C), 71.7 (CH), 41.0 (CH₂), 37.4 (CH₂), 21.6 (CH₃), 14.7 (br s, CH₃), 14.6 (CH₃), 12.7 (br s, CH₃), 12.1 (CH₃) ppm. **FTIR** ν 3267, 2924, 2855, 1712, 1515, 1467, 1361, 1310, 1160, 1114, 1019, 978, 962 cm⁻¹. **HRMS** (ESI⁺) m/z [M + Na]⁺ Calcd. for C₂₄H₂₆BF₂N₃Na 428.2080; Found 428.2081.

2.11. Synthesis of 5h

According to the above-described procedure for the synthesis of **5a, 2** (30.0 mg, 0.076 mmol) was reacted with 4-dimethoxyaniline (17.4 mg, 0.114 mmol) to obtain **5h** as an orange solid (26.8 mg, 70%) upon flash chromatography purification (deactivated silica gel, hexane/Et₂O 9:1→7:3). **¹H NMR** (CD₃CN, 300 MHz) δ 7.36 (d, J = 7.7 Hz, 2H), 7.21 (d, J = 8.1 Hz, 2H), 6.74 (d, J = 8.5 Hz, 1H), 6.30 (d, J = 2.6 Hz, 1H), 6.14 (dd, J = 8.6, 2.6 Hz, 1H), 6.08 (s, 1H), 3.91 (s, 2H), 3.72 (s, 3H), 3.68 (s, 3H), 2.52 (s, 3H), 2.48 (s, 3H), 2.42 (s, 3H), 1.41 (s, 3H), 1.40 (s, 3H) ppm. **¹³C NMR** (CD₃CN, 75 MHz) δ 156.2 (C), 155.9 (C), 151.3 (C), 145.0 (C), 144.6 (C), 143.6 (C), 142.4 (C), 142.2 (C), 140.3 (C), 132.8 (C), 132.4 (C), 131.8 (C), 130.8 (CH), 129.4 (C), 128.9 (CH), 122.2 (CH), 115.3 (CH), 104.4 (CH), 100.1 (CH), 57.4 (CH₃), 56.1 (CH₃), 38.9 (CH₂), 21.4 (CH₃), 14.7 (br s, CH₃), 13.0 (br s, CH₃), 12.3 (CH₃) ppm. **FTIR** ν 3381, 2927, 2832, 1712, 1542, 1512, 1478, 1362, 1311, 1231, 1193, 1163, 1022, 981, 964 cm⁻¹. **HRMS** (ESI⁺) m/z [M]⁺ Calcd. for C₂₉H₃₂BF₂N₃O₂ 503.2550; Found 503.2563.

2.12. Synthesis of 5i

According to the above-described procedure for the synthesis of **5a, 2** (30.0 mg, 0.076 mmol) was reacted with thiophenol (12.5 mg, 0.114 mmol) to obtain **5i** as an orange solid (21.0 mg, 60%) upon flash chromatography purification (deactivated silica gel, hexane/DCM 9:1→8:2). **¹H NMR** (CDCl₃, 300 MHz) δ 7.35-7.21 (m, 7H), 7.12 (d, J = 8.0 Hz, 2H), 5.98 (s, 1H), 3.81 (s, 2H), 2.55 (s, 3H), 2.45 (s, 3H), 2.43 (s, 3H), 1.39 (s, 3H), 1.24 (s, 3H) ppm. **¹³C NMR** (CDCl₃, 75 MHz) δ 155.7 (C), 154.5 (C), 143.6 (C), 142.2 (C), 140.6 (C), 139.0 (C), 136.0 (C), 132.1 (C), 131.9 (C), 131.7 (CH), 129.9 (CH), 129.0 (CH), 128.0 (CH), 127.1 (CH), 125.7 (C), 121.4 (CH), 29.2 (CH₂), 21.6 (CH₃), 14.74 (CH₃), 14.66 (CH₃), 12.6 (CH₃), 11.9 (CH₃) ppm. **FTIR** ν 2924, 2854, 1713, 1539, 1516, 1477, 1362, 1310, 1189, 1162, 1111, 1058, 1004, 982 cm⁻¹. **HRMS** (ESI⁺) m/z [M + H]⁺ Calcd. for C₂₇H₂₈BF₂N₂S 461.2029; Found 461.2034.

2.13. Synthesis of 5j

According to the above-described procedure for the synthesis of **5a, 2** (30.0 mg, 0.076 mmol) was reacted with 3-ethyl-2,4-dimethylpyrrole (16.8 mg, 0.137 mmol) to obtain **5j** as an orange solid (22.4 mg, 52%) upon flash chromatography purification (deactivated silica gel, hexane/Et₂O 9:1→8:2). **¹H NMR** (CD₃CN, 300 MHz) δ 7.85 (br s, 1H), 7.36 (d, J = 7.7 Hz, 2H), 7.21 (d, J =

8.0 Hz, 2H), 6.04 (s, 2H), 3.51 (s, 2H), 2.46 (s, 3H), 2.42 (s, 3H), 2.39 (s, 3H), 2.28 (q, $J = 7.5$ Hz, 2H), 2.01 (s, 3H), 1.89 (s, 3H), 1.38 (s, 3H), 1.34 (s, 3H), 0.97 (t, $J = 7.5$ Hz, 3H) ppm. ^{13}C NMR (CD₃CN, 75 MHz) δ 156.6 (C), 154.5 (C), 142.8 (C), 141.4 (C), 140.2 (C), 132.9 (C), 132.0 (C), 140.2 (C), 130.7 (CH and C, two signals by HMBC), 129.0 (CH), 122.4 (C), 121.5 (CH), 120.1 (C), 113.1 (C), 21.4 (CH₃), 20.9 (CH₂), 18.2 (CH₂), 16.2 (CH₃), 14.6 (CH₃), 12.4 (CH₃), 10.7 (CH₃), 9.3 (CH₃), 9.0 (CH₃) ppm. FTIR ν 3420, 2962, 2925, 2862, 1710, 1542, 1516, 1472, 1312, 1265, 1195, 1162, 1064, 1013, 984, 915 cm⁻¹. HRMS (ESI⁺) m/z [M + H]⁺ Calcd. for C₂₉H₃₅BF₂N₃ 474.2887; Found 474.2885.

2.14. Synthesis of 8

Based on the previously described microwave-assisted procedure described by Wacharasindhu,⁵ a solution of **1** (139.0 mg, 0.411 mmol, 1.0 mol equiv.), 4-fluorobenzaldehyde (153.0 g, 1.774 mmol, 3.0 mol equiv.), AcOH (124.4 mg, 2.055 mmol, 5.0 mol equiv.) and piperidine (175.0 mg, 2.055 mmol, 5.0 mol equiv.) in 2 mL of anhydrous *N,N*-dimethylformamide (DMF, 2 mL) was submitted to microwave (MW) irradiation at 120 °C for 60 min. Then, the mixture was diluted with AcOEt (30 mL), washed with water (2 × 20 mL) and brine (2 × 30 mL), and dried over Na₂SO₄. After filtration and solvent evaporation under reduced pressure, the crude product was purified by flash chromatography (silica gel, toluene) to afford **8** as a blue solid (108.4 mg, 48%). ^1H NMR (CDCl₃, 300 MHz) δ 7.65 (d, $J = 15.7$ Hz, 2H), 7.60 (m, $J = 8.7, 5.4, 2.0$ Hz, 4H), 7.31 (d, $J = 7.7$ Hz, 2H), 7.20 (d, $J = 16.3$ Hz, 2H), 7.19 (d, $J = 8.1$ Hz, 2H), 7.09 (m, $J = 8.7, 8.7, 2.0$ Hz, 4H), 6.61 (s, 2H), 2.45 (s, 3H), 1.47 (s, 6H) ppm. ^{13}C NMR (CDCl₃, 75 MHz) δ 163.2 (d, $J_{\text{CF}} = 249.7$ Hz, C), 152.4 (C), 142.5 (C), 139.8 (C), 139.1 (C), 134.9 (CH), 133.7 (C), 133.0 (d, $J_{\text{CF}} = 3.3$ Hz, C), 132.1 (C), 129.9 (CH), 129.3 (d, $J_{\text{CF}} = 8.1$ Hz, CH), 128.3 (CH), 119.2 (CH), 117.8 (CH), 116.0 (d, $J_{\text{CF}} = 21.8$ Hz, CH), 21.6 (CH₃), 14.9 (CH₃) ppm. FTIR ν 2921, 2850, 1621, 1597, 1483, 1198, 1152, 1109, 989 cm⁻¹. HRMS (ESI⁺) m/z [M + H]⁺ Calcd. for C₃₄H₂₈BF₄N₂ 551.2276; Found 551.2276.

2.15. Synthesis of 9

According to the above-described procedure for the synthesis of **2**, **6** (commercial PM505, 1,3,5,7-tetramethyl-*F*-BODIPY, 50.0 mg, 0.202 mmol) was reacted with Eschenmoser's salt (111.8 mg, 0.605 mmol) to obtain **9** as a red solid (52.4 mg, 85%) upon flash chromatography purification (deactivated silica gel, hexane/DCM 1:1 → DCM/MeOH 9:1). ^1H NMR (CDCl₃, 300 MHz) δ = 7.04 (s, 1H), 6.03 (s, 1H), 3.21 (s, 2H), 2.55 (s, 3H), 2.53 (s, 3H), 2.24 (s, 3H), 2.232 (s, 3H) 2.225 (s, 6H) ppm. ^{13}C NMR (CDCl₃, 75 MHz) δ = 157.2 (C), 156.6 (C), 141.0 (C), 139.9 (C), 133.4 (C), 132.8 (C), 126.5 (C), 120.0 (CH), 119.0 (CH), 53.0 (CH₂), 45.3 (CH₃), 14.8 (br s, CH₃), 13.0 (br s, CH₃), 11.4 (CH₃), 9.9 (CH₃) ppm. FTIR ν 2978, 2942, 2856, 2811, 2760, 1599,

1513, 1470, 1355, 1224, 1195, 1156, 1066, 1031, 976, 916 cm^{-1} . **HRMS** (ESI⁺) m/z [M + H]⁺ Calcd. for C₁₆H₂₃BF₂N₃ 306.1948; Found 306.1950.

2.16. Synthesis of 10

According to the above-described procedure for the synthesis of **2**, **7** (commercial PM546, 1,3,5,7,8-pentamethyl-*F*-BODIPY, 50.0 mg, 0.191 mmol) was reacted with Eschenmoser's salt (105.9 mg, 0.572 mmol) to obtain **10** as an orange solid (49.4 mg, 81%) upon flash chromatography purification (deactivated silica gel, DCM→DCM/MeOH 95:5). **¹H NMR** (CDCl₃, 300 MHz) δ 6.03 (s, 1H), 3.19 (s, 2H), 2.58 (s, 3H), 2.54 (s, 3H), 2.51 (s, 3H), 2.39 (s, 6H), 2.21 (s, 6H) ppm. **¹³C NMR** (CDCl₃, 75 MHz) δ 154.2 (C), 153.3 (C), 141.4 (C), 140.8 (C), 139.8 (C), 132.2 (C), 131.9 (C), 127.6 (C), 121.3 (CH), 52.8 (CH₂), 45.3 (CH₃), 17.5 (CH₃), 16.8 (CH₃), 14.8 (CH₃), 14.5 (t, J = 2.3 Hz, CH₃), 12.7 (t, J = 2.7 Hz, CH₃) ppm. **FTIR** ν 2978, 2942, 2856, 2811, 2760, 1599, 1513, 1470, 1355, 1224, 1195, 1156, 1066, 1031, 976, 916 cm^{-1} . **HRMS** (ESI⁺) m/z [M + H]⁺ Calcd. for C₁₇H₂₅BF₂N₃ 320.2104; Found 320.2105.

2.17. Synthesis of 11

According to the above-described procedure for the synthesis of **2**, **8** (36.0 mg, 0.065 mmol) was reacted with Eschenmoser's salt (36.3 mg, 0.065 mmol) to obtain **11** as a blue solid (27.7 mg, 70%) upon flash chromatography purification (deactivated silica gel, DCM→DCM/MeOH 9.8:0.2). **¹H NMR** (CDCl₃, 500 MHz) δ 7.89 (d, J = 16.3 Hz, 1H), 7.70 (d, J = 16.4 Hz, 1H), 7.67-7.57 (m, 16.3 Hz, 5H), 7.31 (d, J = 7.8 Hz, 2H), 7.22-7.16 (m, 3H), 7.12-7.06 (m, 4H), 6.61 (s, 1H), 3.21 (s, 2H), 2.46 (s, 3H), 2.26 (s, 6H), 1.45 (s, 3H), 1.44 (s, 3) ppm. **¹³C NMR** (CDCl₃, 126 MHz) δ 163.2 (d, J_{CF} = 249.7 Hz, C), 163.1 (d, J_{CF} = 248.9 Hz, C), 153.1 (C), 152.5 (C), 142.5 (C), 141.5 (C), 140.0 (C), 139.1 (C), 138.4 (CH), 134.8 (CH), 134.1 (d, J_{CF} = 3.2 Hz, C), 133.9 (C), 133.0 (d, J_{CF} = 3.3 Hz, C), 132.7 (C), 132.5 (C), 130.0 (CH), 129.3 (d, J_{CF} = 8.1 Hz, CH), 129.3 (d, J_{CF} = 8.1 Hz, CH), 128.7 (C), 128.4 (CH), 119.3 (CH), 117.9 (CH), 116.0 (d, J_{CF} = 21.8 Hz, CH), 115.8 (d, J_{CF} = 21.8 Hz, CH), 53.1 (CH₂), 44.9 (CH₃), 21.6 (CH₃), 14.9 (CH₃), 12.6 (CH₃) ppm. **¹⁹F NMR** (CDCl₃, 282 MHz) δ -111.7 (s), -112.4 (s), -138.7 (q, $J_{\text{F-B}}$ = 33.5 Hz) ppm. **FTIR** ν 2922, 2851, 1619, 1598, 1536, 1507, 1460, 1364, 1155, 1097, 1068, 1000 cm^{-1} . **HRMS** (ESI⁺) m/z [M + H]⁺ Calcd. for C₃₇H₃₅BF₄N₃ 608.2845; Found 608.2845.

2.18. Synthesis of 12

According to the above-described procedure for the synthesis of **5a**, **6** (30.0 mg, 0.098 mmol) was reacted with BnOH (15.9 mg, 0.147 mmol) to obtain **12** as an orange solid (28.9 mg, 80%) upon flash chromatography purification (deactivated silica gel, toluene). **¹H NMR** (CDCl₃, 300 MHz) δ 7.37-7.27 (m, 5H), 7.06 (s, 1H), 6.06 (s, 1H), 4.52 (s, 2H), 4.35 (s, 2H), 2.53 (br s, 6H), 2.25 (s,

3H), 2.23 (s, 3H) ppm. ^{13}C NMR (CDCl₃, 75 MHz) δ 157.4 (C), 156.4 (C), 141.7 (C), 139.8 (C), 138.3 (C), 133.8 (C), 132.5 (C), 128.6 (CH), 128.0 (CH), 127.9 (CH), 126.0 (C), 120.3 (CH), 119.4 (CH), 72.1 (CH₂), 61.9 (CH₂), 14.8 (br s, CH₃), 12.8 (br s, CH₃), 11.4 (CH₃), 9.7 (CH₃) ppm. FTIR ν 3031, 2922, 2854, 1599, 1225, 1195, 1154, 1064, 975, 918 cm⁻¹. HRMS (ESI⁺) m/z [M + Na]⁺ Calcd. for C₂₁H₂₃BF₂N₂ONa 391.1764; Found 391.1772.

2.19. Synthesis of 13

According to the above-described procedure for the synthesis of **5a**, **7** (20.0 mg, 0.063 mmol) was reacted with BnOH (10.2 mg, 0.093 mmol) to obtain **13** as an orange solid (20.2 mg, 84%) upon flash chromatography purification (deactivated silica gel, hexane/Et₂O 9:1). ^1H NMR (CDCl₃, 500 MHz) δ 7.38-7.34 (m, 4H), 7.32-7.27 (m, 1H), 6.07 (s, 1H), 4.53 (s, 2H), 4.36 (s, 2H), 2.61 (s, 3H), 2.52 (s, 6H), 2.42 (s, 3H), 2.40 (s, 3H) ppm. ^{13}C NMR (CDCl₃, 126 MHz) δ 154.4 (C), 153.4 (C), 141.8 (C), 141.5 (C), 139.6 (C), 138.4 (C), 132.6 (C), 131.7 (C), 128.6 (CH), 128.0 (CH), 127.9 (CH), 121.7 (CH), 126.7 (C), 72.0 (CH₂), 61.7 (CH₂), 17.6 (CH₃), 16.9 (CH₃), 14.7 (CH₃), 14.6 (t, J = 2.6 Hz, CH₃), 12.5 (t, J = 2.8 Hz, CH₃) ppm. FTIR ν 3030, 2925, 2855, 1726, 1552, 1486, 1314, 1201, 1167, 1064, 982 cm⁻¹. HRMS (ESI⁺) m/z [M + Na]⁺ Calcd. for C₂₂H₂₅BF₂N₂ONa 405.1920; Found 405.1924.

2.20. Synthesis of 14

According to the above-described procedure for the synthesis of **5a**, **11** (27.0 mg, 0.045 mmol) was reacted with BnOH (7.2 mg, 0.067 mmol) to obtain **14** as a blue solid (15.2 mg, 51%) upon flash chromatography purification (deactivated silica gel, hexane/toluene 9:1). ^1H NMR (CDCl₃, 300 MHz) δ 7.66 (d, J = 16.8 Hz, 1H), 7.64 (d, J = 15.4 Hz, 1H), 7.61-7.50 (m, 4H), 7.45 (d, J = 16.6 Hz, 1H), 7.39-7.24 (m, 7H), 7.27 (d, J = 15.5 Hz, 1H), 7.18 (d, J = 8.1 Hz, 2H), 7.10 (d, J = 8.0 Hz, 2H), 7.07 (d, J = 8.0 Hz, 2H), 6.63 (s, 1H), 4.60 (s, 2H), 4.41 (s, 2H), 2.46 (s, 3H), 1.46 (s, 3H), 1.44 (s, 3H) ppm. ^{13}C NMR (CDCl₃, 75 MHz) δ 162.5 (d, J_{CF} = 259.9 Hz, C), 153.5 (C), 151.8 (C), 140.6 (C), 139.2 (C), 138.2 (C), 136.5 (CH), 135.7 (CH), 134.3 (C), 133.74 (C), 133.70 (C), 132.8 (C), 132.3 (C), 130.0 (CH), 129.5 (d, J_{CF} = 12.8 Hz, CH), 129.3 (d, J_{CF} = 12.8 Hz, CH), 128.6 (CH), 128.3 (CH), 128.0 (CH), 127.9 (CH), 126.8 (C), 119.0 (br s, CH), 118.3 (CH), 116.0 (d, J_{CF} = 21.9 Hz, CH), 115.8 (d, J_{CF} = 21.8 Hz, CH), 72.3 (CH₂), 62.5 (CH₂), 21.6 (CH₃), 15.0 (CH₃), 12.1 (CH₃) ppm. ^{19}F NMR (CDCl₃, 282 MHz) δ -111.4 (s), -112.32 (s), -138.85 (q, $J_{\text{F-B}}$ = 33.6 Hz) ppm. FTIR ν 2923, 2854, 1630, 1509, 1460, 1378, 1100 cm⁻¹. HRMS (ESI⁺) m/z [M + Na]⁺ Calcd. for C₄₂H₃₅BF₄N₂ONa 693.2672; Found 693.2671.

2.21. Synthesis of 15

Based on the procedure described for the synthesis of **2**, **2** (50.0 mg, 0.126 mmol) was reacted with Eschenmoser's salt (70.2 mg, 0.379 mmol) and K_2CO_3 (104.9 mg, 0.759 mmol) to obtain **15** as an orange solid (23.7 mg, 41%) upon flash chromatography purification (deactivated silica gel, DCM→AcOEt). 1H NMR ($CDCl_3$, 300 MHz) δ = 7.27 (d, J = 8.1 Hz, 2H), 7.12 (d, J = 7.8 Hz, 2H), 3.15 (s, 4H), 2.58 (s, 6H), 2.43 (s, 3H), 2.19 (s, 12H), 1.37 (s, 6H) ppm. ^{13}C NMR ($CDCl_3$, 75 MHz) δ 155.6 (C), 142.0 (C), 141.7 (C), 139.0 (C), 132.4 (C), 131.3 (C), 129.9 (CH), 128.0 (CH), 127.2 (C), 52.5 (CH_2), 45.1 (CH_3), 21.6 (CH_3), 12.9 (br s, CH_3), 12.3 (CH_3) ppm. FTIR ν 2972, 2939, 2856, 2811, 2762, 1537, 1477, 1407, 1372, 1349, 1315, 1197, 1175, 1074, 1043, 1017, 956 cm^{-1} . HRMS (ESI⁺) m/z [$M + H$]⁺ Calcd. for $C_{26}H_{36}BF_2N_4$ 453.2996; Found 453.2999.

2.22. Synthesis of 16

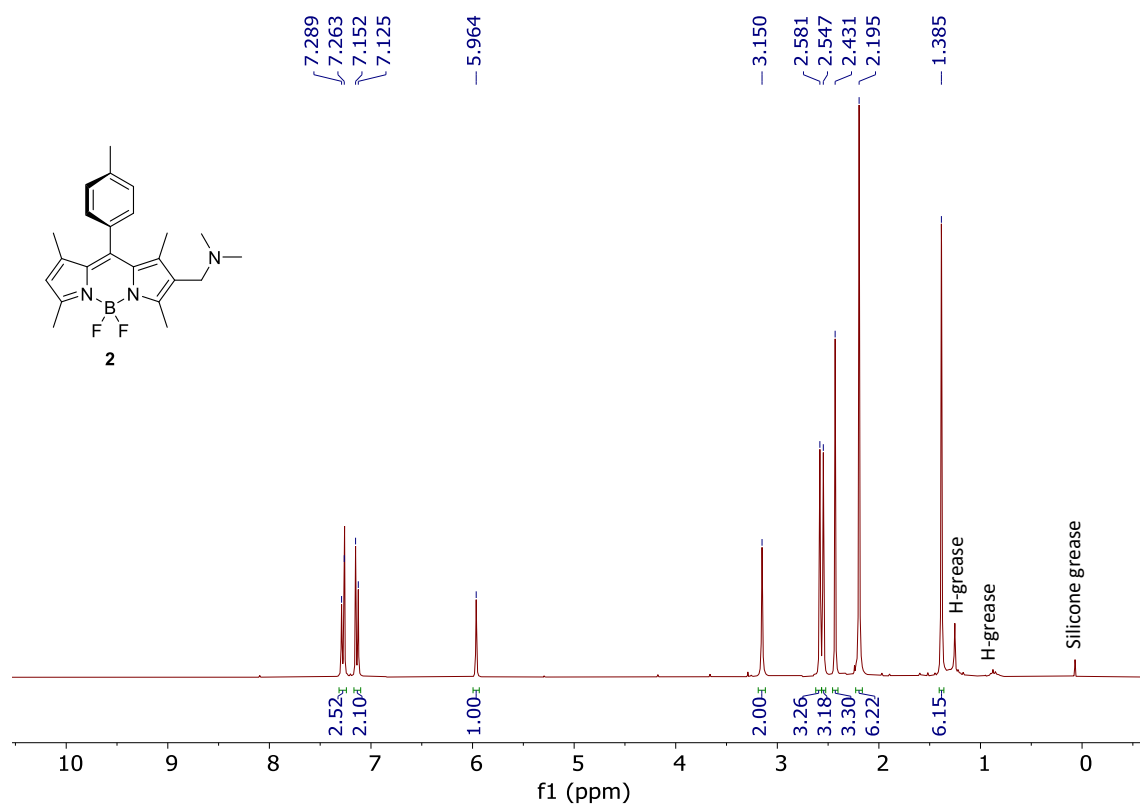
According to the above-described procedure for the synthesis of **5a**, **15** (30.0 mg, 0.066 mmol) was reacted with double amount of BnOH (21.5 mg, 0.199 mmol) to obtain **16** as an orange solid (22.2 mg, 58%) upon flash chromatography purification (deactivated silica gel, hexane/Et₂O/AcOEt 6.0:3.5:0.5). 1H NMR ($CDCl_3$, 300 MHz) δ 7.37-7.26 (m, 12H), 7.12 (d, J = 8.0 Hz, 2H), 4.48 (s, 4H), 4.25 (s, 4H), 2.56 (s, 6H), 2.48 (s, 3H), 1.37 (s, 6H) ppm. ^{13}C NMR ($CDCl_3$, 75 MHz) δ 155.7 (C), 142.8 (C), 142.1 (C), 139.1 (C), 138.3 (C), 132.3 (C), 131.4 (C), 130.0 (CH), 128.6 (CH), 127.98 (CH), 127.96 (CH), 127.8 (CH), 127.2 (C), 72.2 (CH_2), 61.7 (CH_2), 21.6 (CH_3), 12.7 (CH_3), 12.2 (CH_3) ppm. FTIR ν 2921, 2851, 1540, 1480, 1316, 1198, 1066, 964 cm^{-1} . HRMS (ESI⁺) m/z [$M + Na$]⁺ Calcd. for $C_{36}H_{37}BF_2N_2O_2Na$ 601.2808; Found 601.2812.

2.23. Synthesis of 17

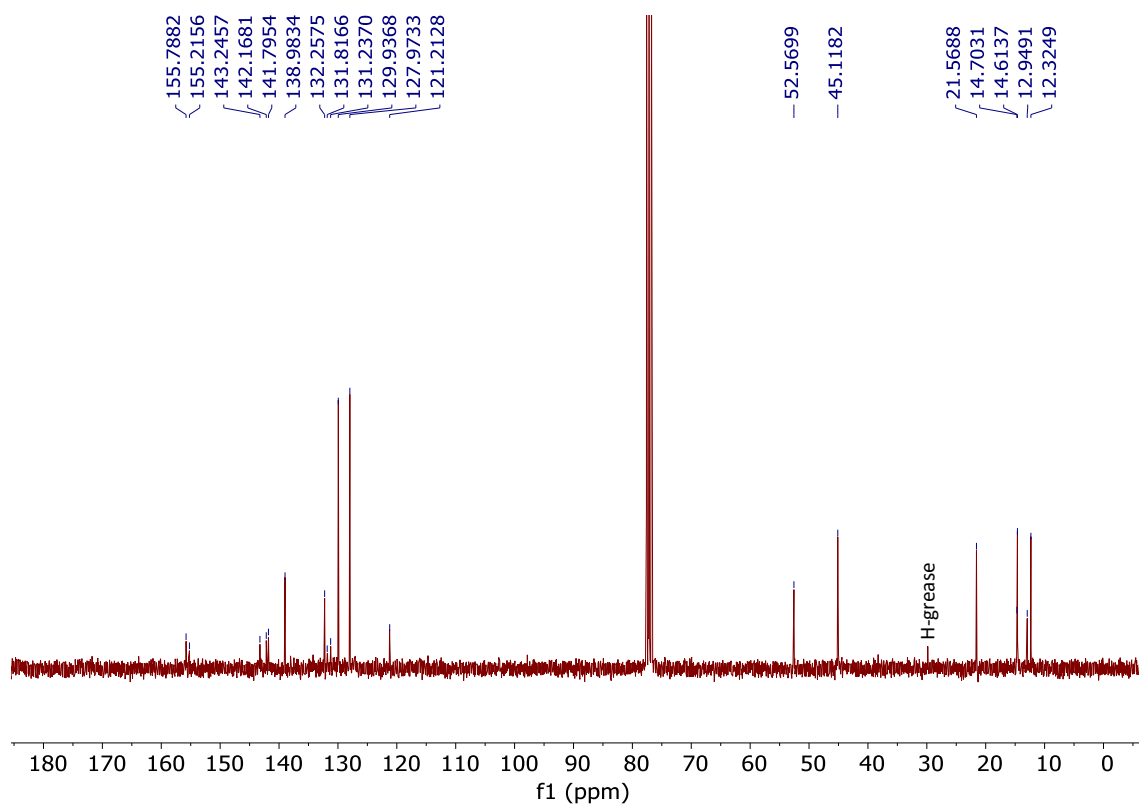
According to the above-described procedure for the synthesis of **3**, **15** (88.0 mg, 0.164 mmol) was reacted with MeI 477.2 mg, 3.363 mmol) to obtain **17** as a red solid (118.4 mg, 98%) upon filtration and washed with DCM (2 × 10 mL). 1H NMR (MeOD, 500 MHz) δ 7.48 (d, J = 7.7 Hz, 2H), 7.31 (d, J = 8.0 Hz, 2H), 4.41 (s, 4H), 3.09 (s, 18H), 2.70 (s, 6H), 2.48 (s, 3H), 1.60 (s, 6H) ppm. ^{13}C NMR (MeOD, 126 MHz) δ 158.8 (C), 147.9 (C), 147.5 (C), 141.8 (C), 133.4 (C), 132.5 (C), 131.8 (CH), 128.9 (CH), 120.3 (C), 60.0 (CH_2), 53.0 (t, J = 3.6 Hz, CH_3), 21.4 (C), 14.2 (CH_3), 13.9 (br s, CH_3) ppm. FTIR ν 3412 2950, 1626, 1529, 1487, 1362, 1319, 1195, 1090, 969 cm^{-1} . HRMS (ESI⁺) m/z [M]²⁺ 241.1691 Calcd. for $C_{28}H_{41}BF_2N_4$; Found 241.1694.

3. NMR spectra of new compounds

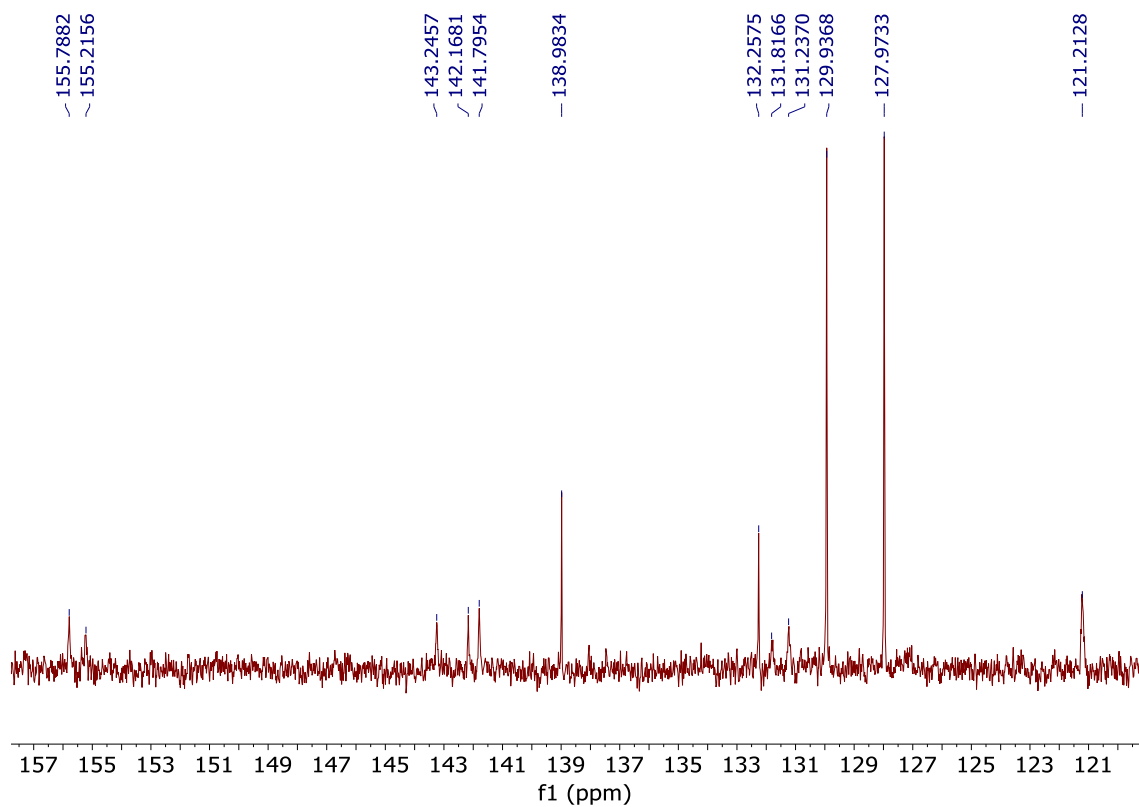
¹H NMR (CDCl₃, 300 MHz) of 2



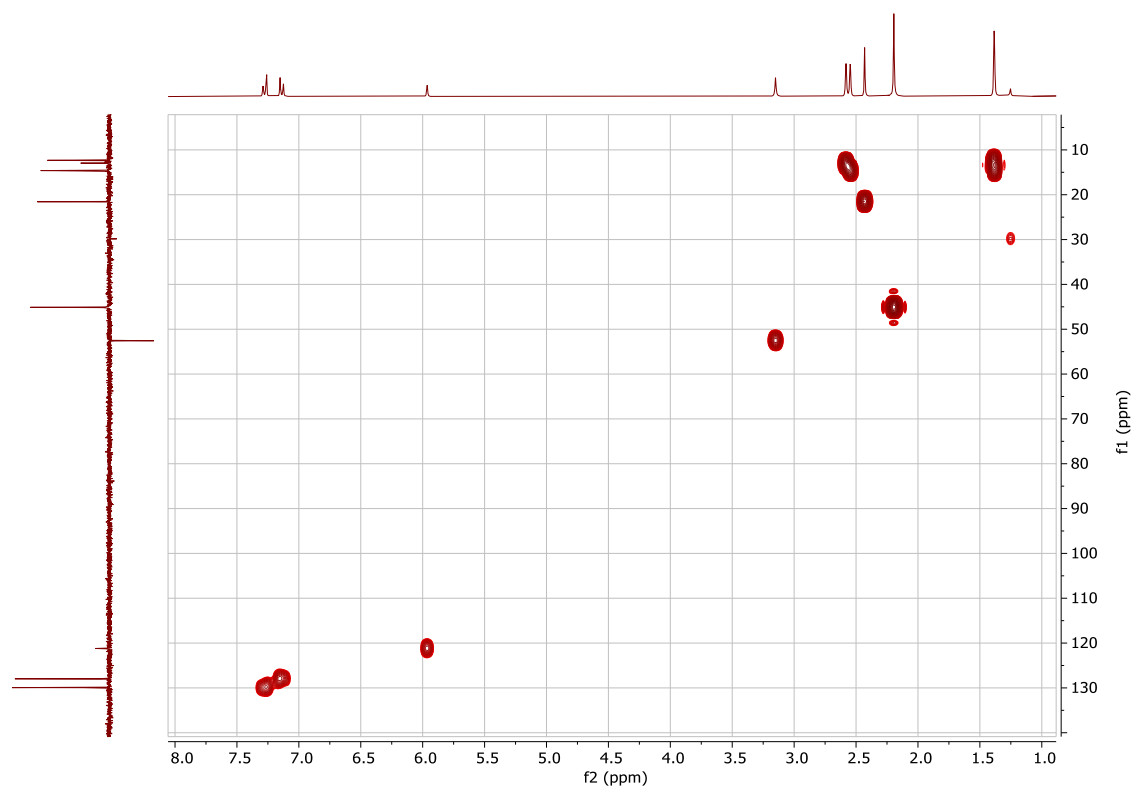
^{13}C NMR (CDCl_3 , 75 MHz) of 2



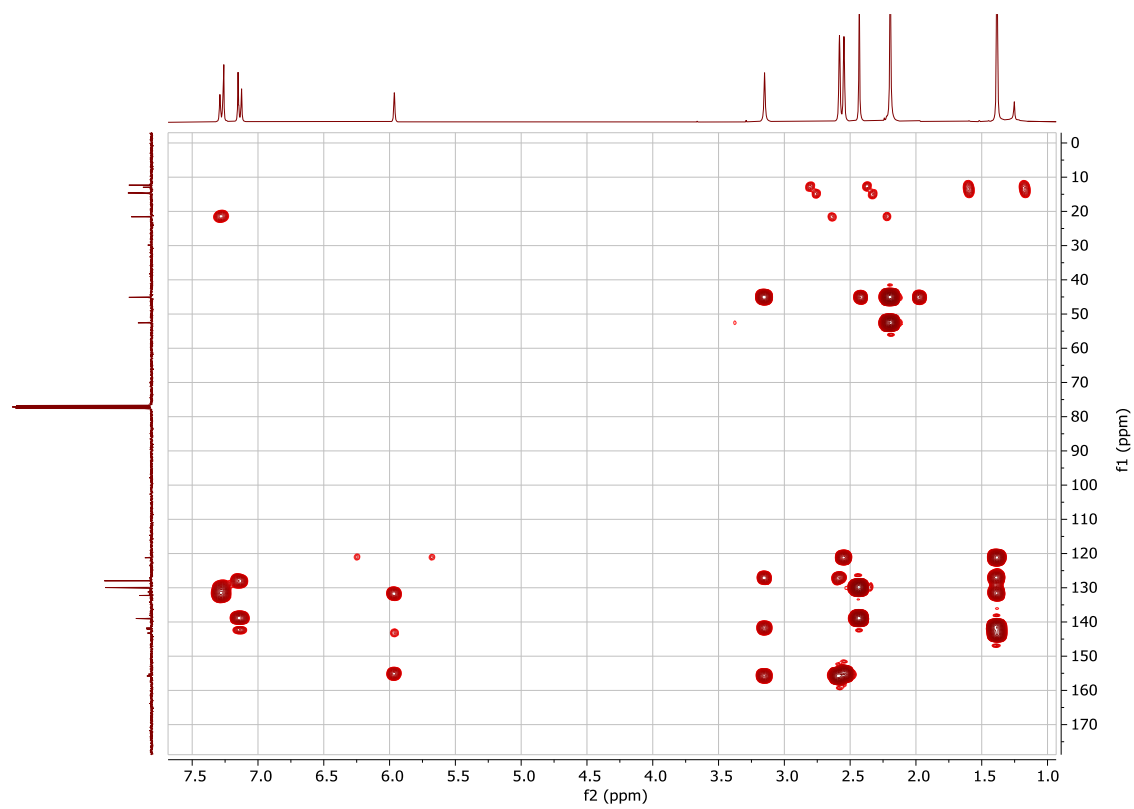
Expansion of the ^{13}C NMR spectrum of 2 (aromatic region)



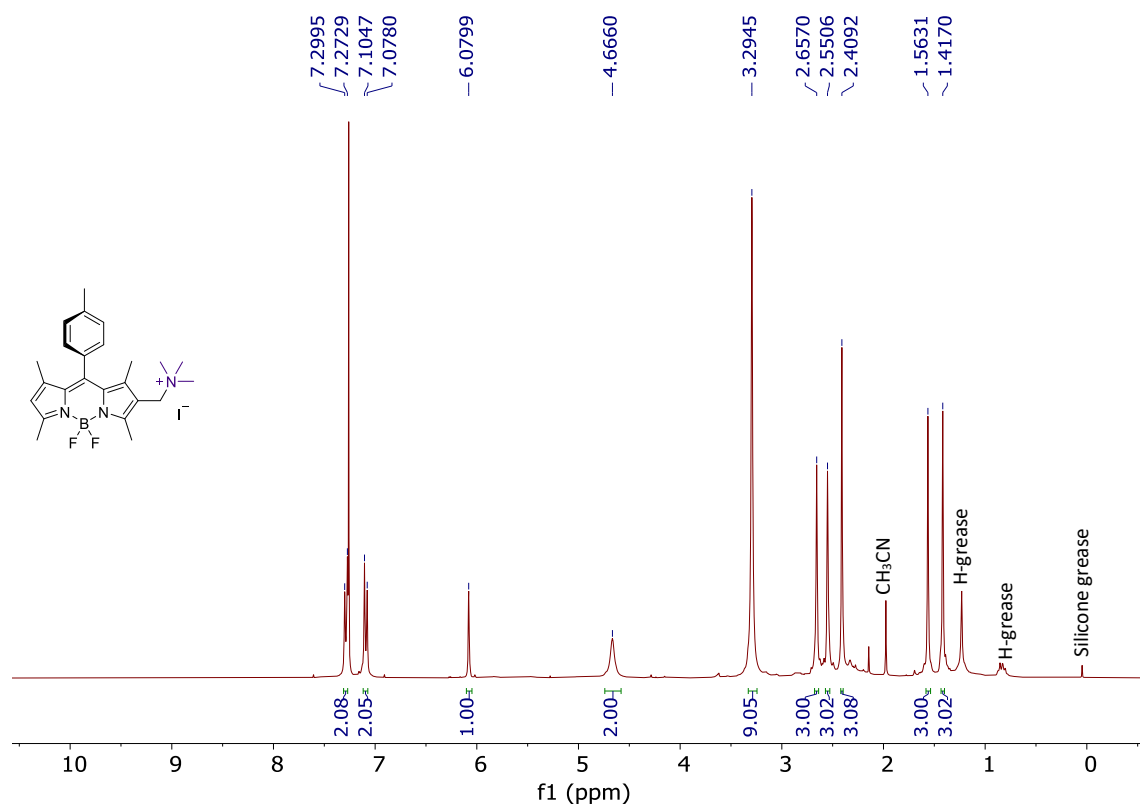
HMQC spectrum of 2



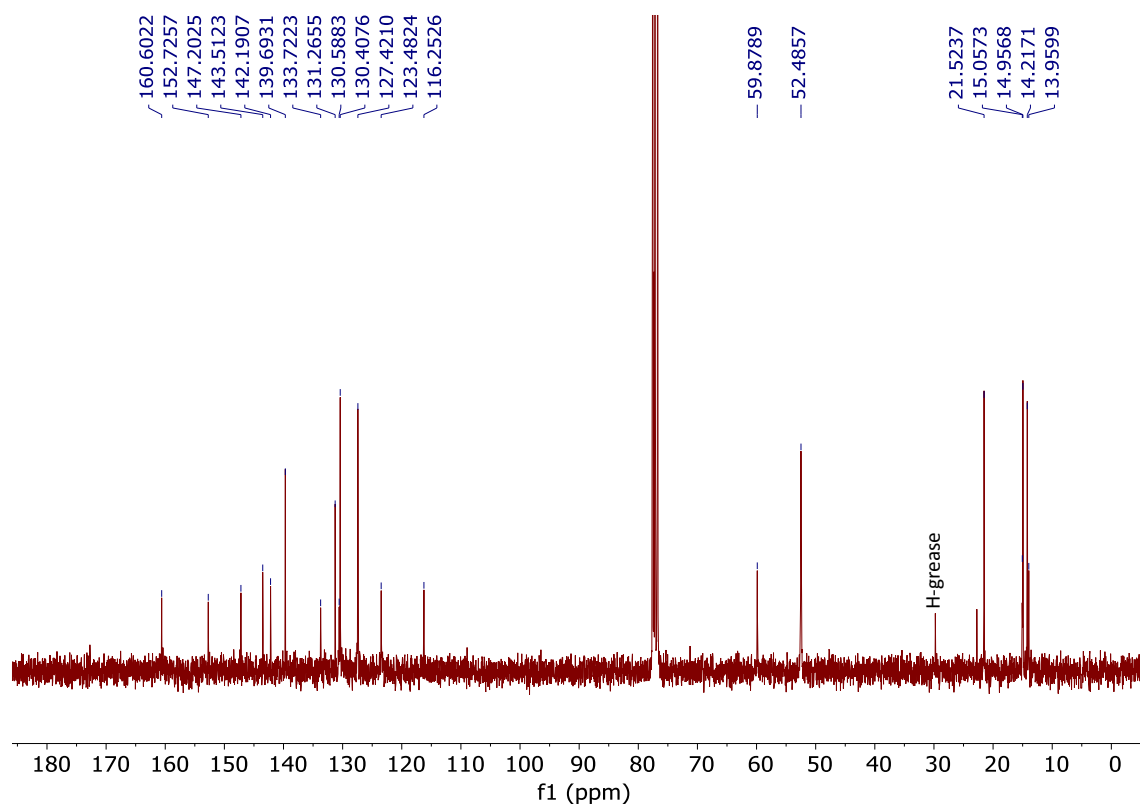
HMBC spectrum of 2



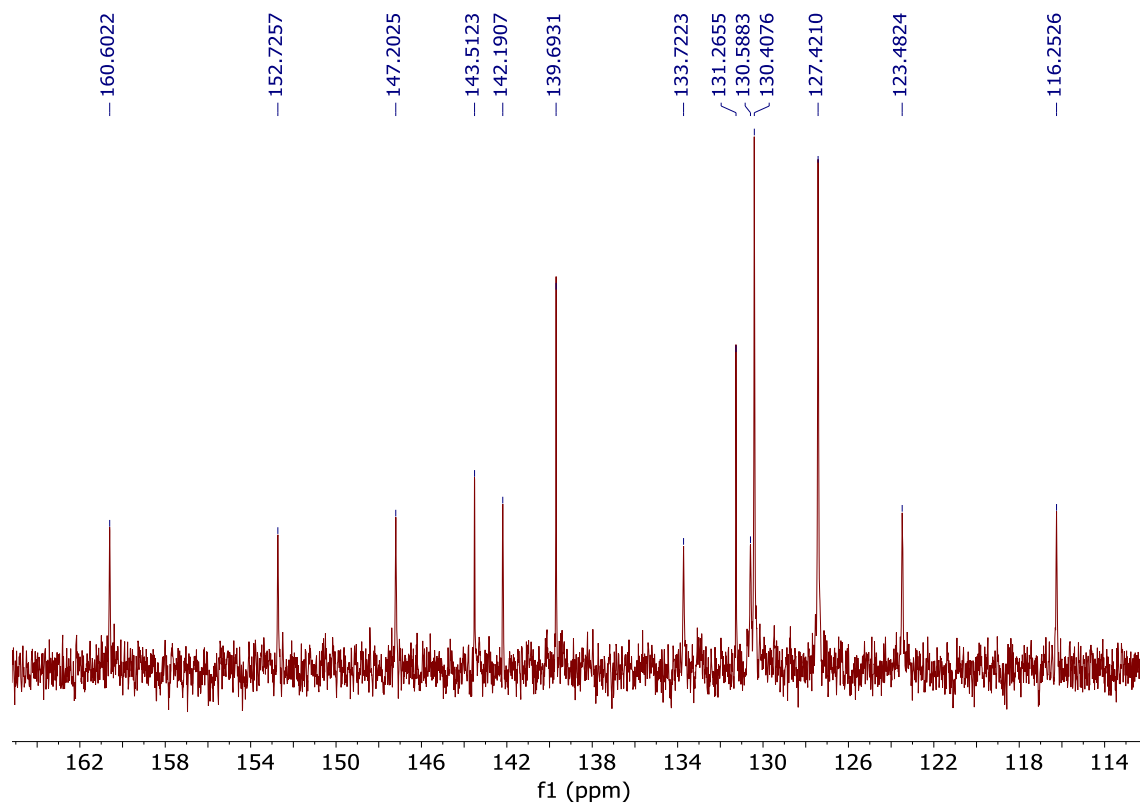
¹H NMR (CDCl₃, 300 MHz) of 3



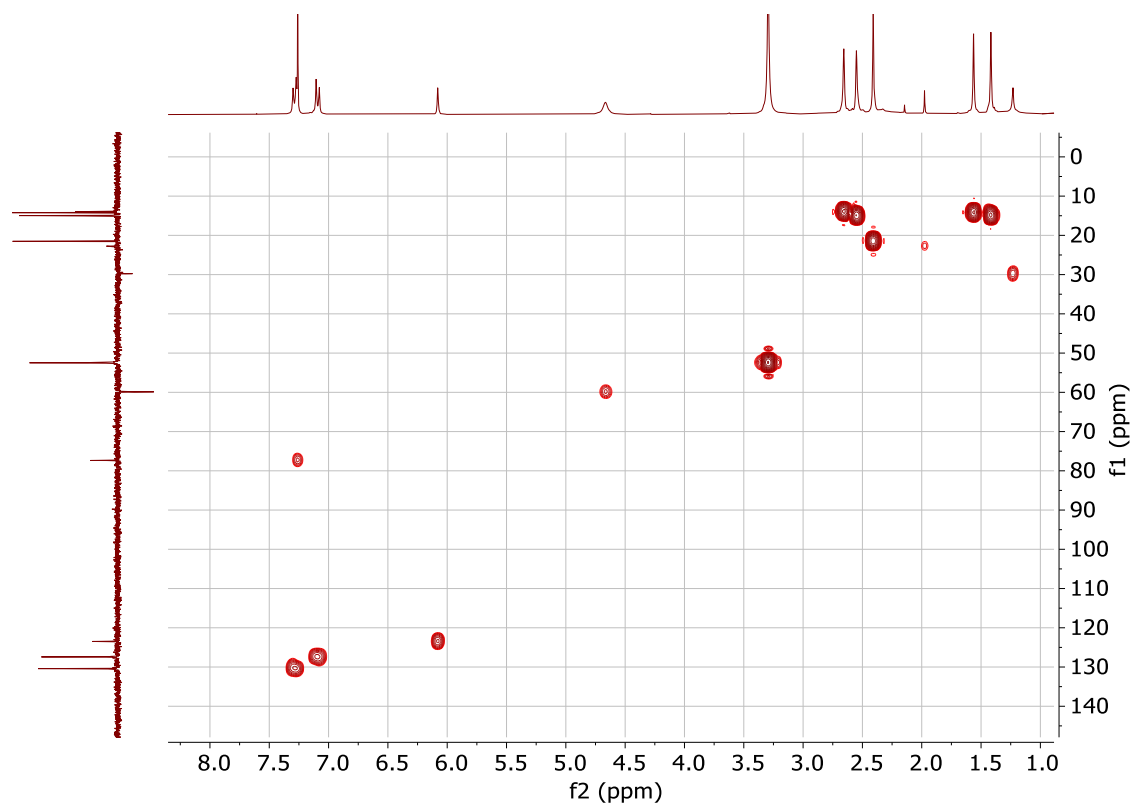
^{13}C NMR (CDCl₃, 75 MHz) of 3



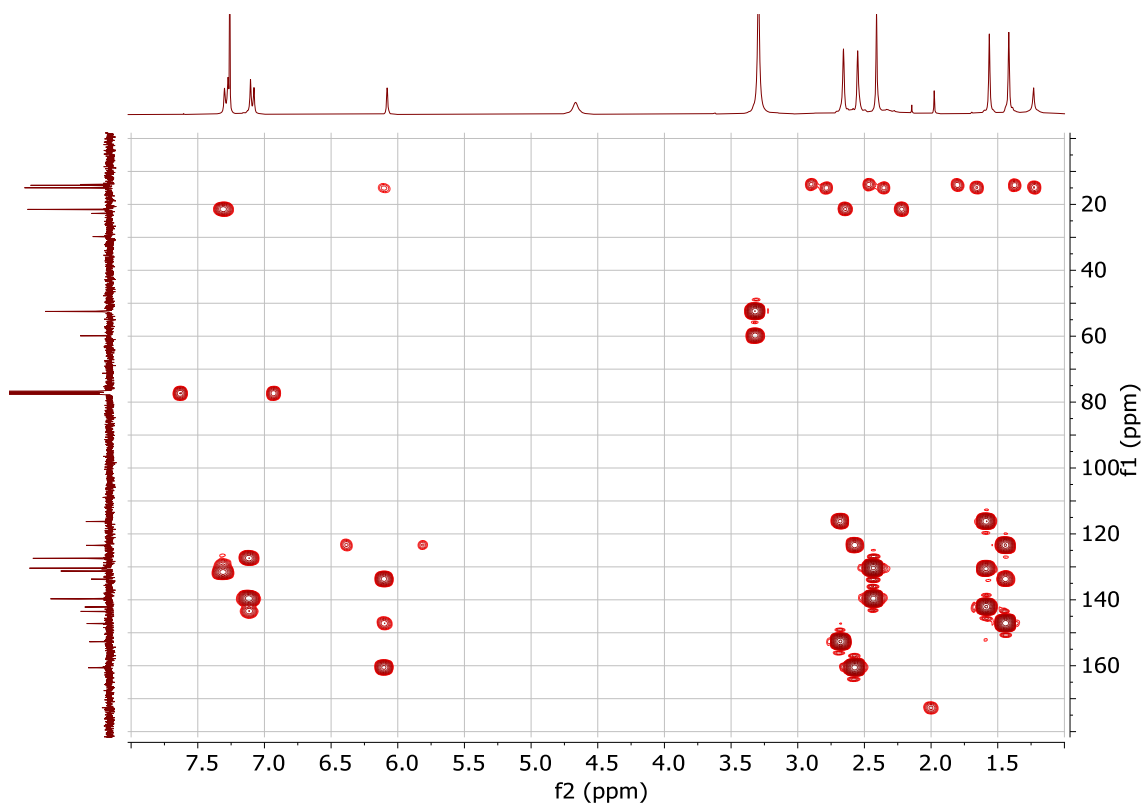
Expansion of the ^{13}C NMR spectrum of 3 (aromatic region)



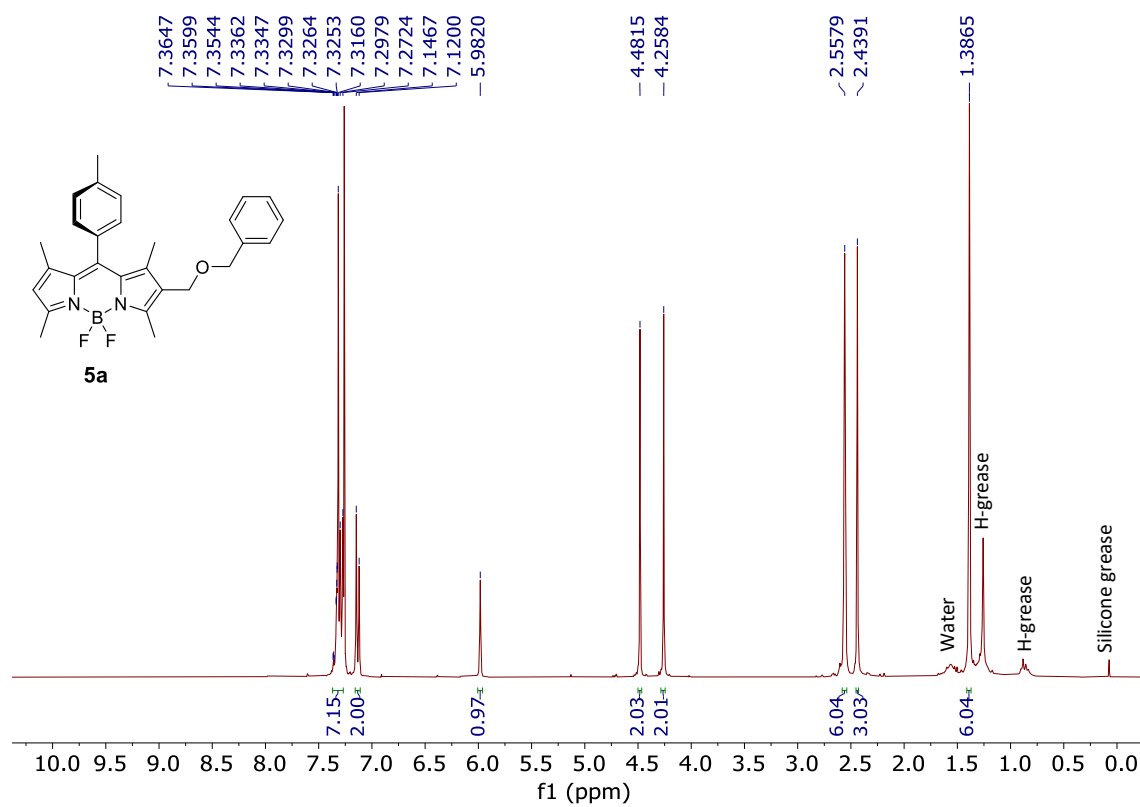
HMQC spectrum (CDCl₃, 300 MHz) of 3



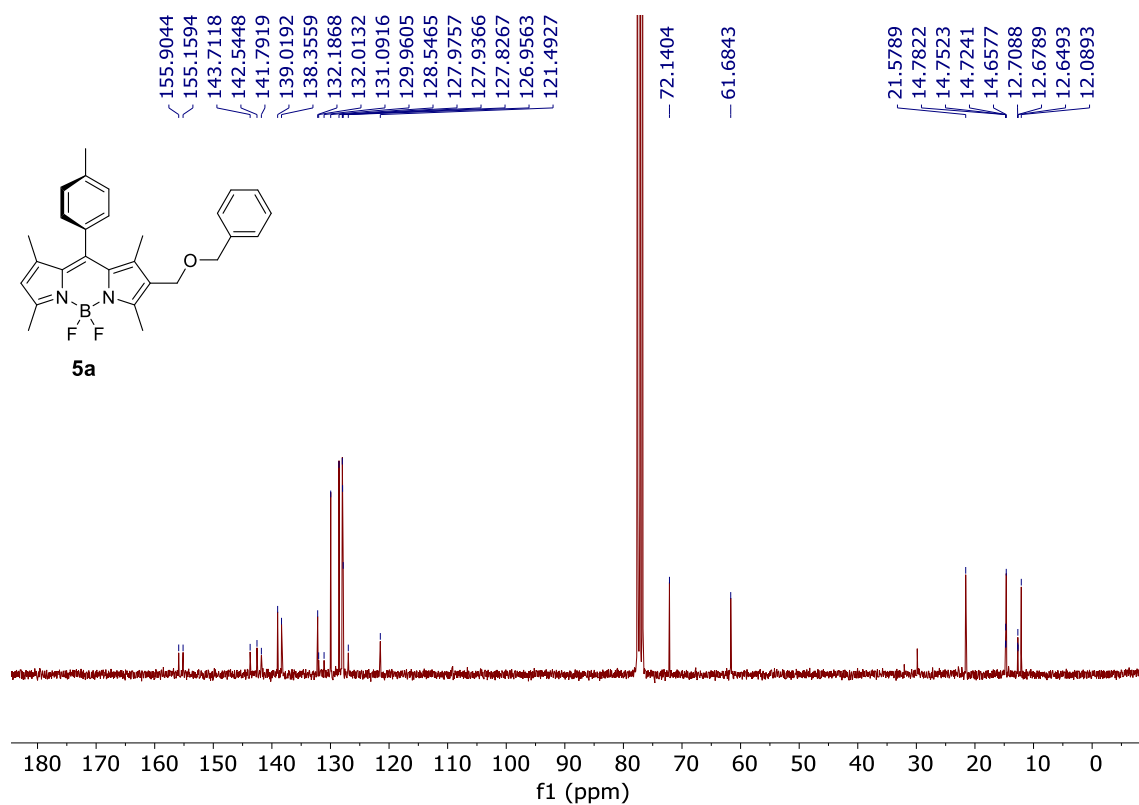
HMBC spectrum of 3



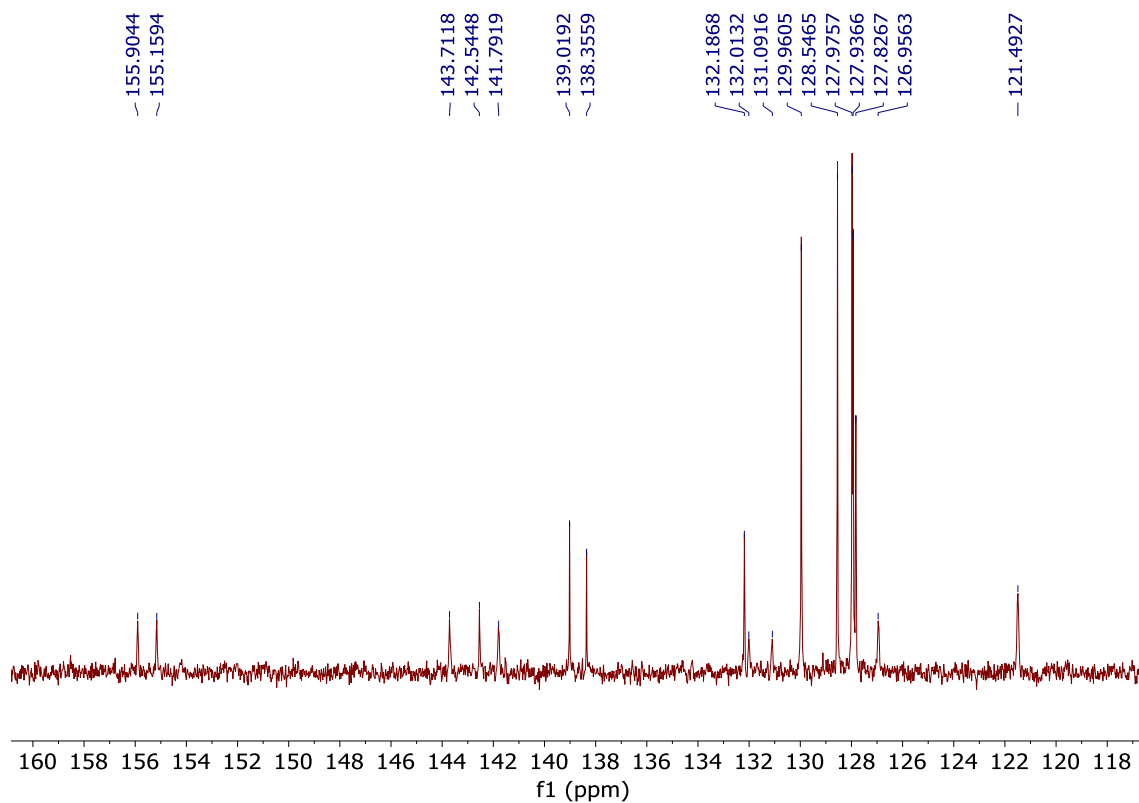
¹H NMR (CDCl₃, 300 MHz) of 5a



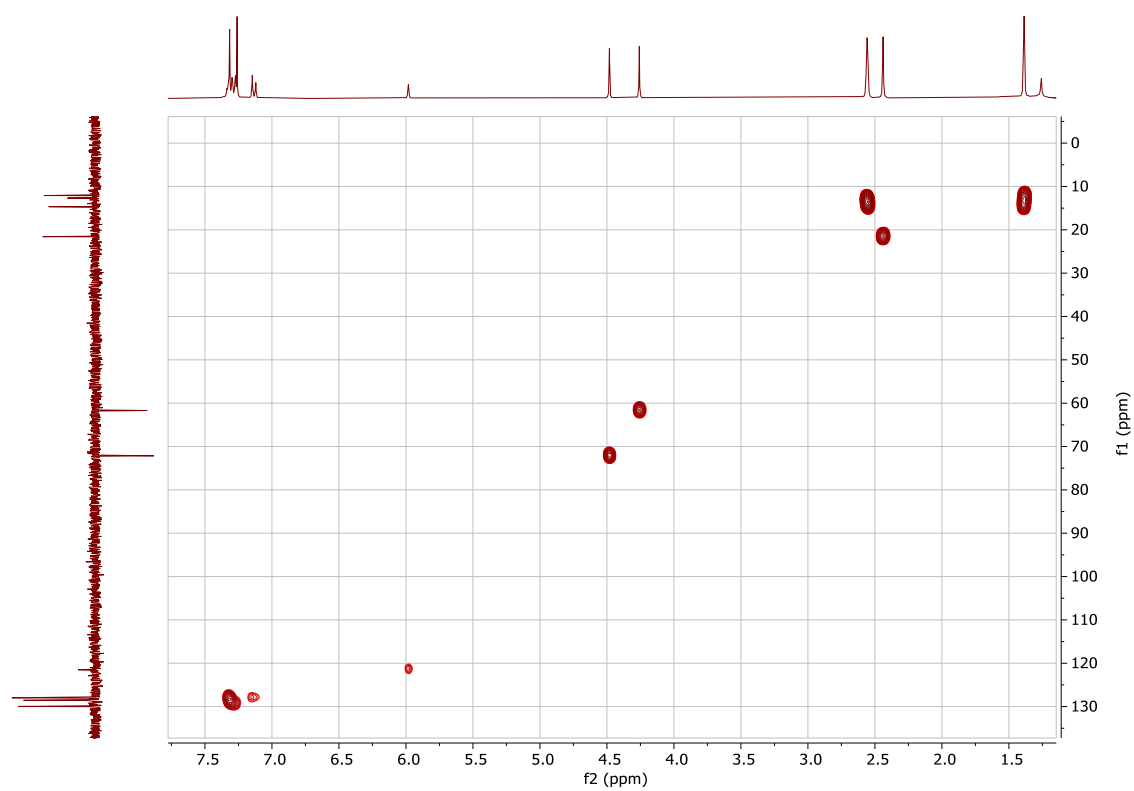
^{13}C NMR (CDCl_3 , 75 MHz) of **5a**



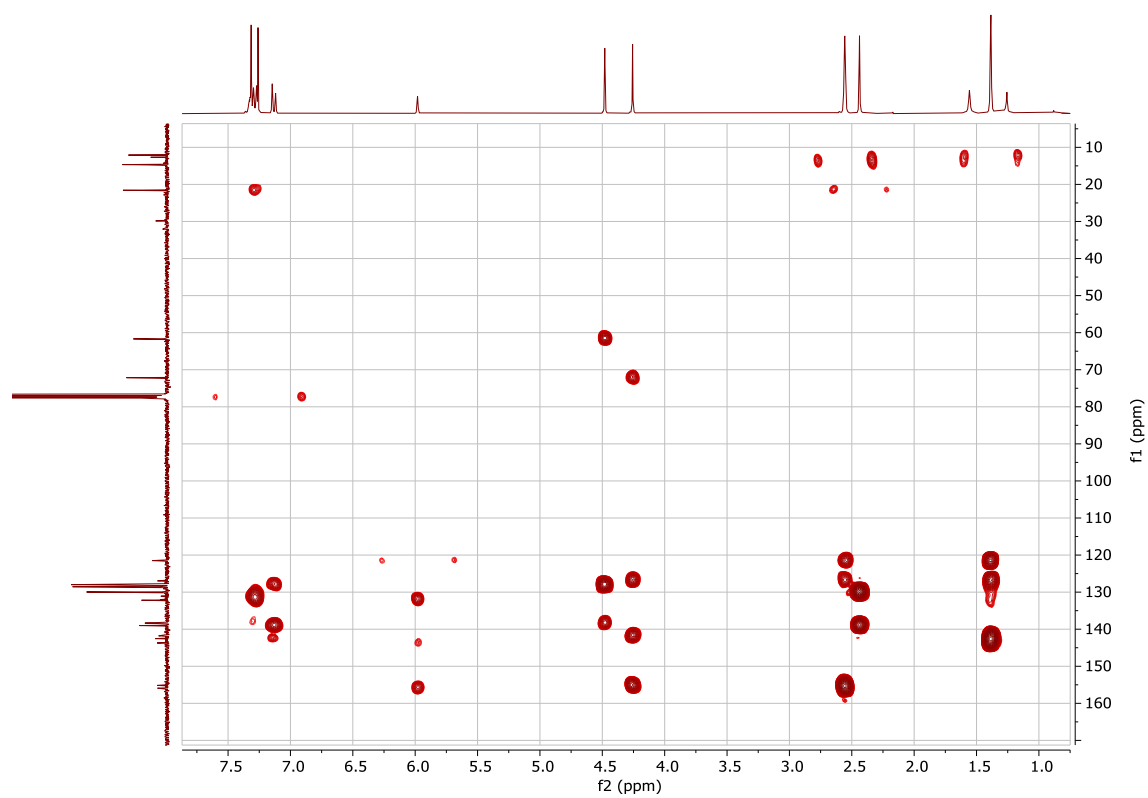
Expansion of the ^{13}C NMR spectrum of **5a** (aromatic region)



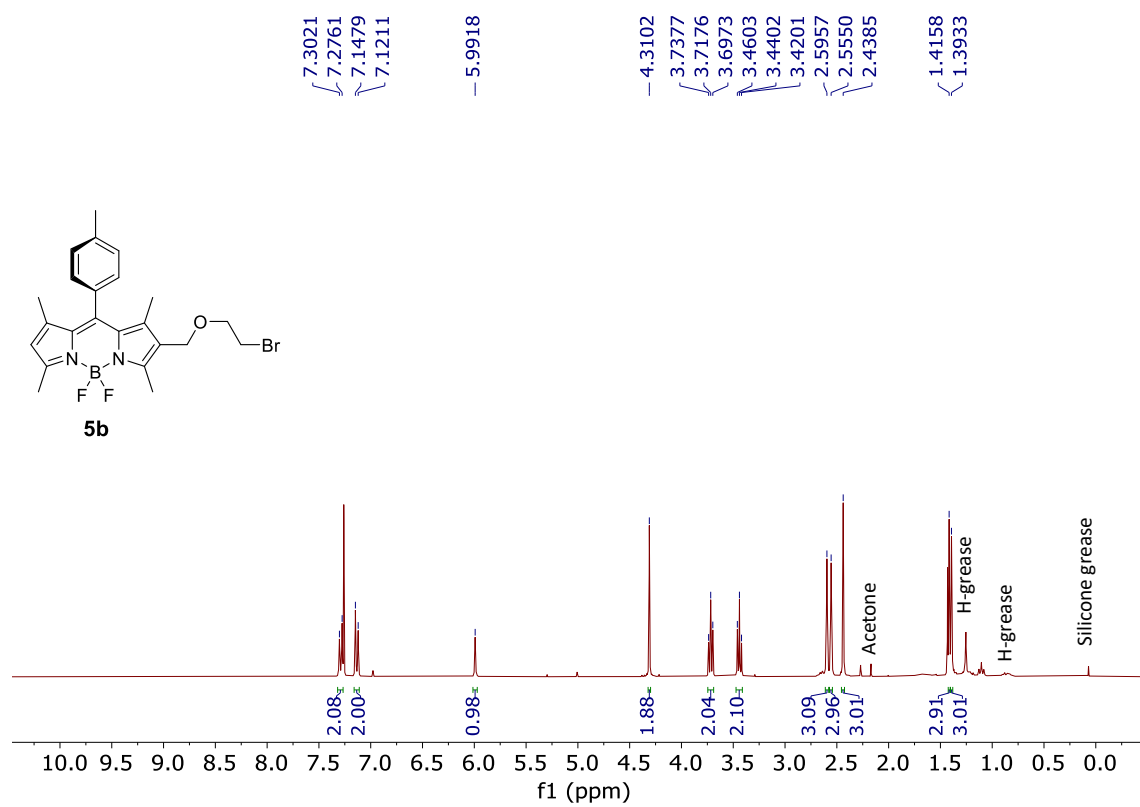
HMQC spectrum of 5a



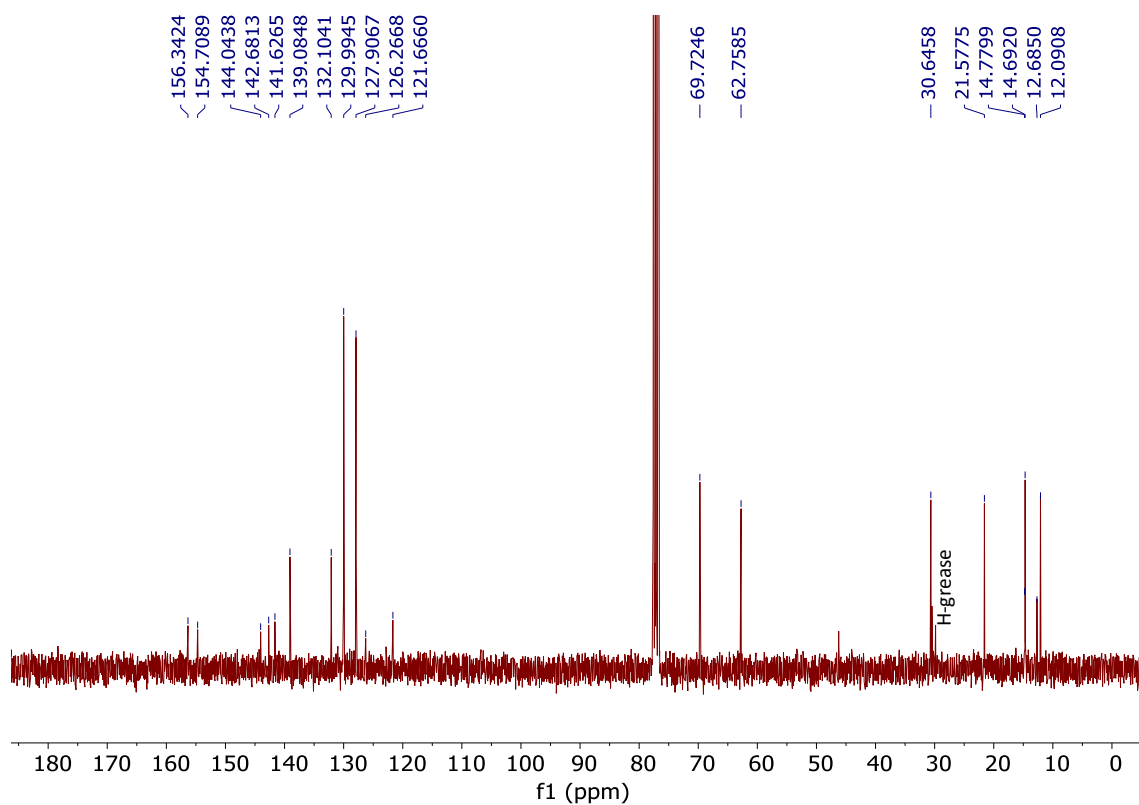
HMBC spectrum of 5a



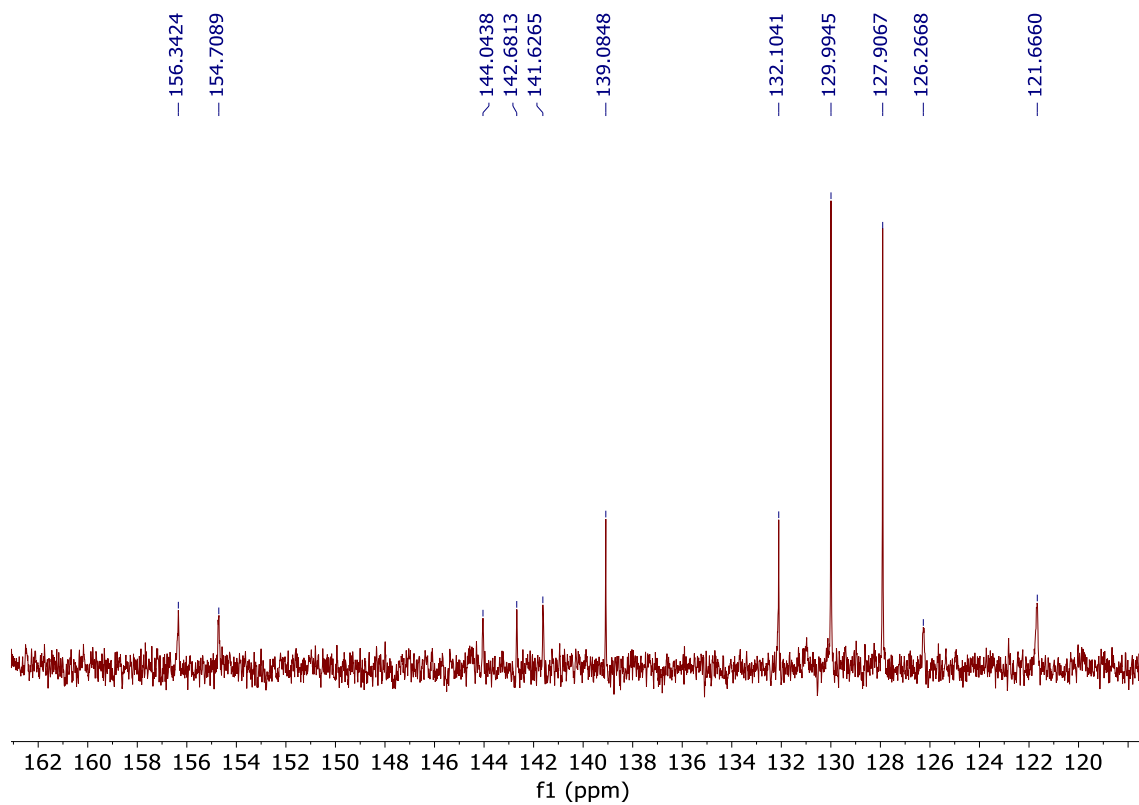
¹H NMR (CDCl₃, 300 MHz) of 5b



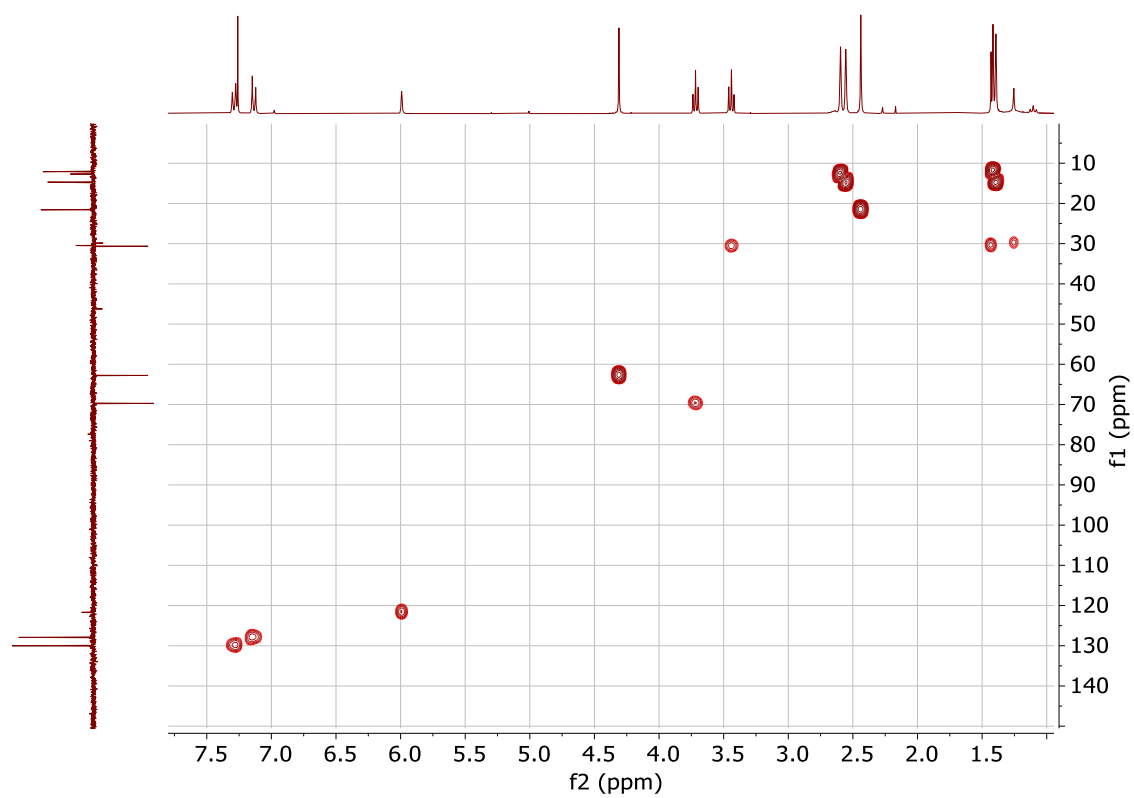
^{13}C NMR (CDCl_3 , 75 MHz) of 5b



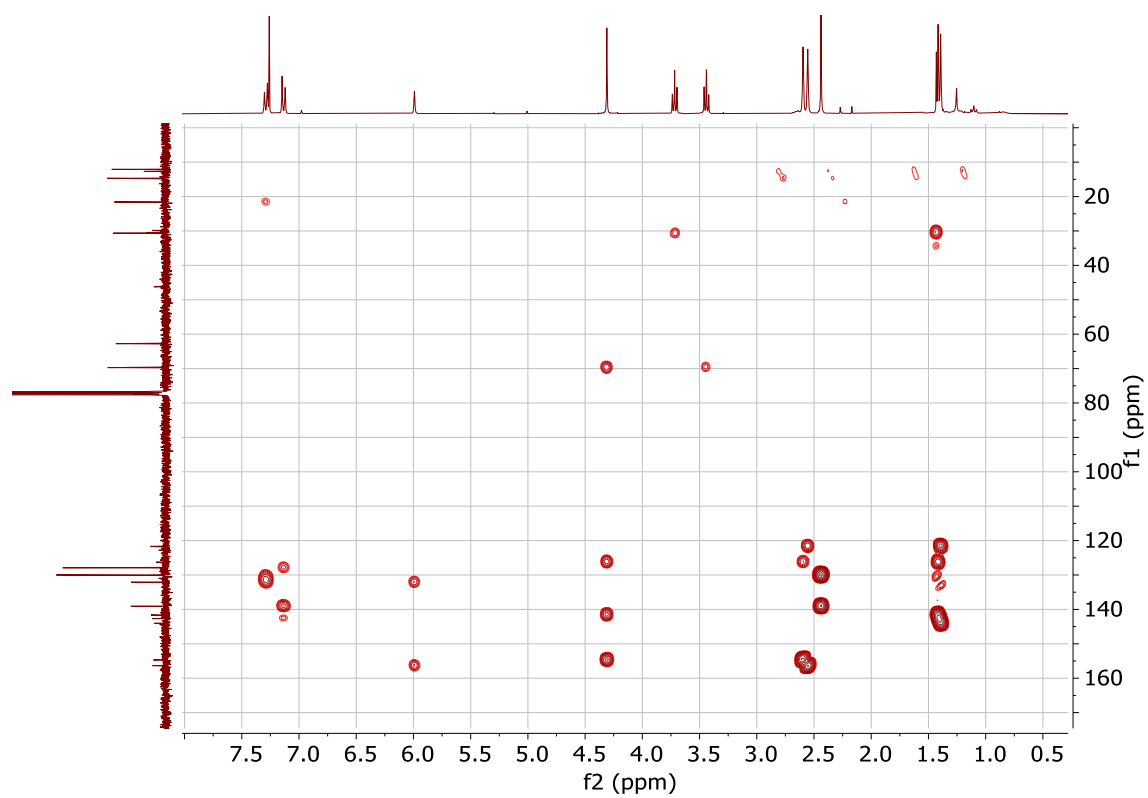
Expansion of the ^{13}C NMR spectrum of 5b (aromatic region)



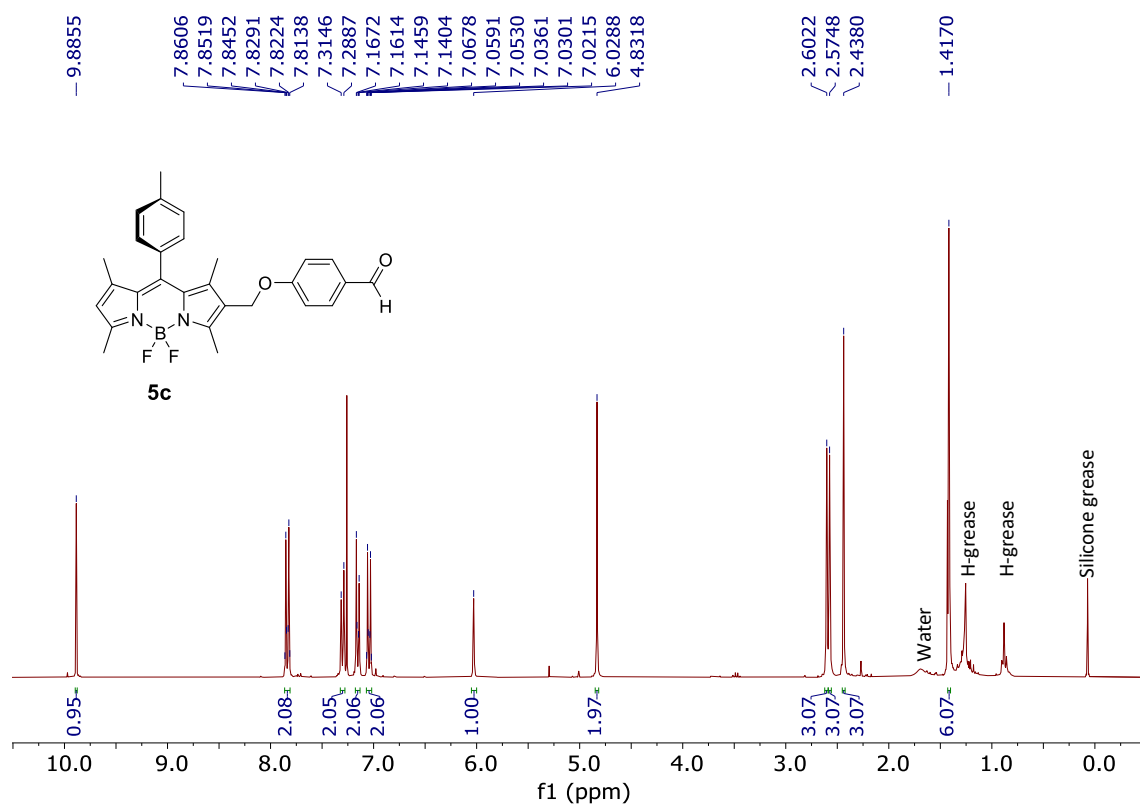
HMQC spectrum of 5b



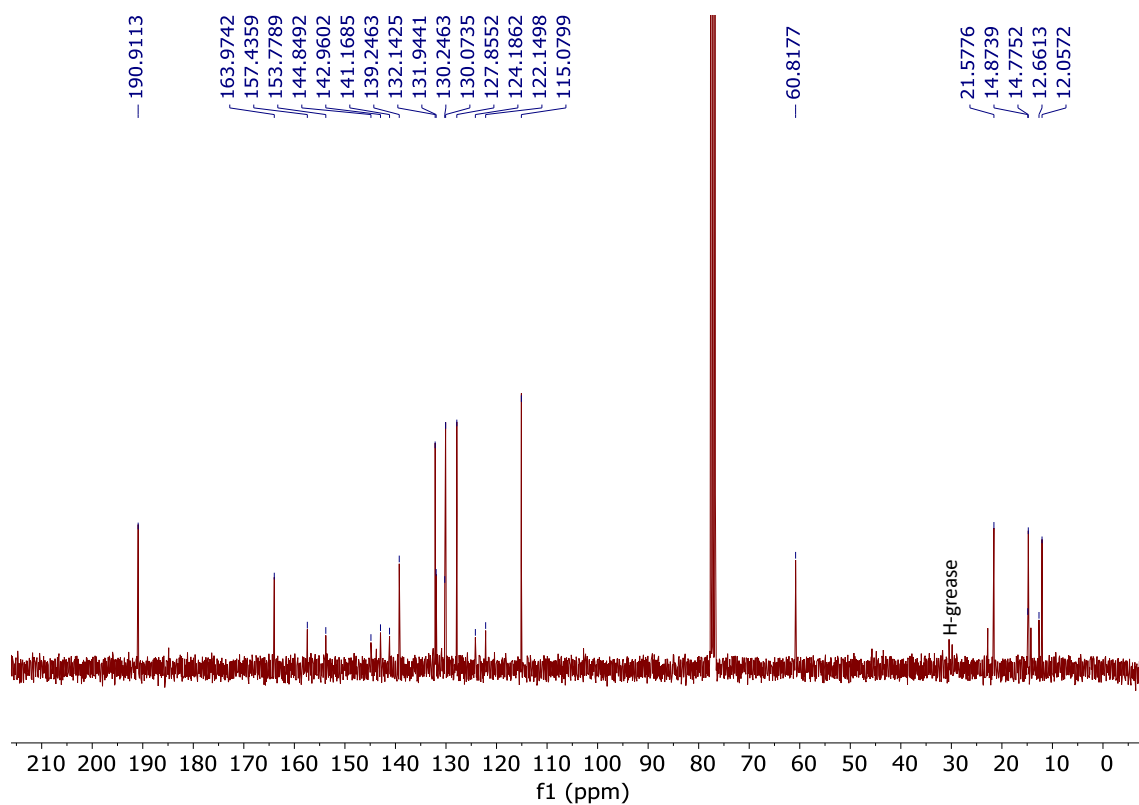
HMBC spectrum of 5b



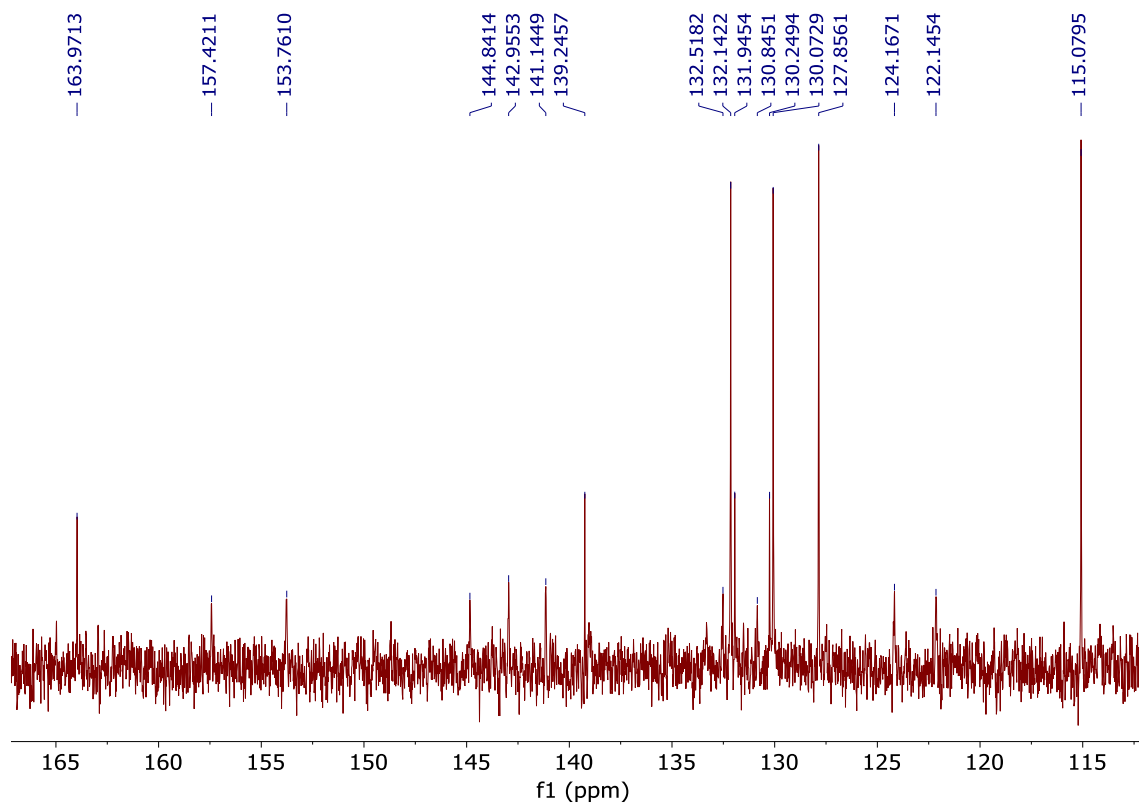
¹H NMR (CDCl₃, 300 MHz) of 5c



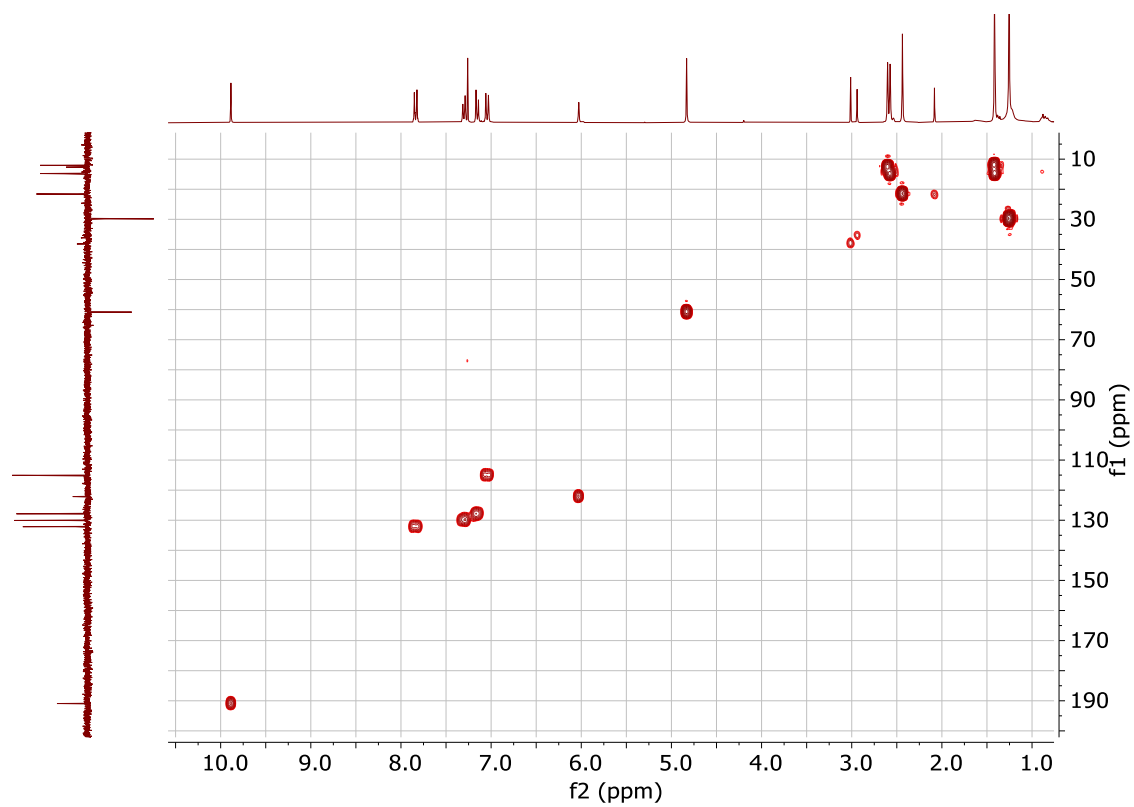
^{13}C NMR (CDCl₃, 75 MHz) of 5c



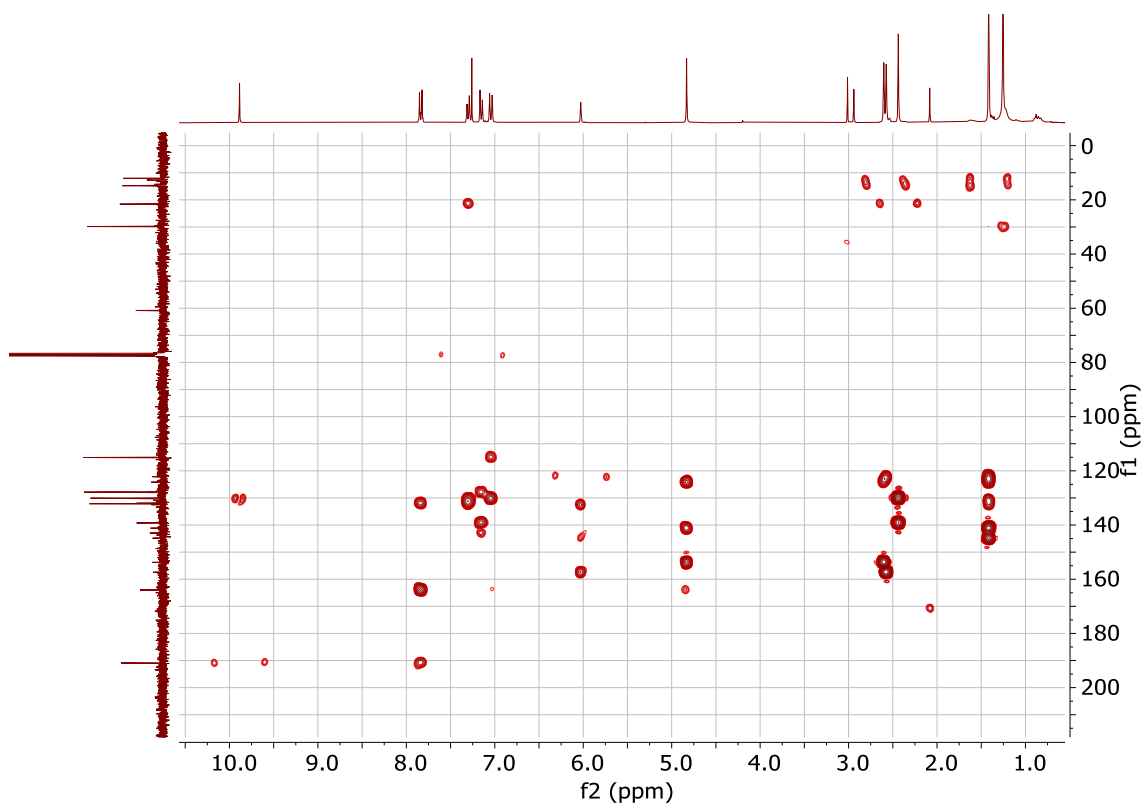
Expansion of the ^{13}C NMR spectrum of 5c (aromatic region)



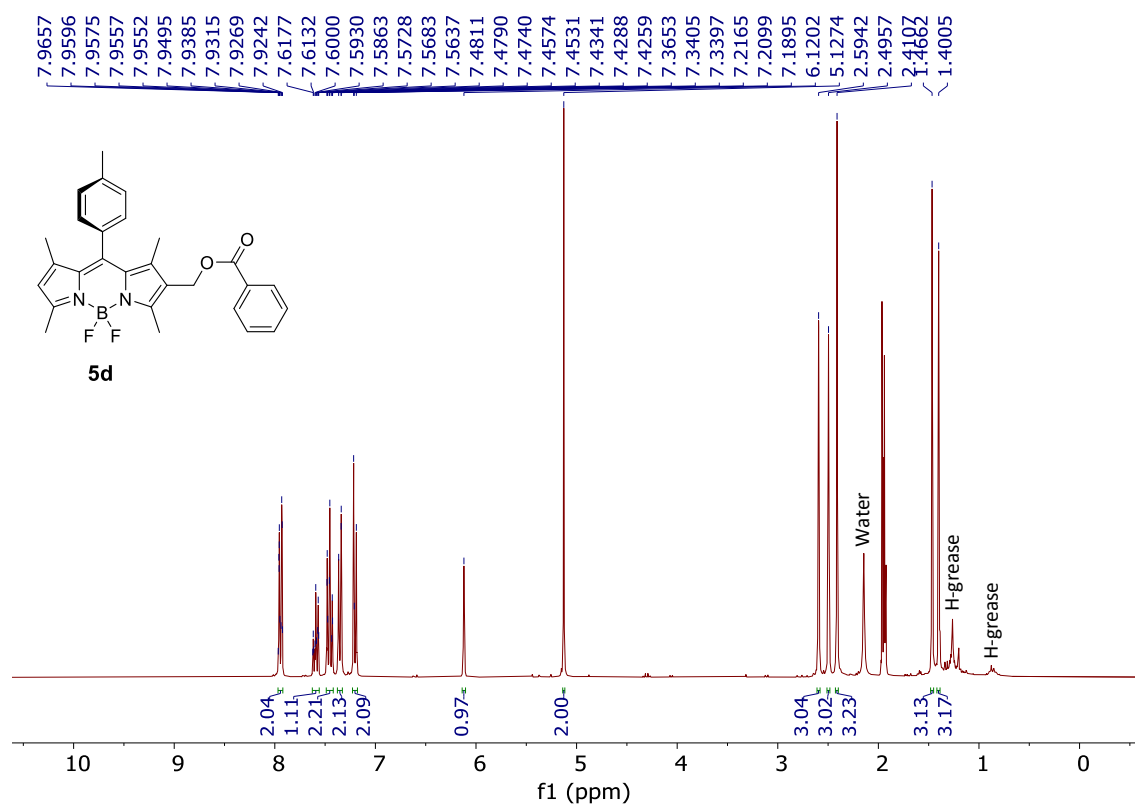
HMQC spectrum of 5c



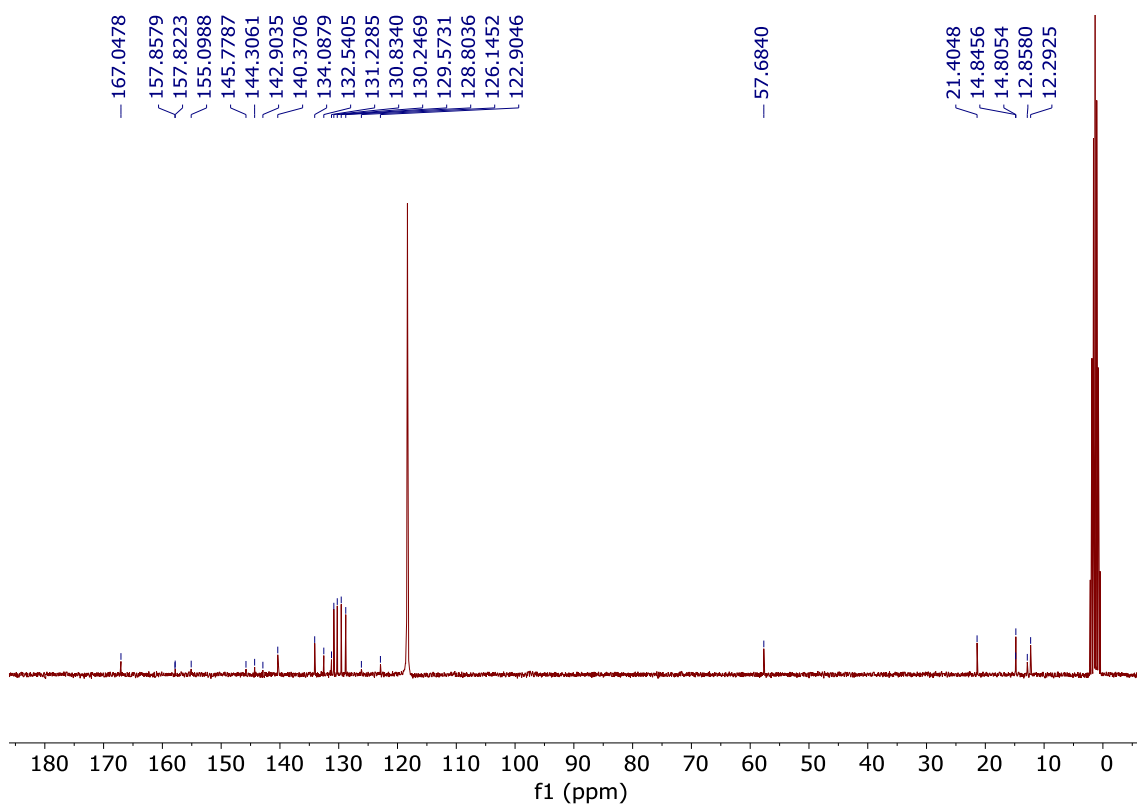
HMBC spectrum of 5c



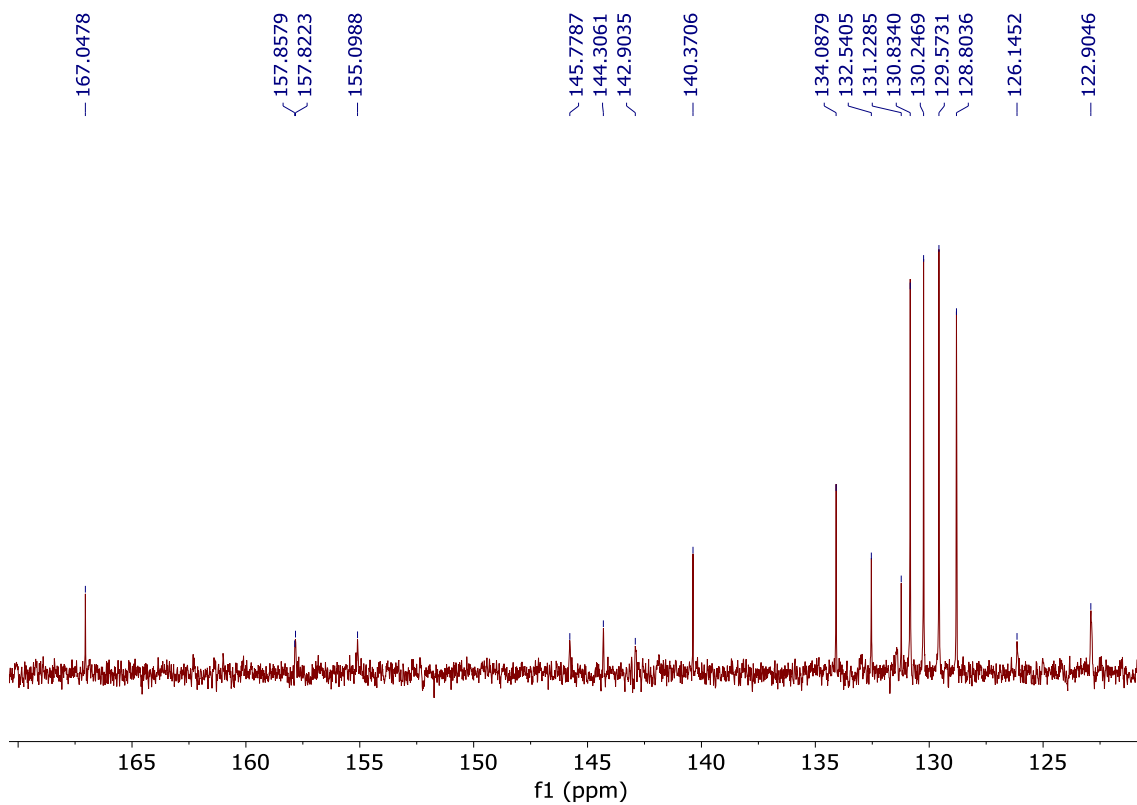
¹H NMR (CD₃CN, 300 MHz) of 5d



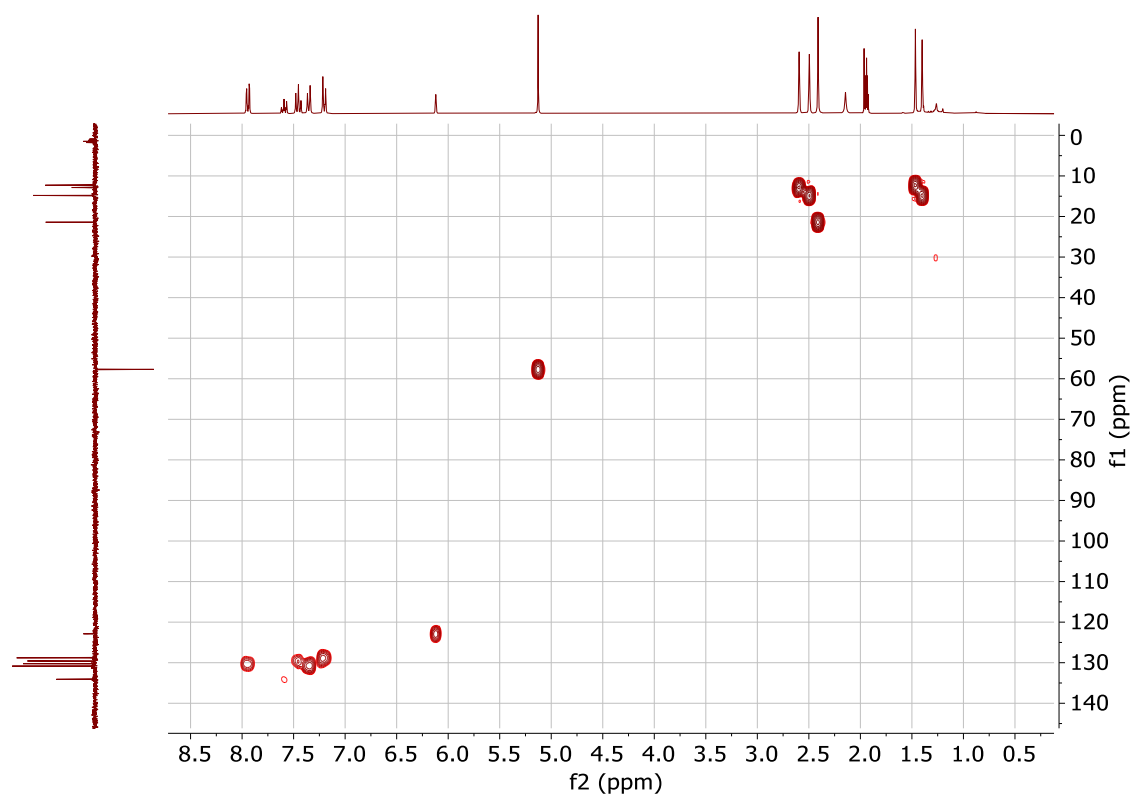
^{13}C NMR (CD_3CN , 75 MHz) of 5d



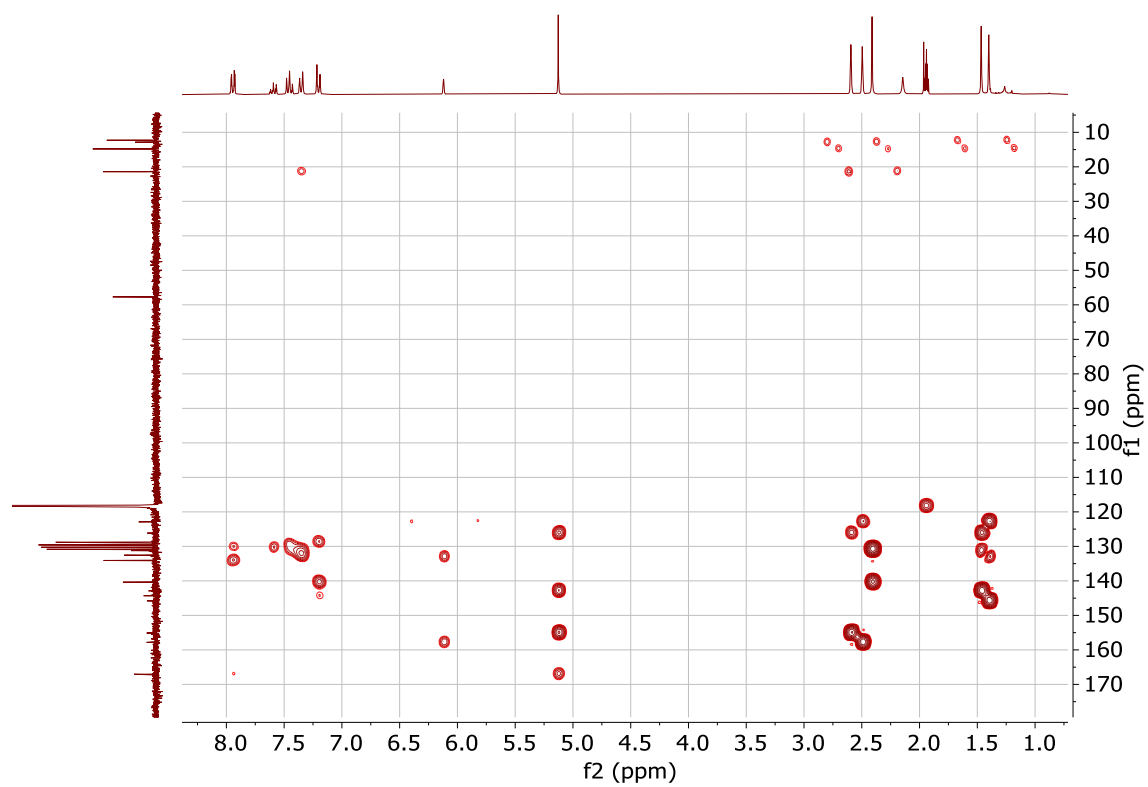
Expansion of the ^{13}C NMR spectrum of 5d (aromatic region)



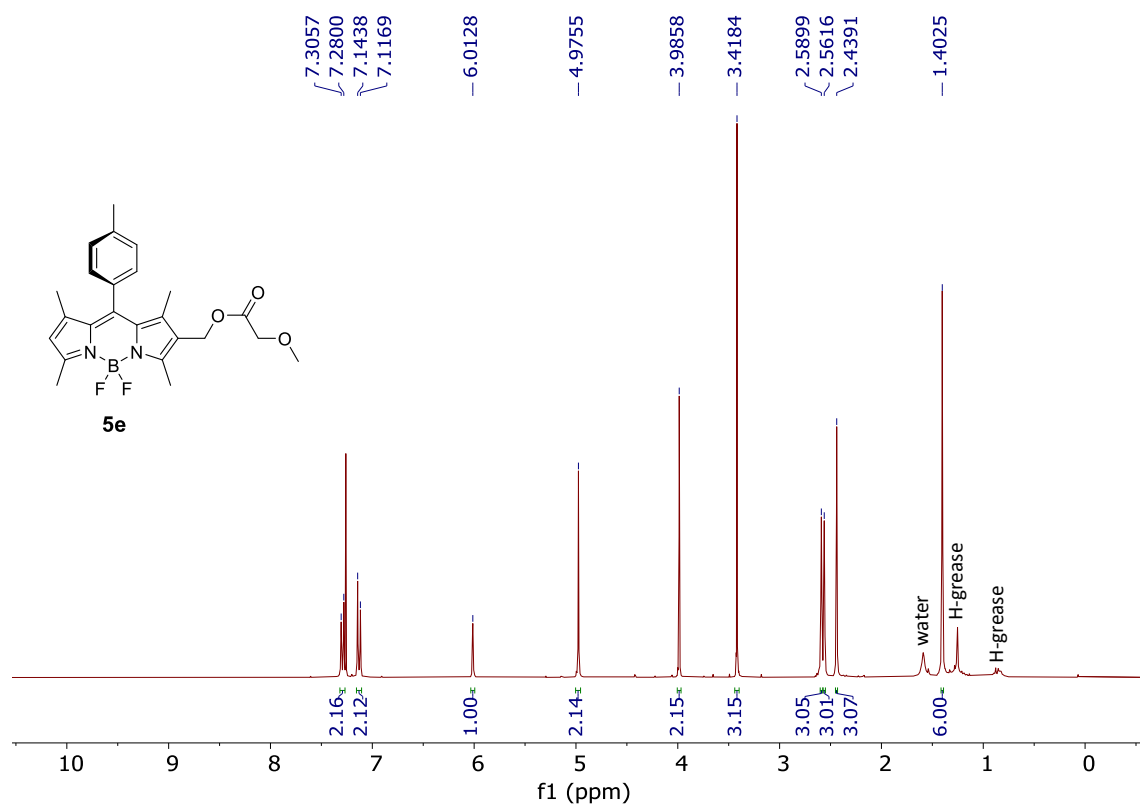
HMQC spectrum of 5d



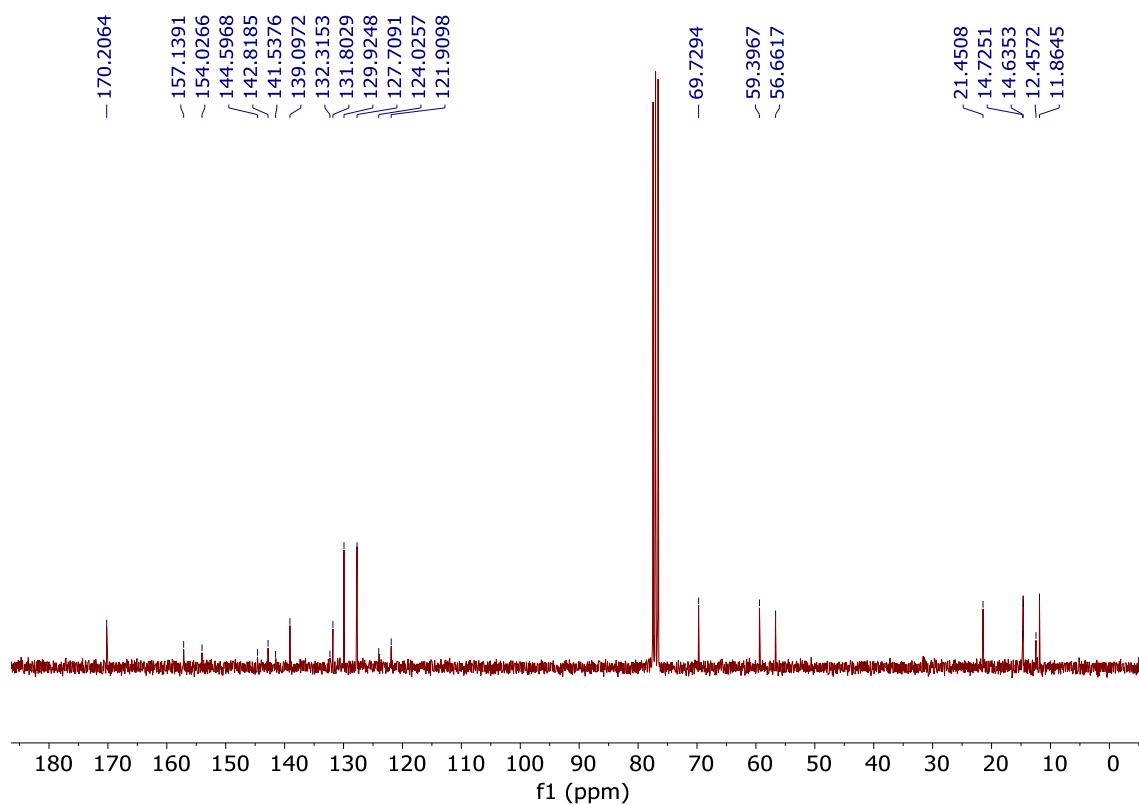
HMBC spectrum of 5d



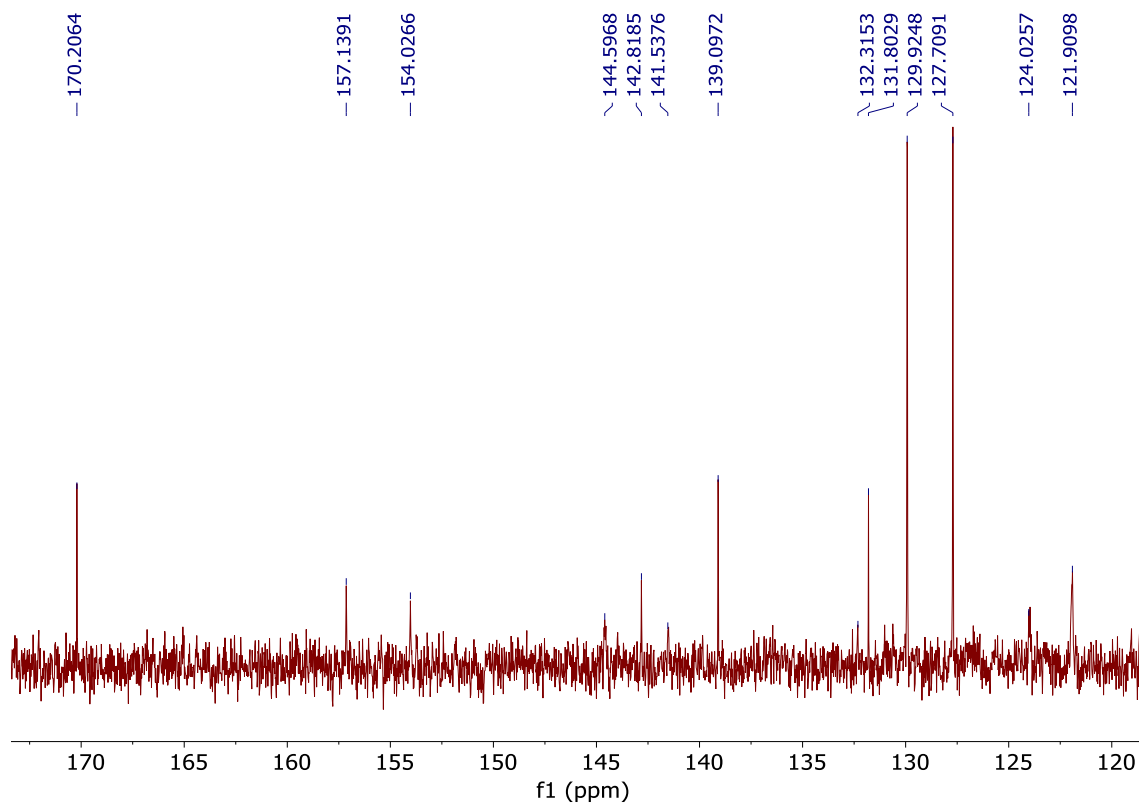
¹H NMR (CDCl₃, 300 MHz) of 5e



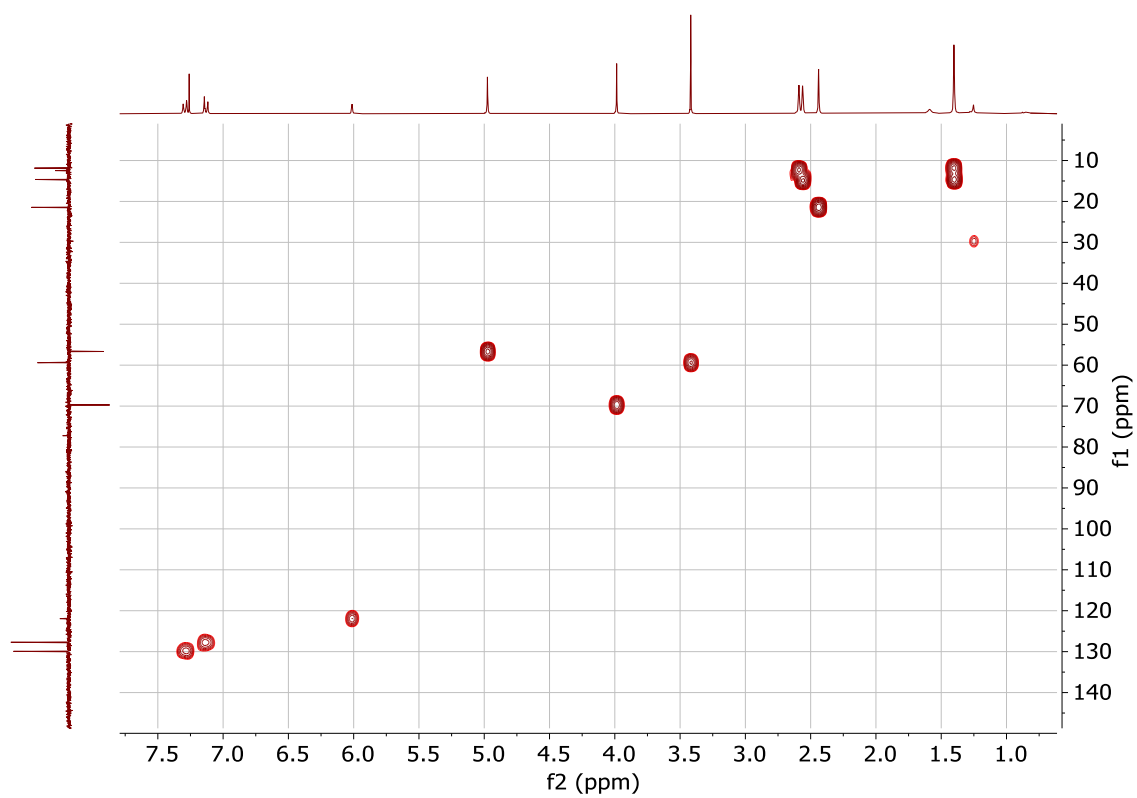
^{13}C NMR (CDCl₃, 75 MHz) of 5e



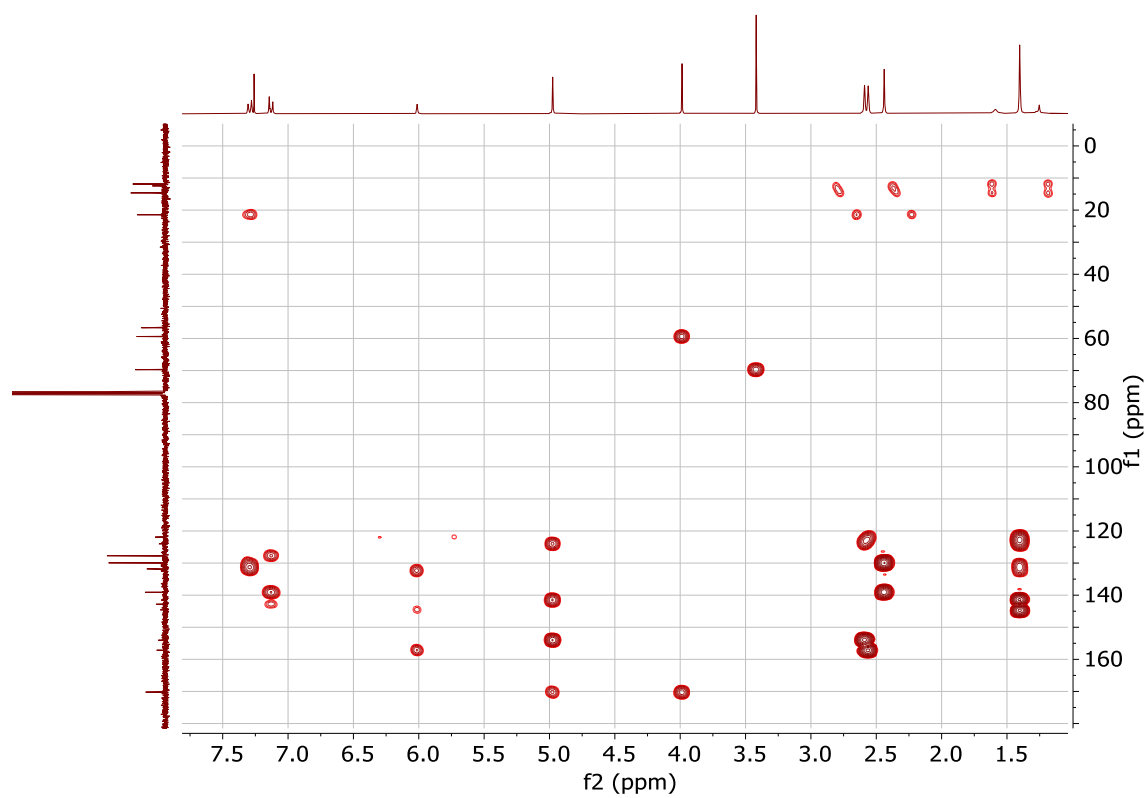
Expansion of the ^{13}C NMR spectrum of 5e (aromatic region)



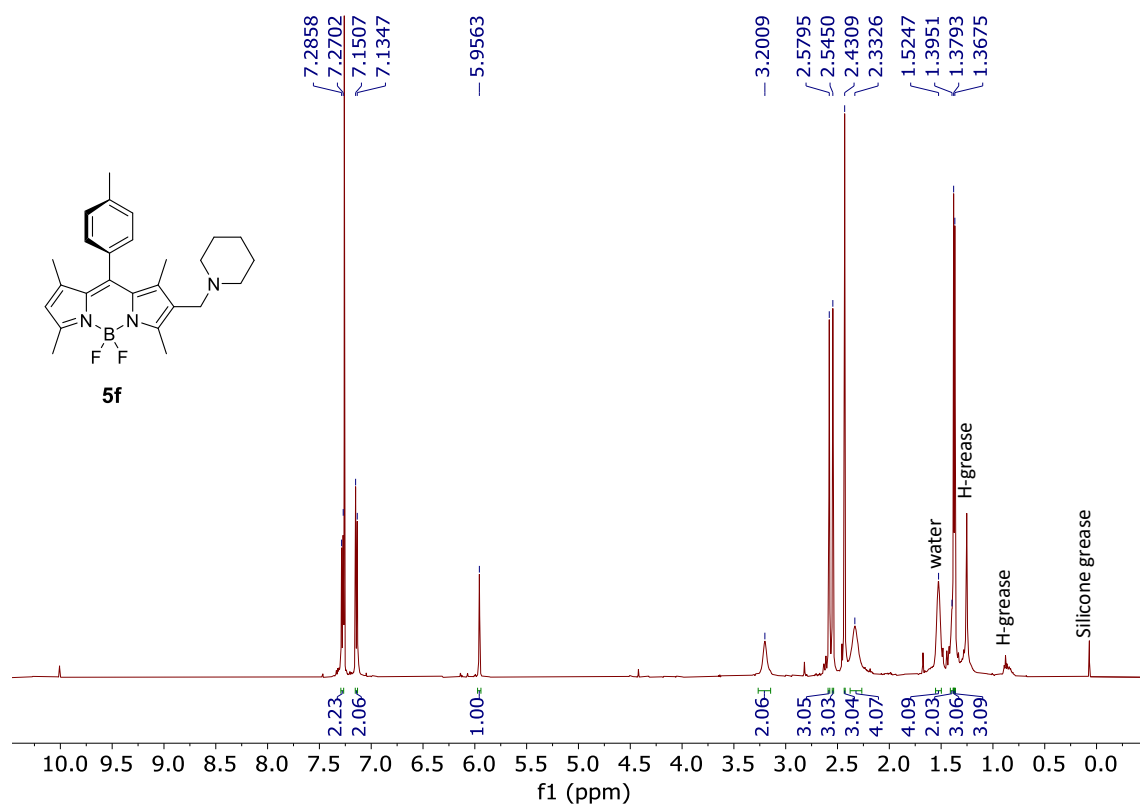
HMQC spectrum of 5e



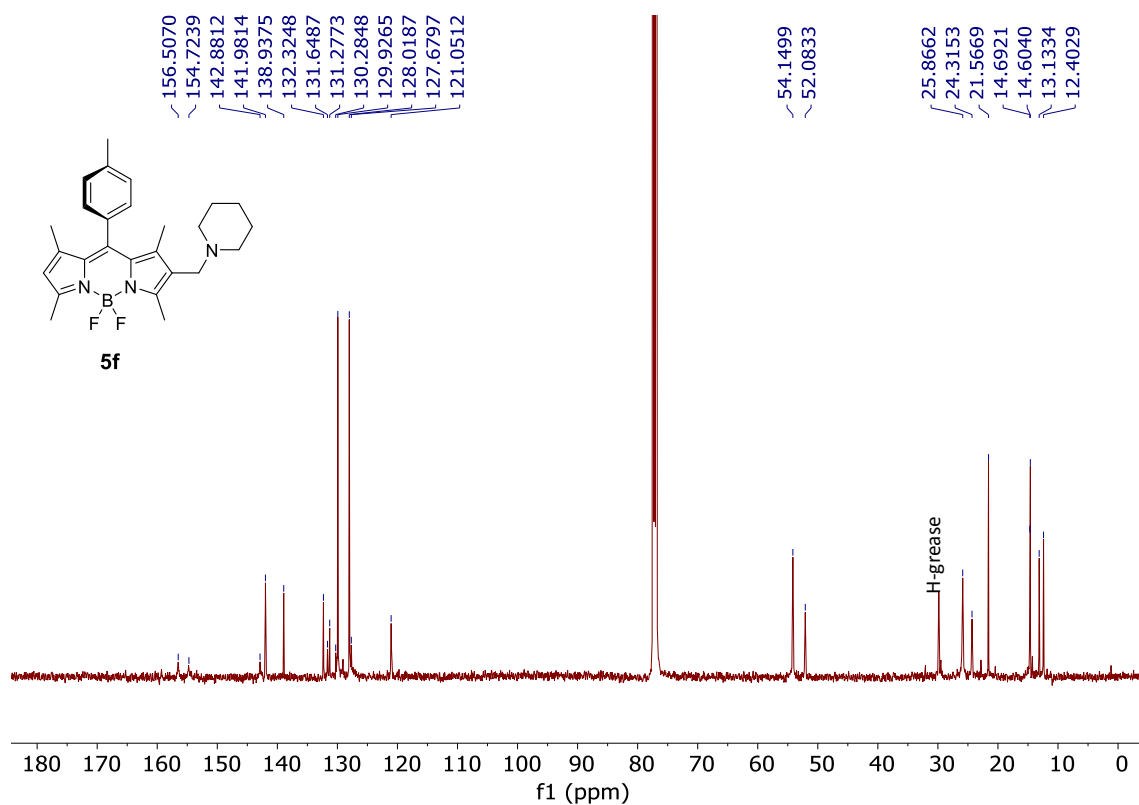
HMBC spectrum of 5e



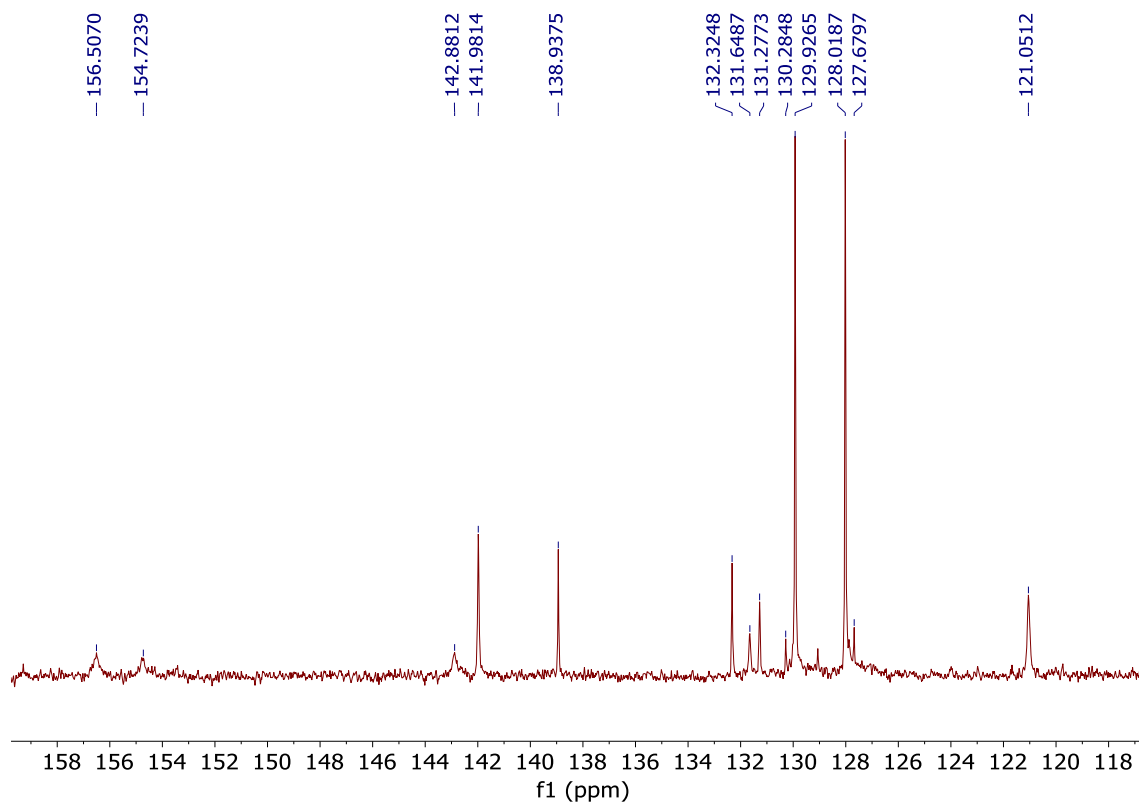
¹H NMR (CDCl₃, 500 MHz) of **5f**



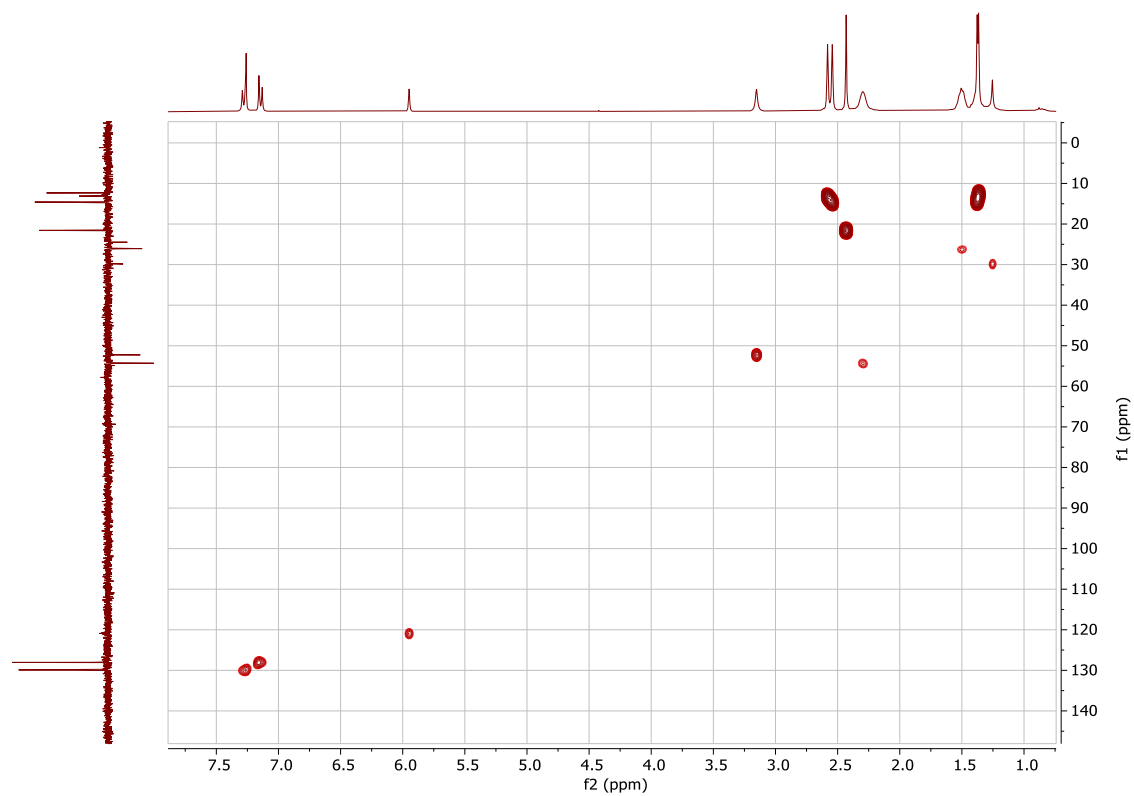
^{13}C NMR (CDCl_3 , 126 MHz) of 5f



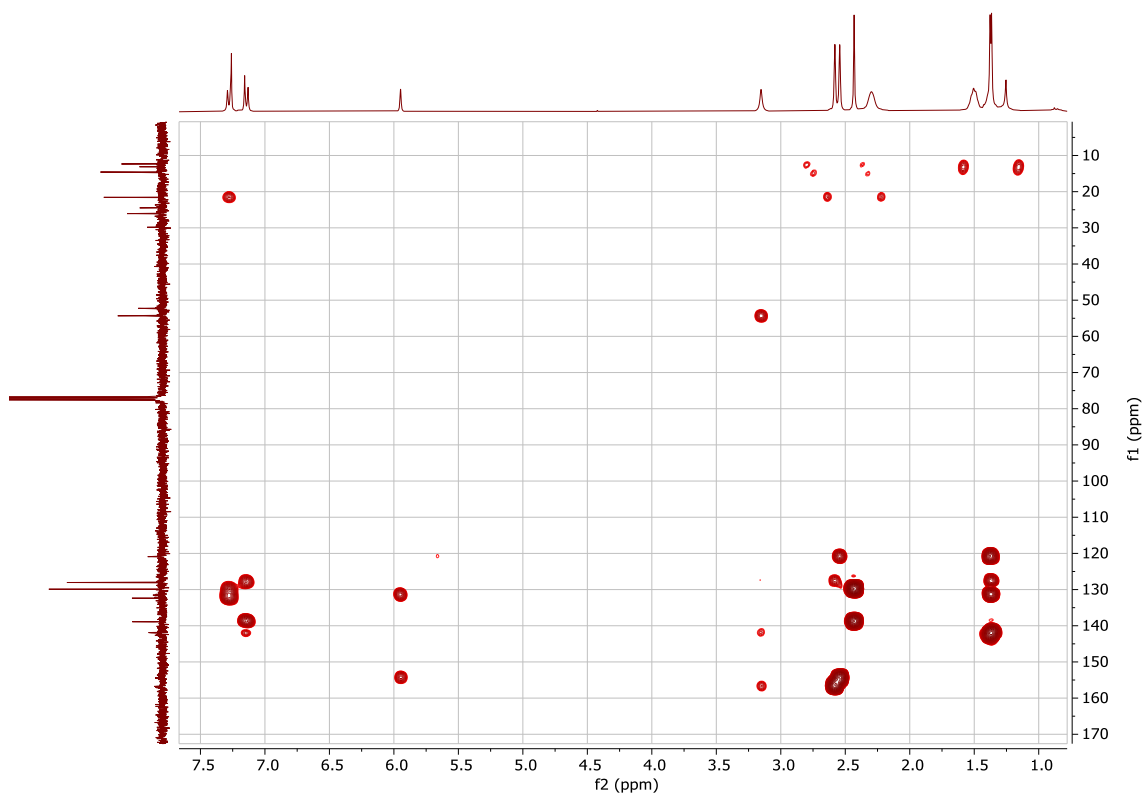
Expansion of the ^{13}C NMR spectrum of 5f (aromatic region)



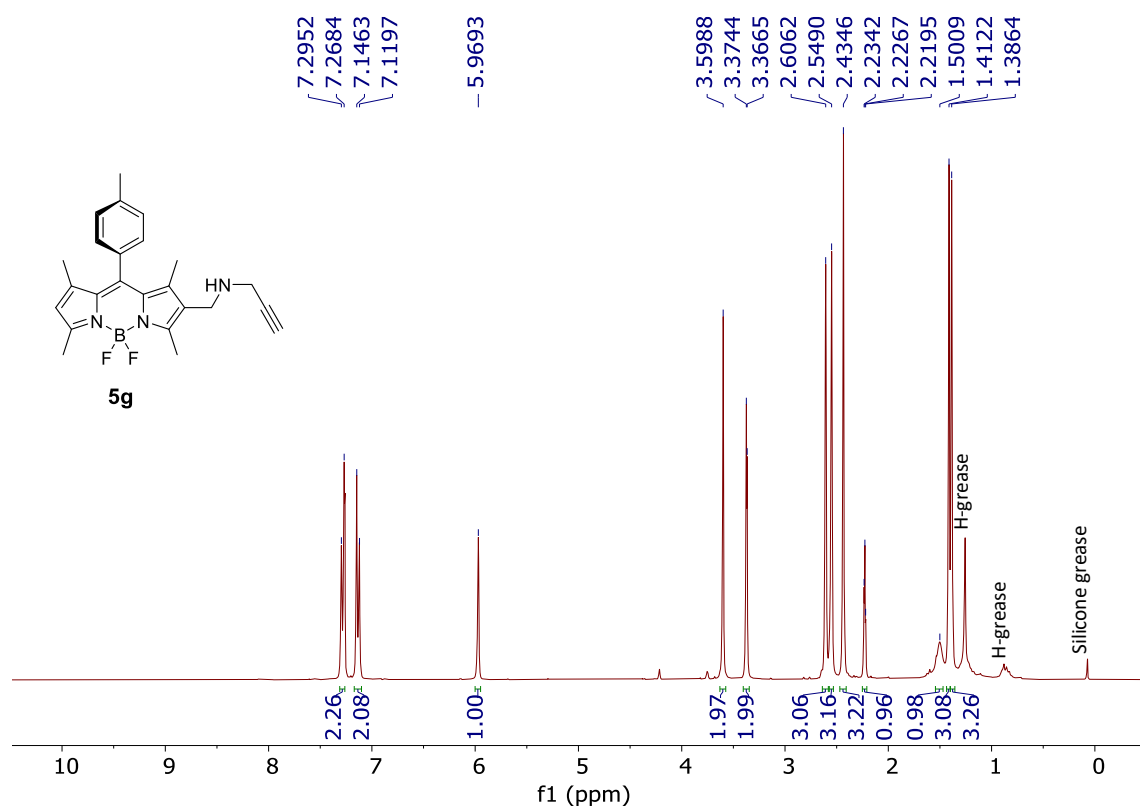
HMQC spectrum of 5f



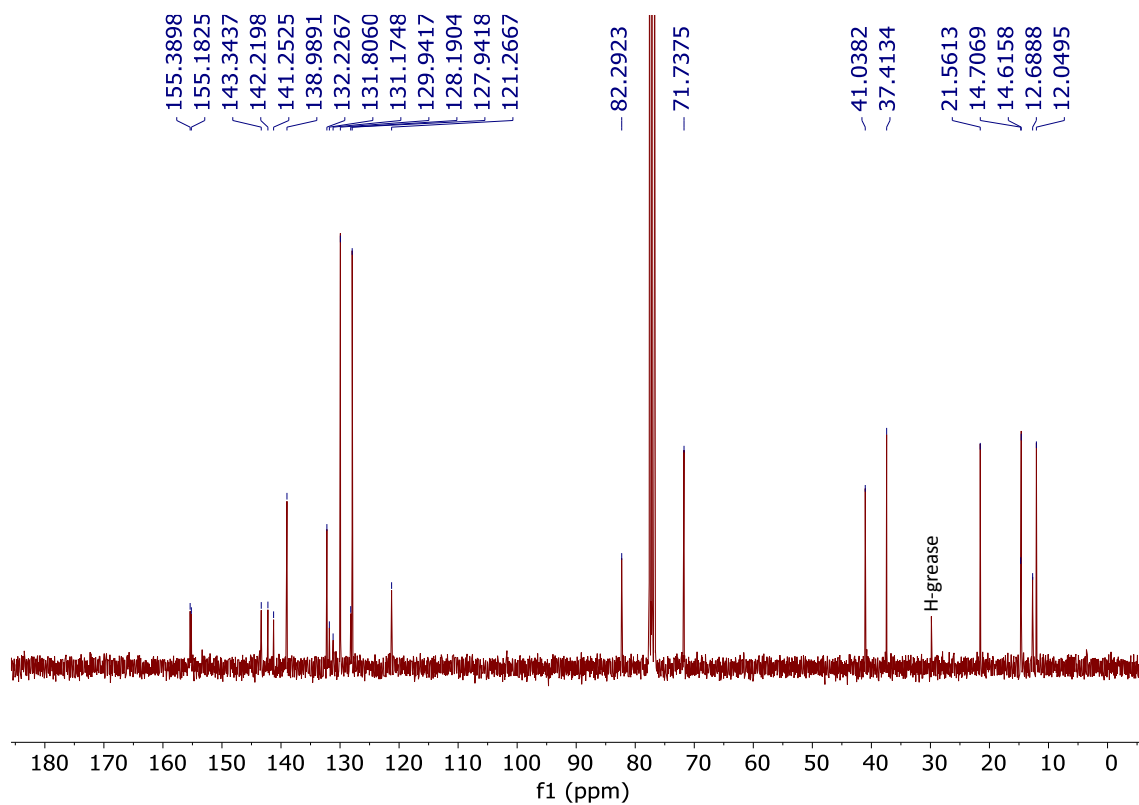
HMBC spectrum of 5f



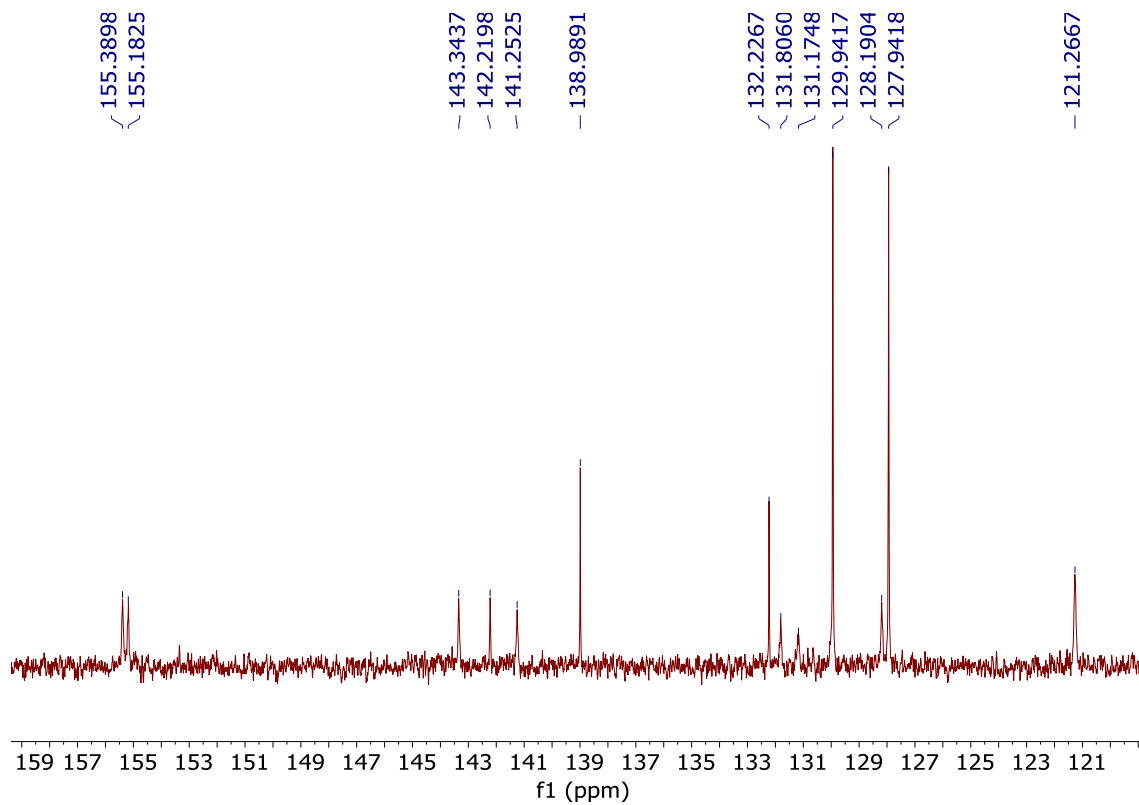
¹H NMR (CDCl₃, 300 MHz) of 5g



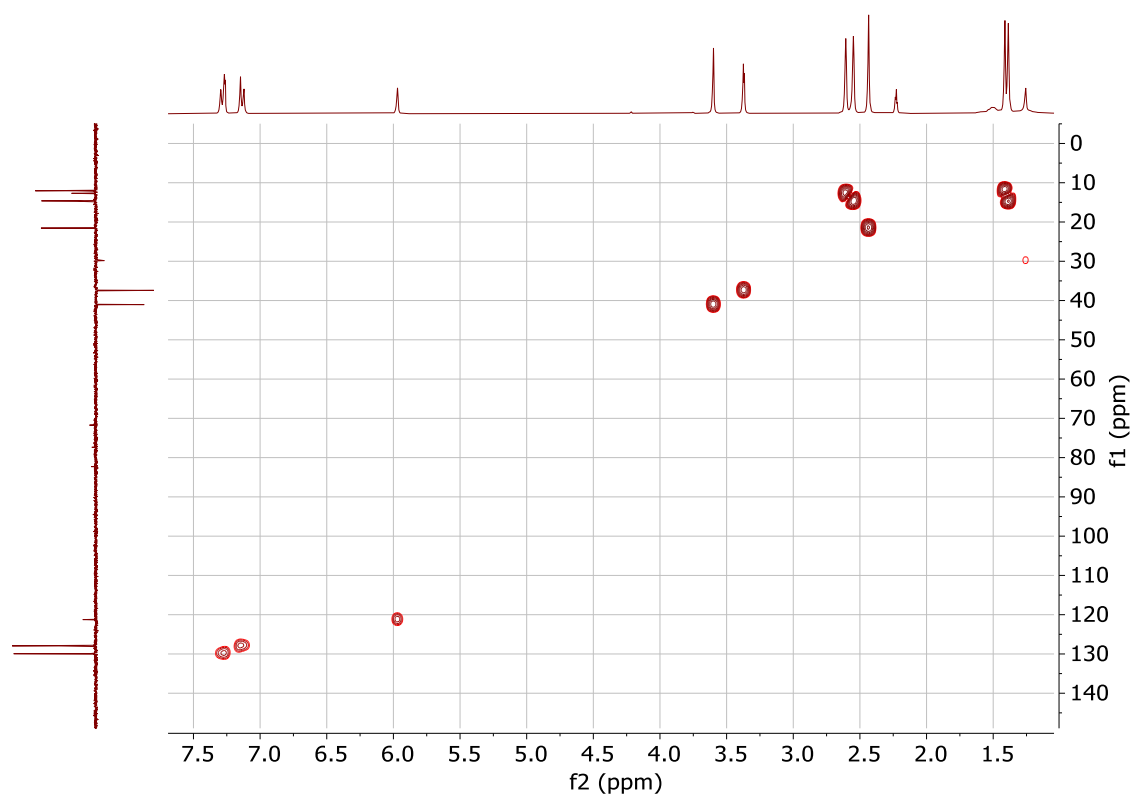
^{13}C NMR (CDCl_3 , 75 MHz) of 5g



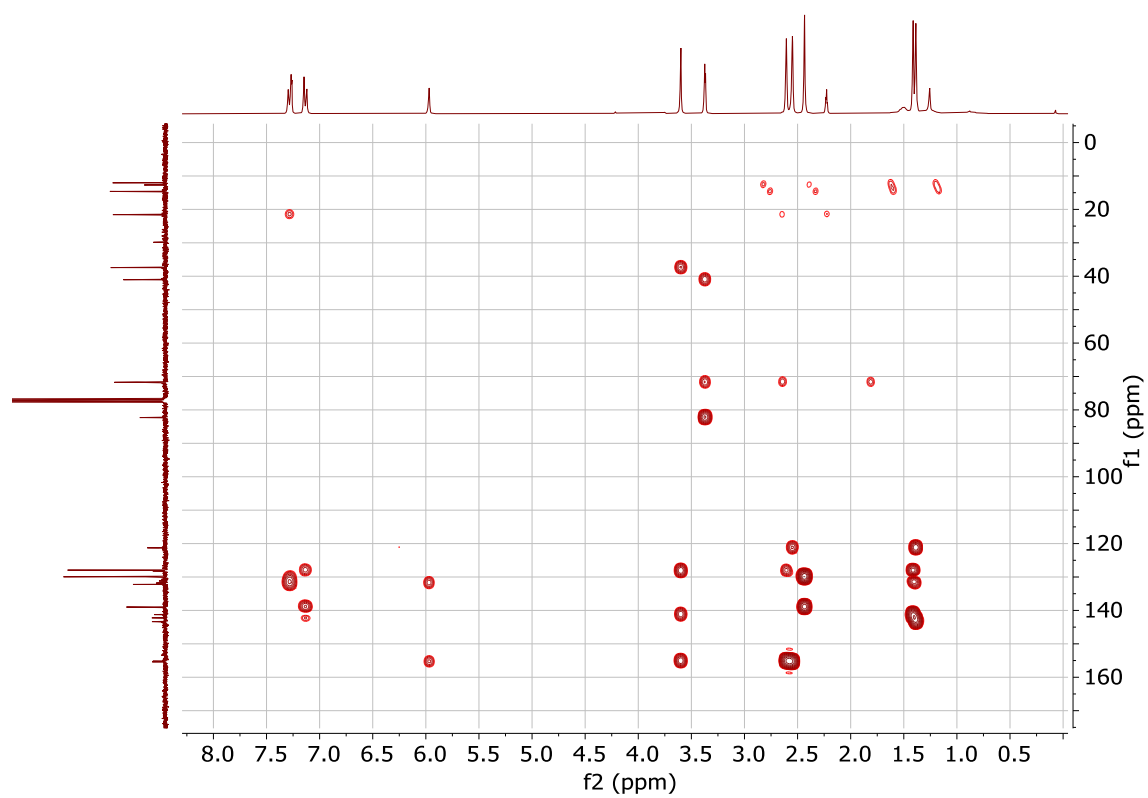
Expansion of the ^{13}C NMR spectrum of 5g (aromatic region)



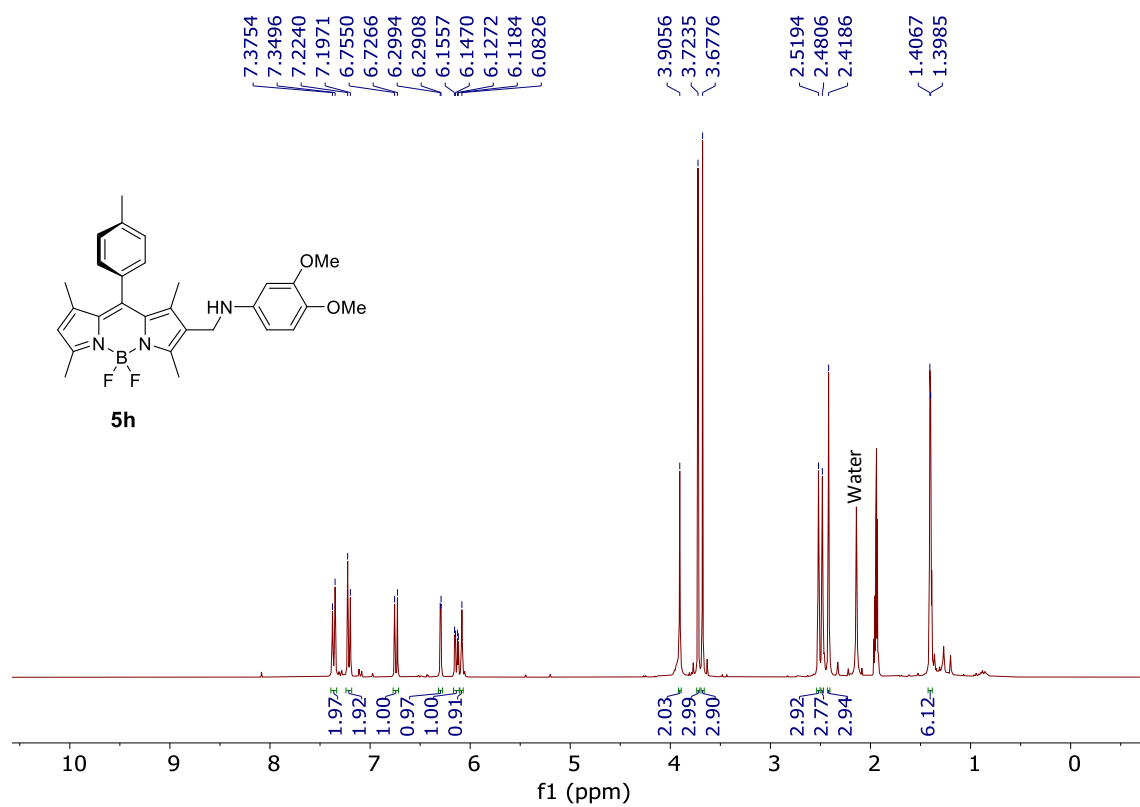
HMQC spectrum of 5g



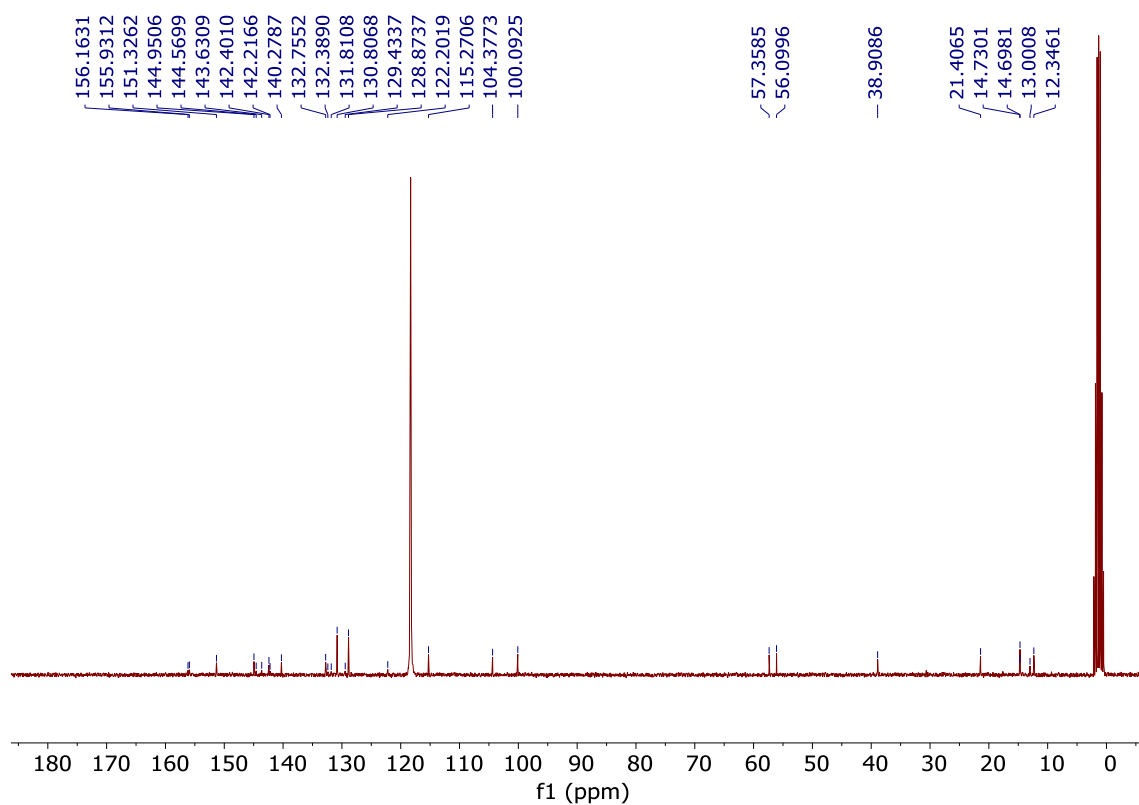
HMBC spectrum of 5g



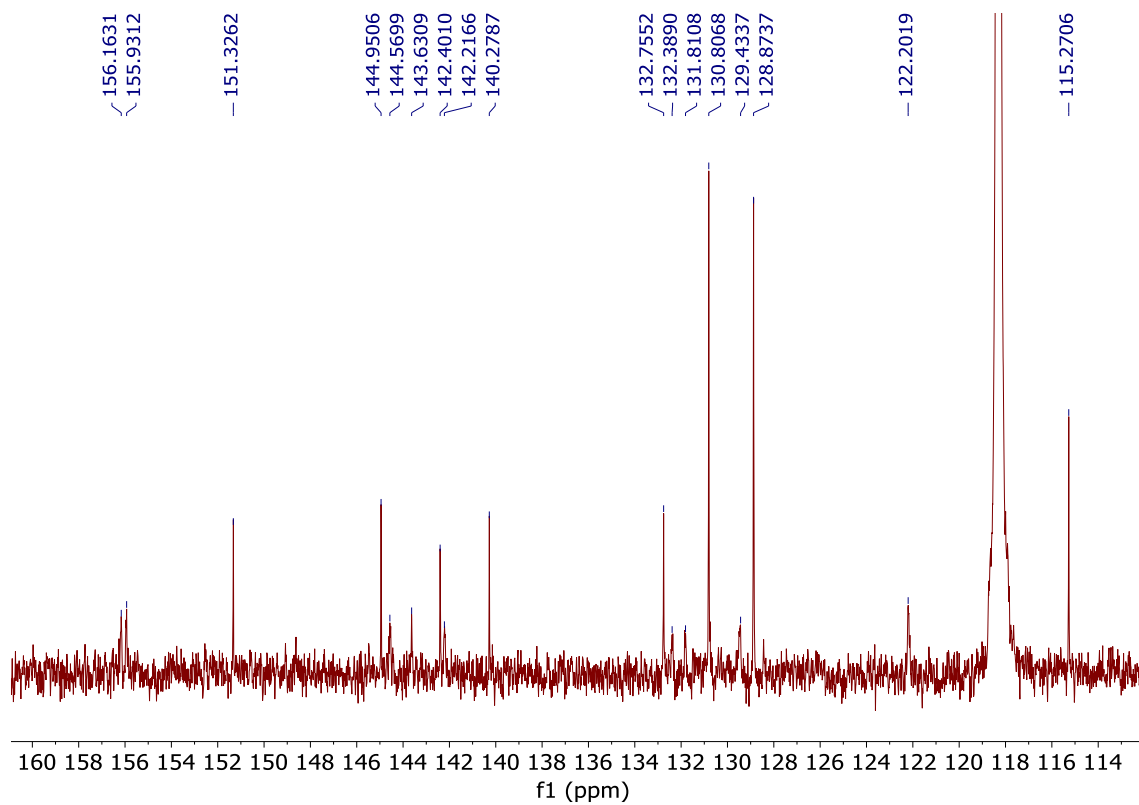
^1H NMR (CD_3CN , 300 MHz) of **5h**



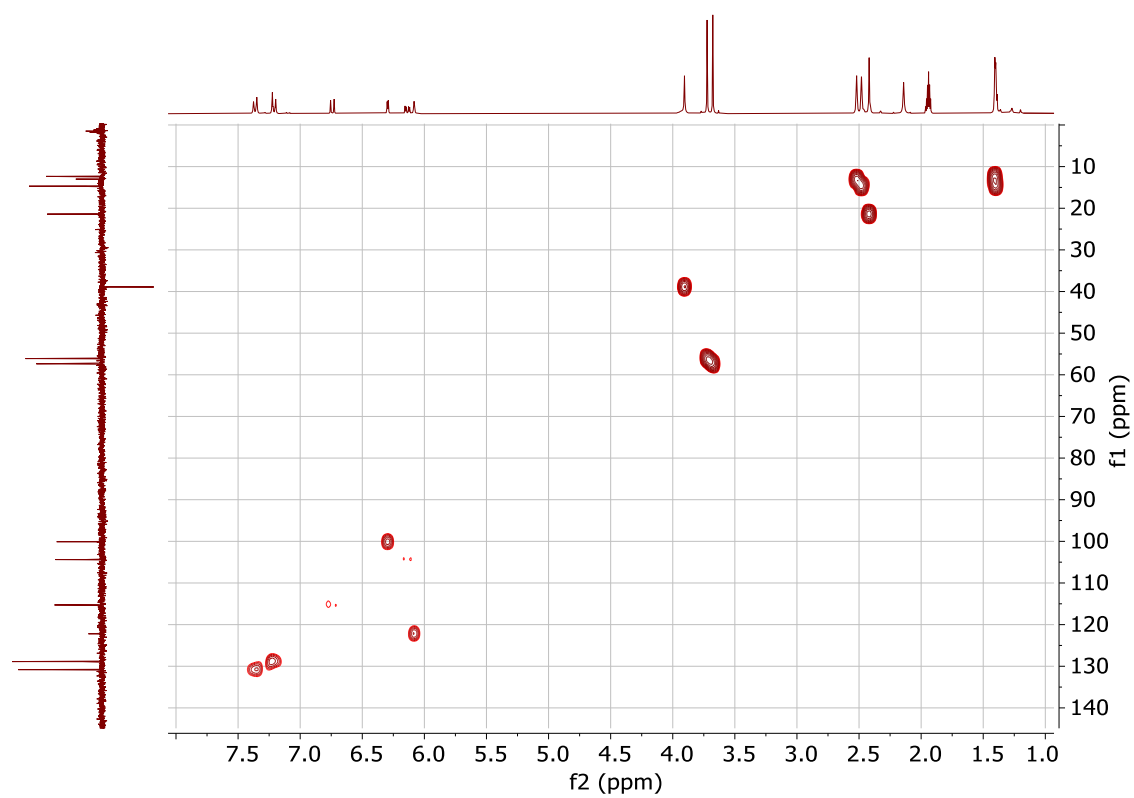
^{13}C NMR (CD_3CN , 75 MHz) of 5h



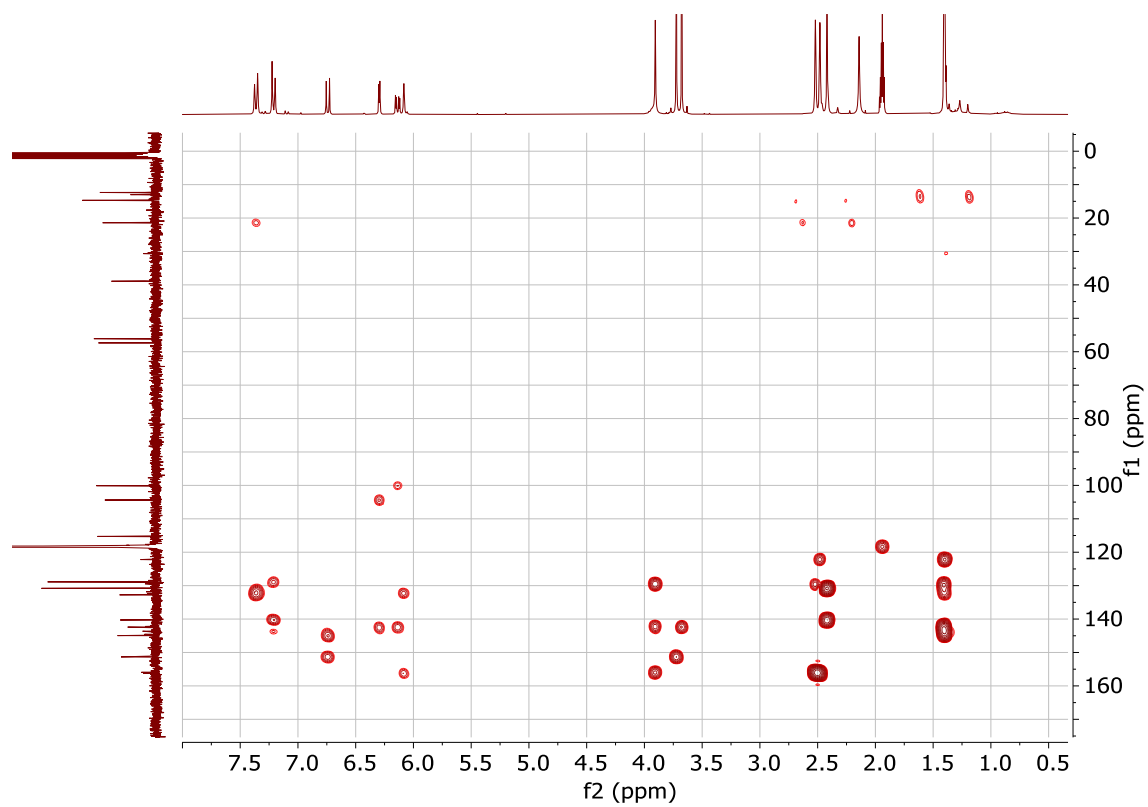
Expansion of the ^{13}C NMR spectrum of 5h (aromatic region)



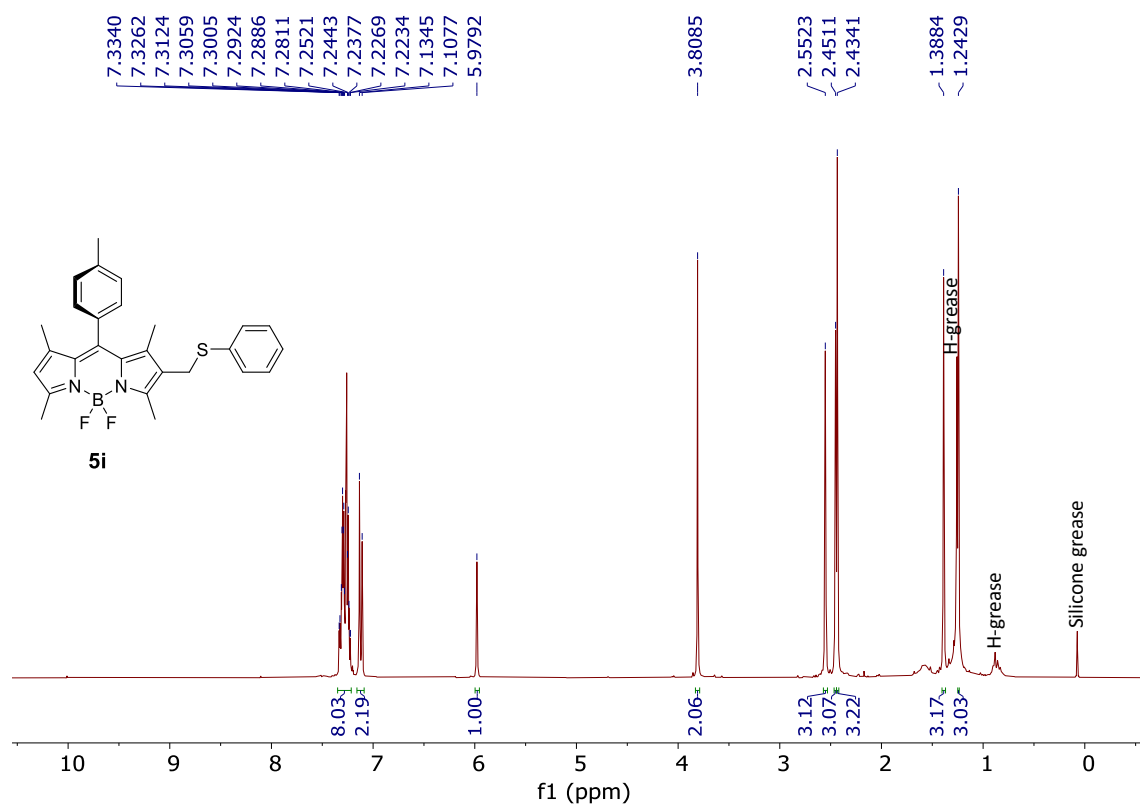
HMQC spectrum of 5h



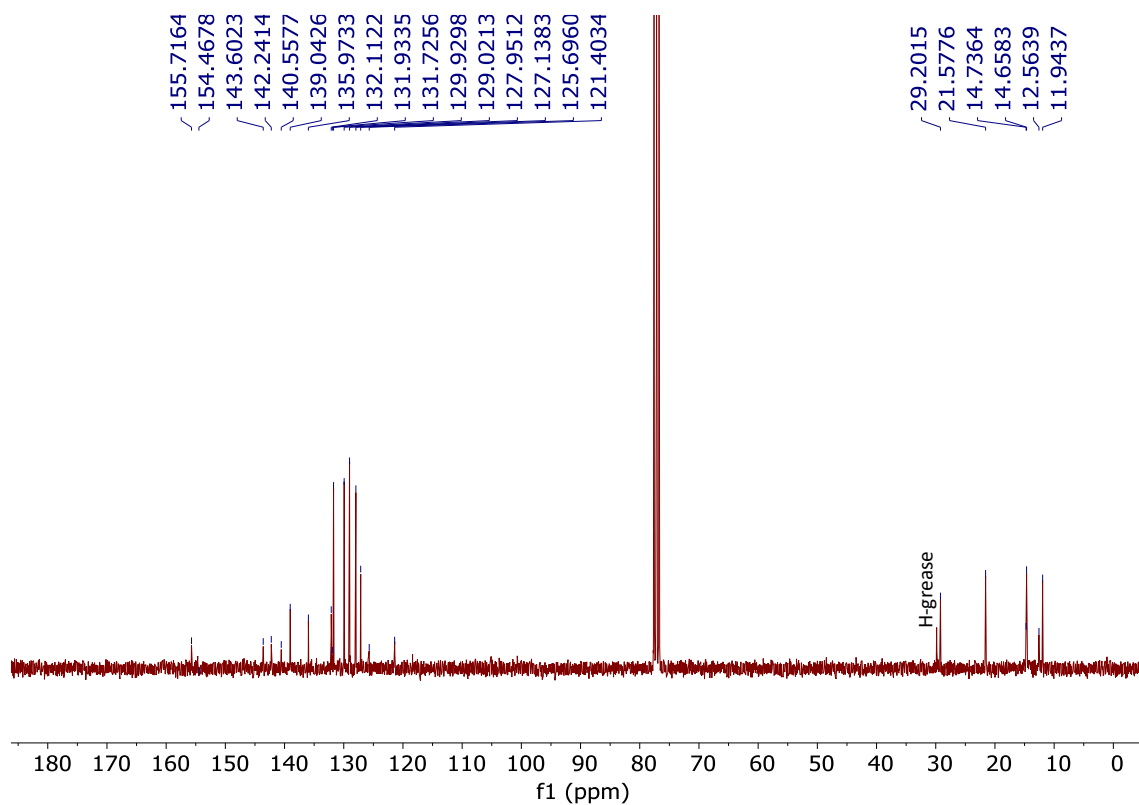
HMBC spectrum of 5h



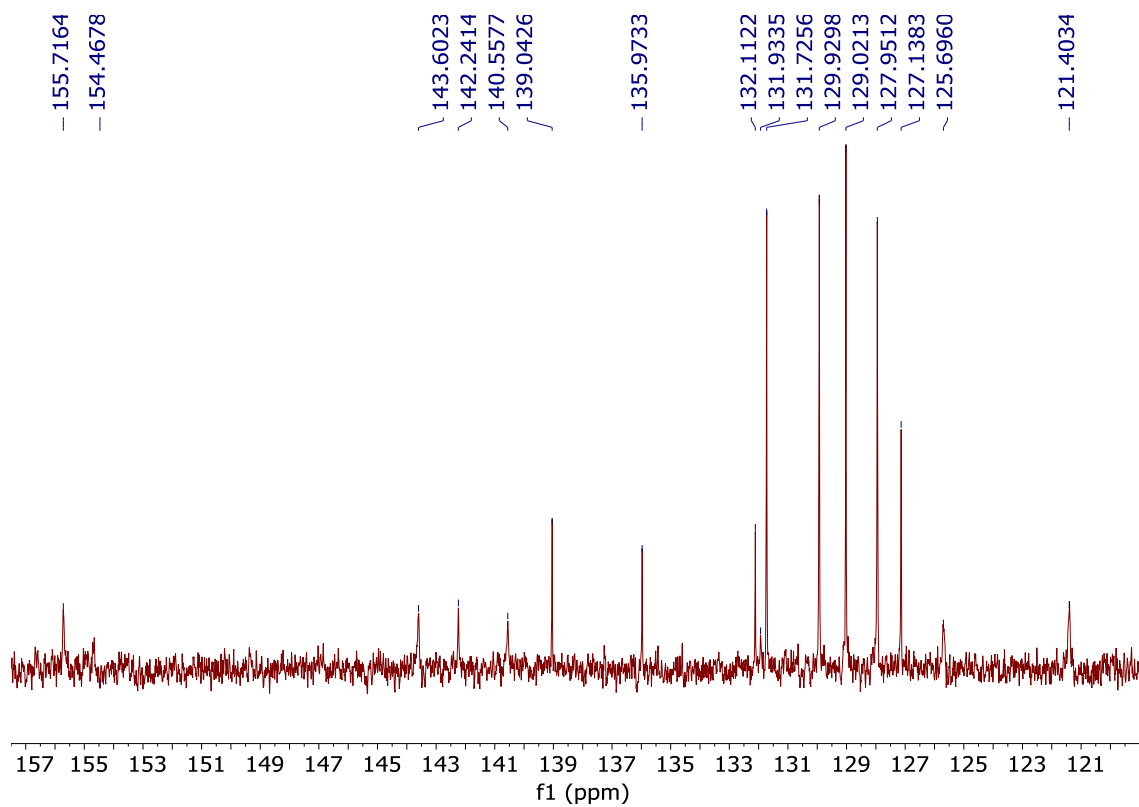
¹H NMR (CDCl₃, 300 MHz) of 5i



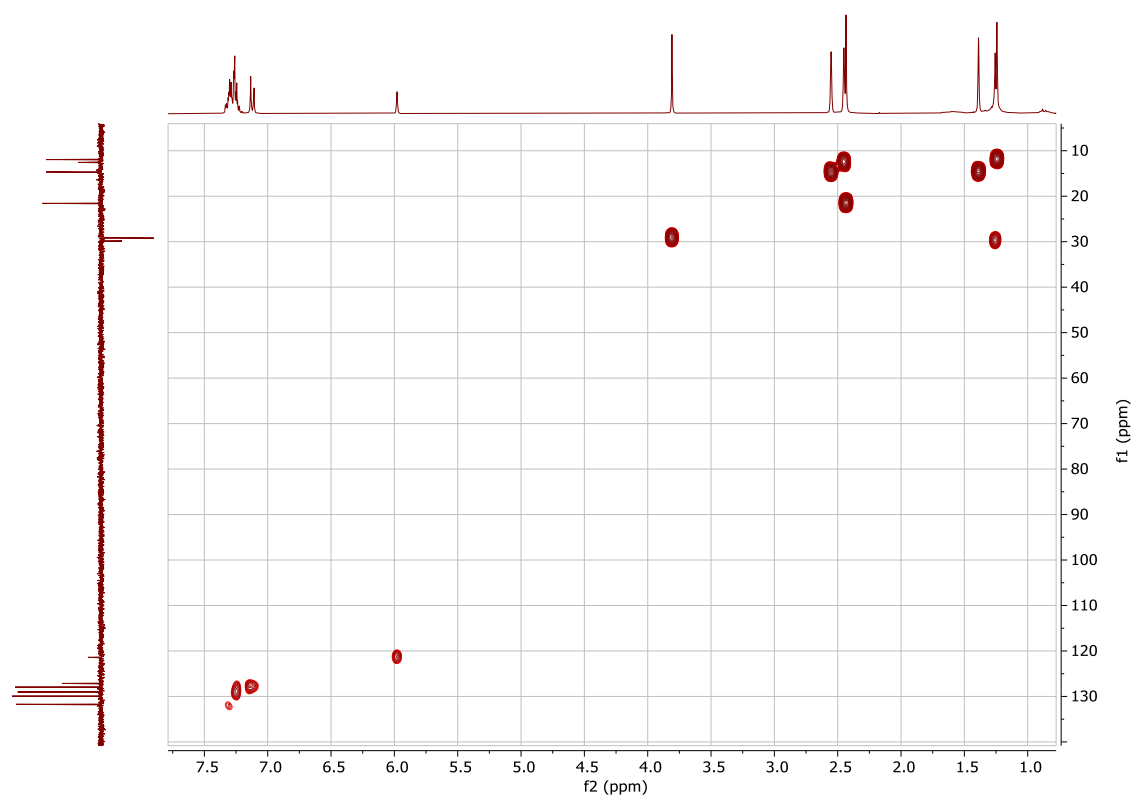
^{13}C NMR (CDCl₃, 75 MHz) of 5i



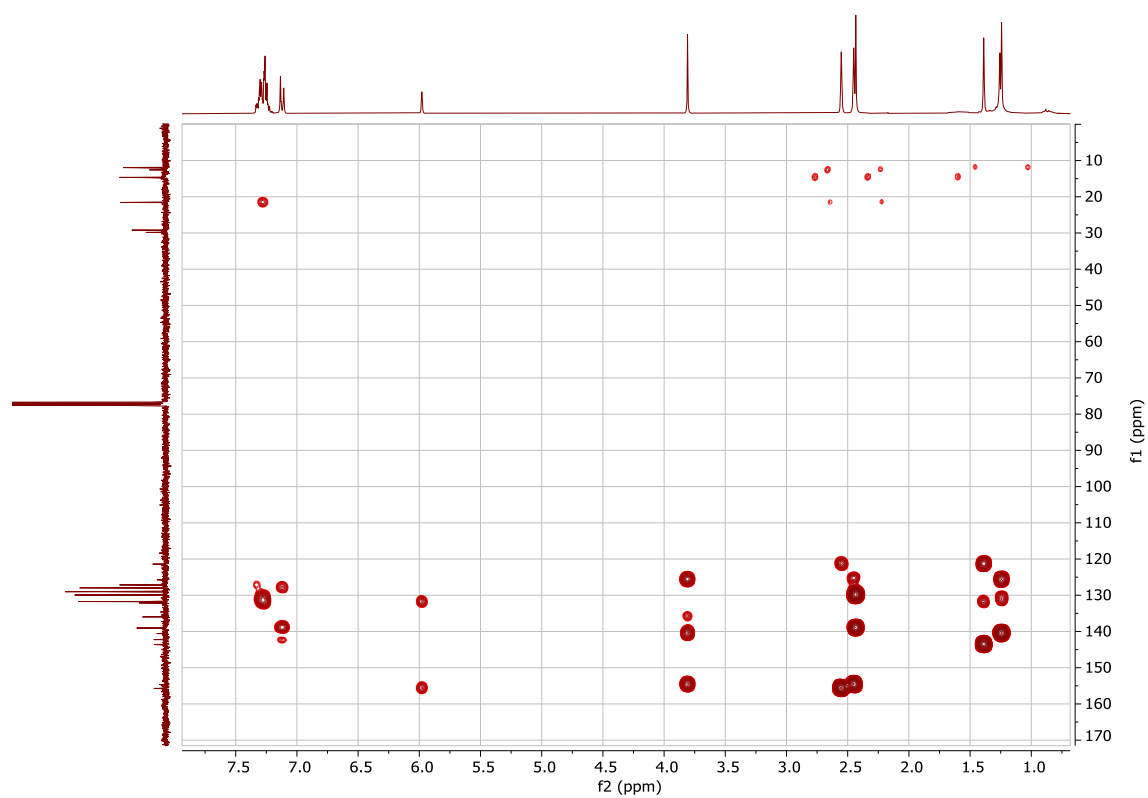
Expansion of the ^{13}C NMR spectrum of 5i (aromatic region)



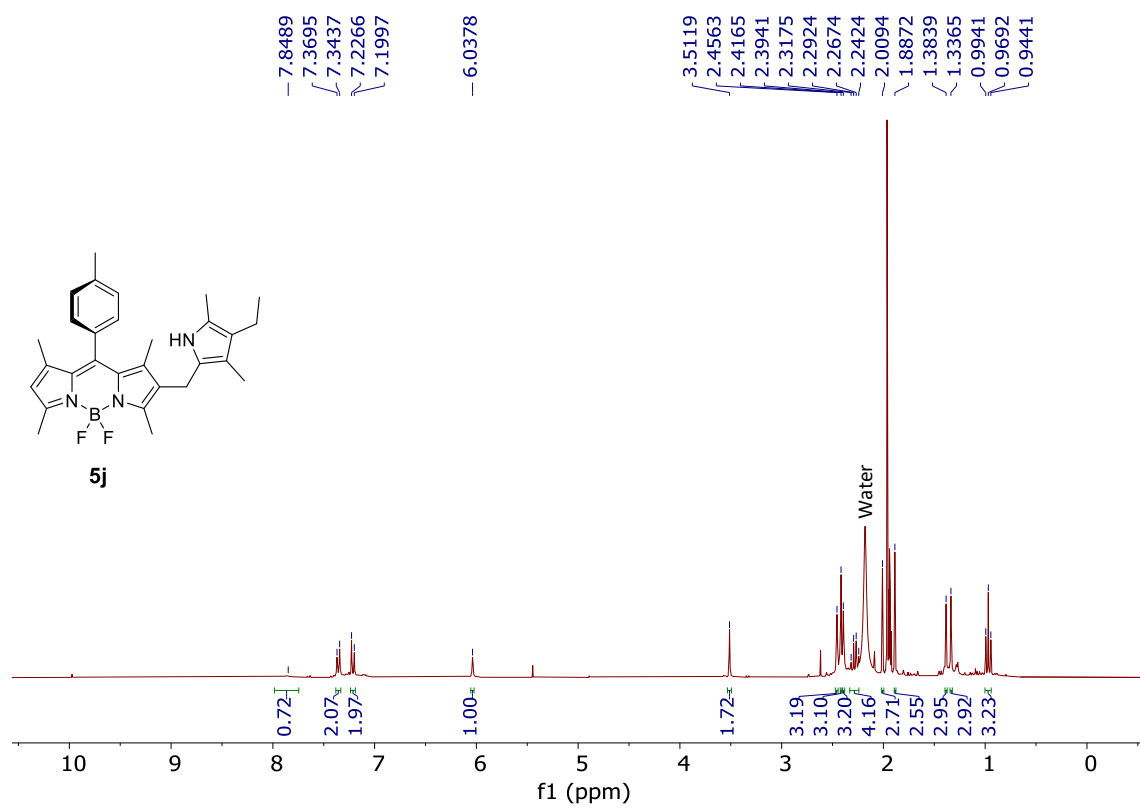
HMQC spectrum of 5i



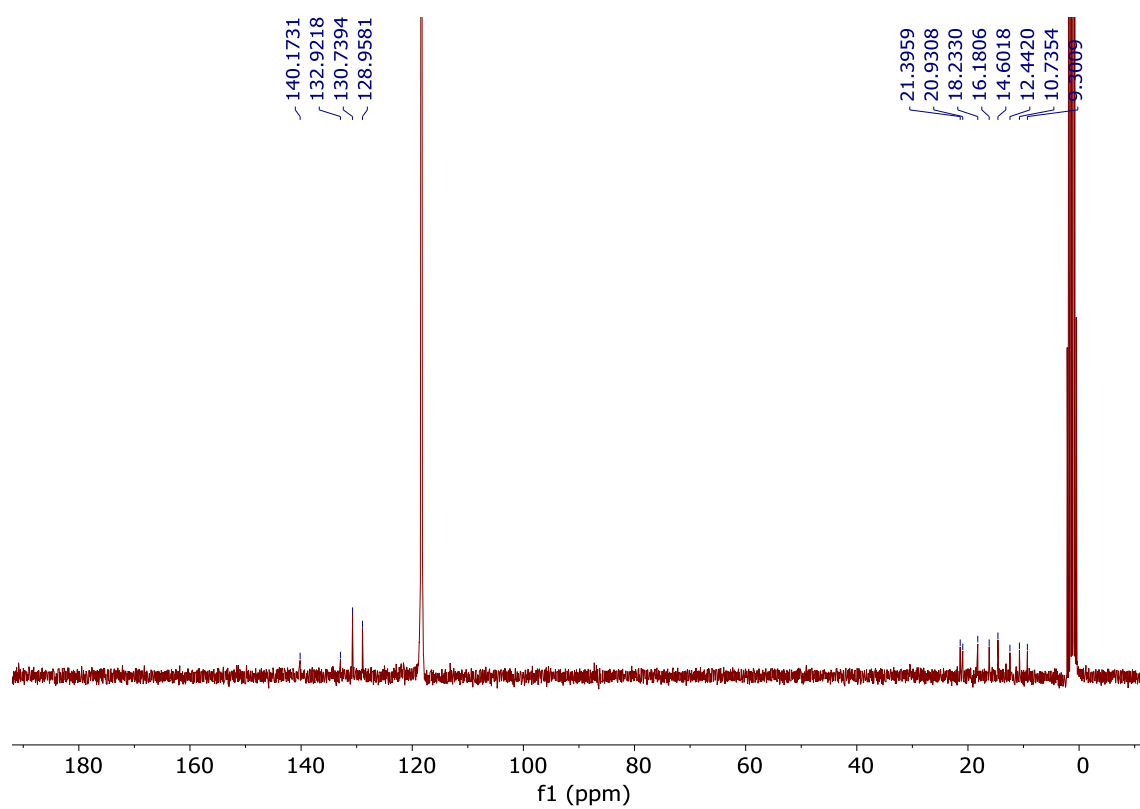
HMBC spectrum of 5i



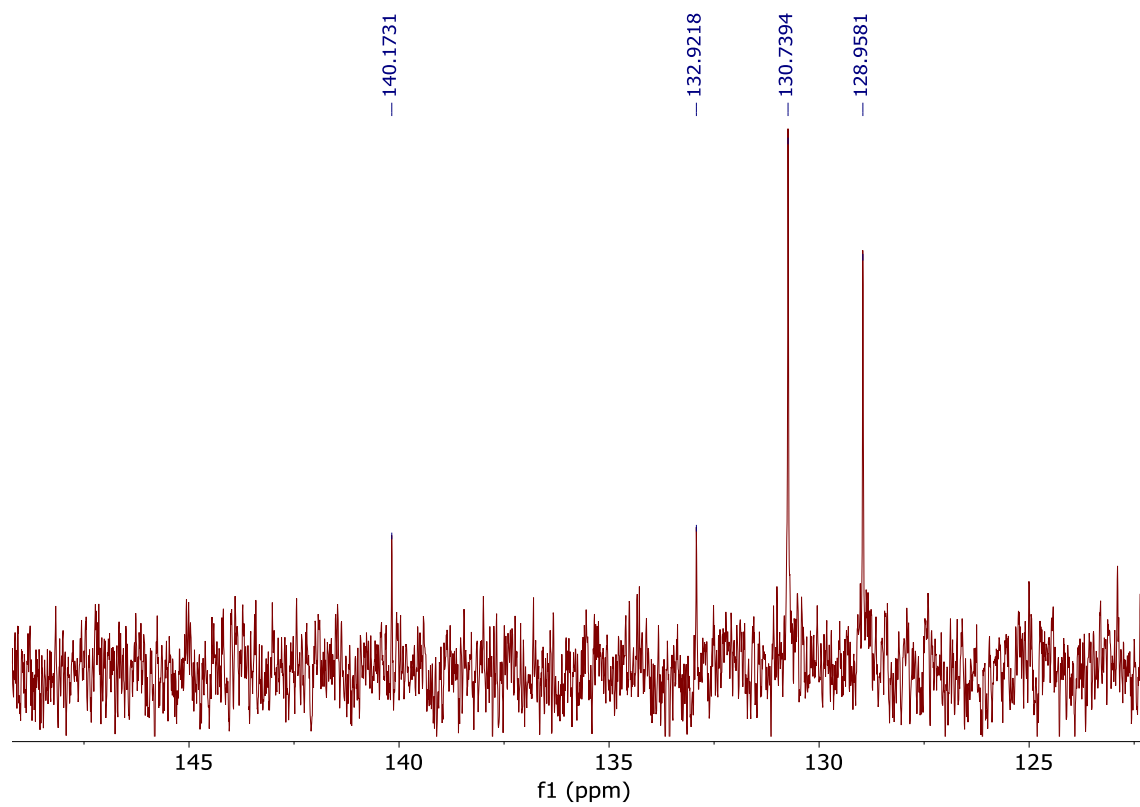
¹H NMR (CD₃CN, 300 MHz) of 5j



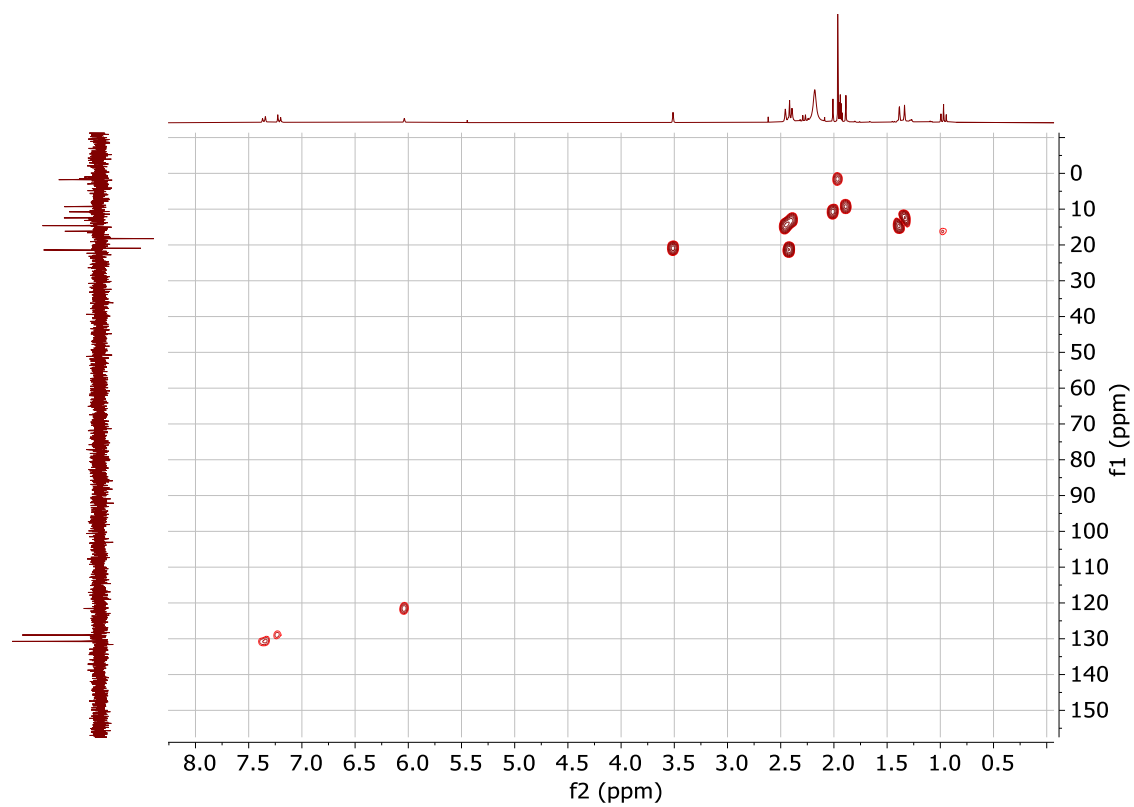
^{13}C NMR (CD_3CN , 75 MHz) of 5j



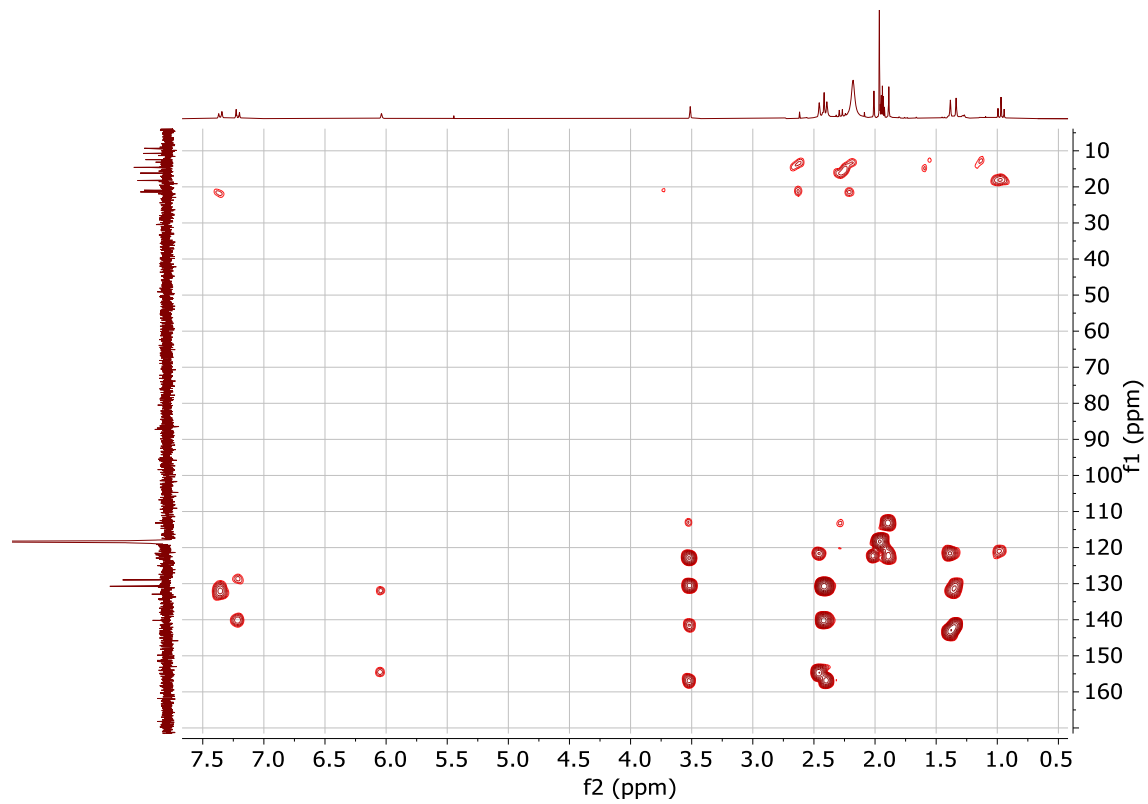
Expansion of the ^{13}C NMR spectrum of 5j (aromatic region)



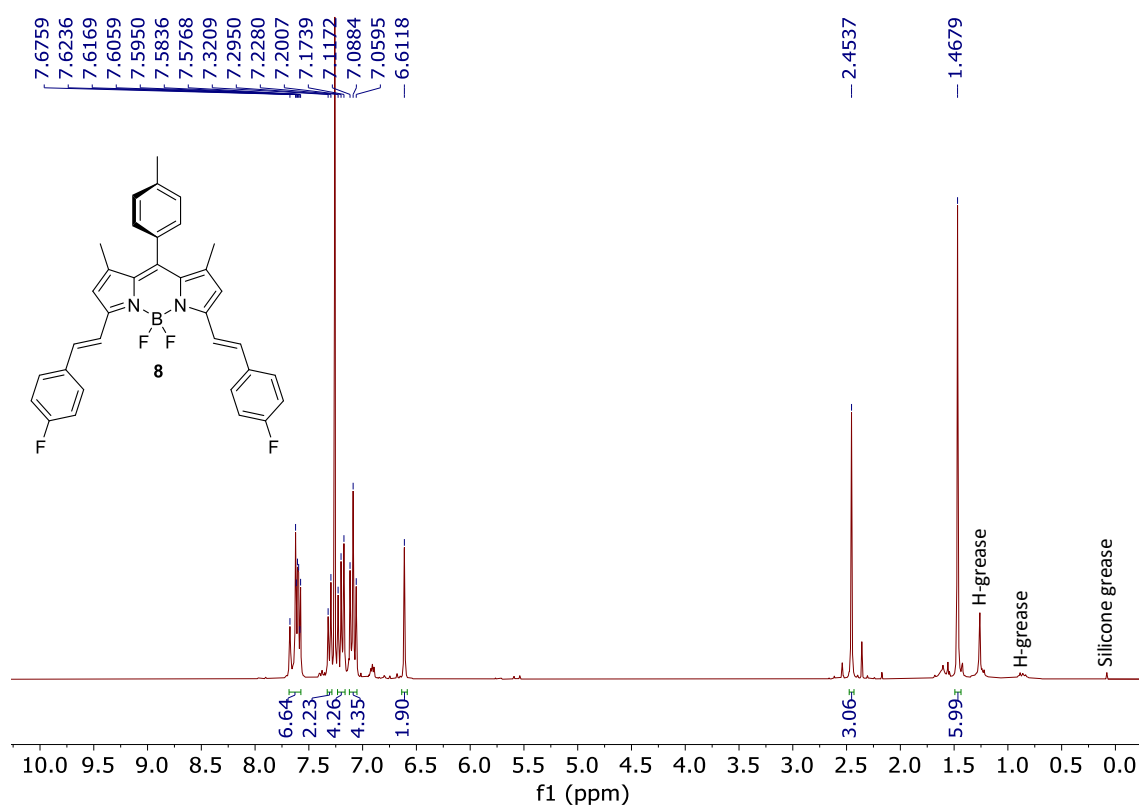
HMQC spectrum of 5j



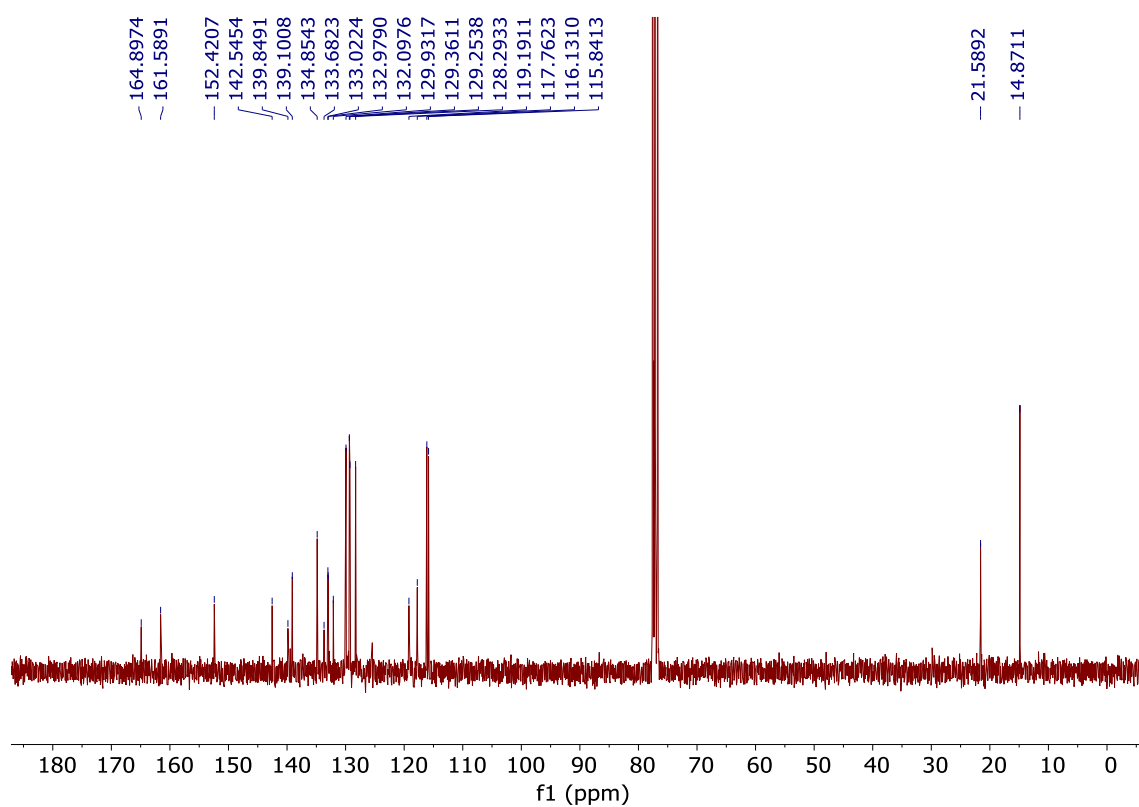
HMBC spectrum of 5j



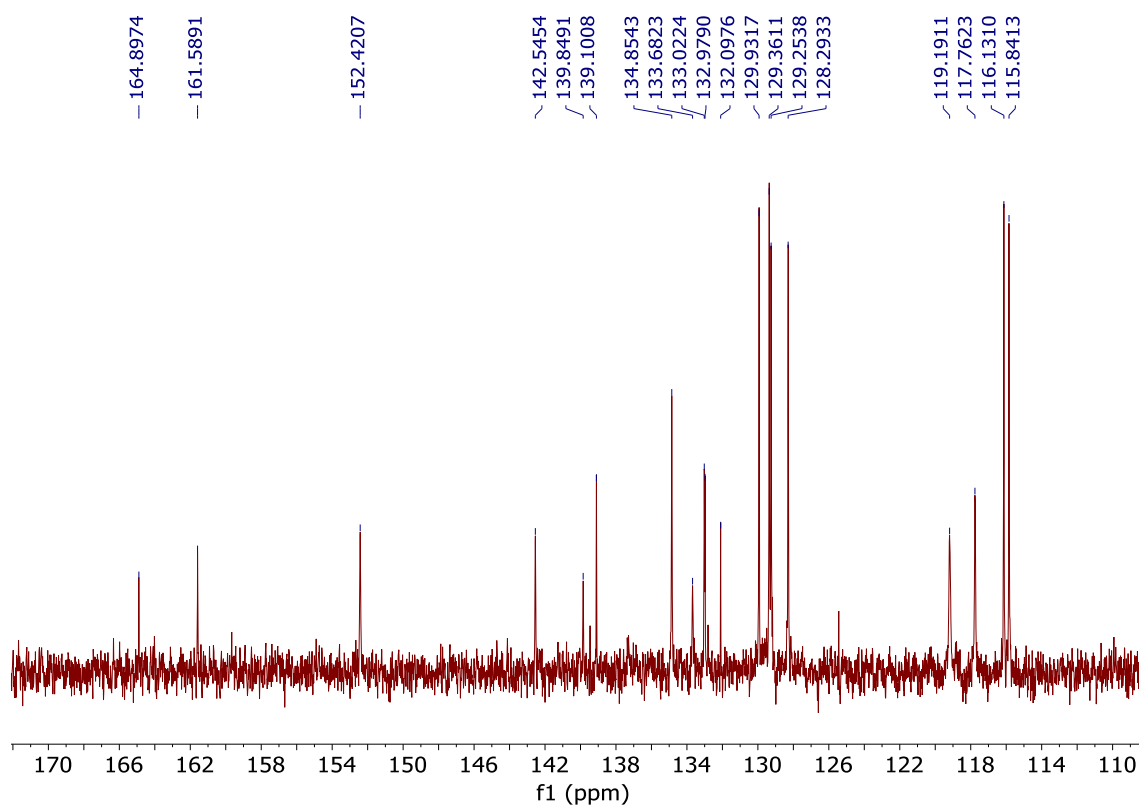
¹H NMR (CDCl₃, 300 MHz) of 8



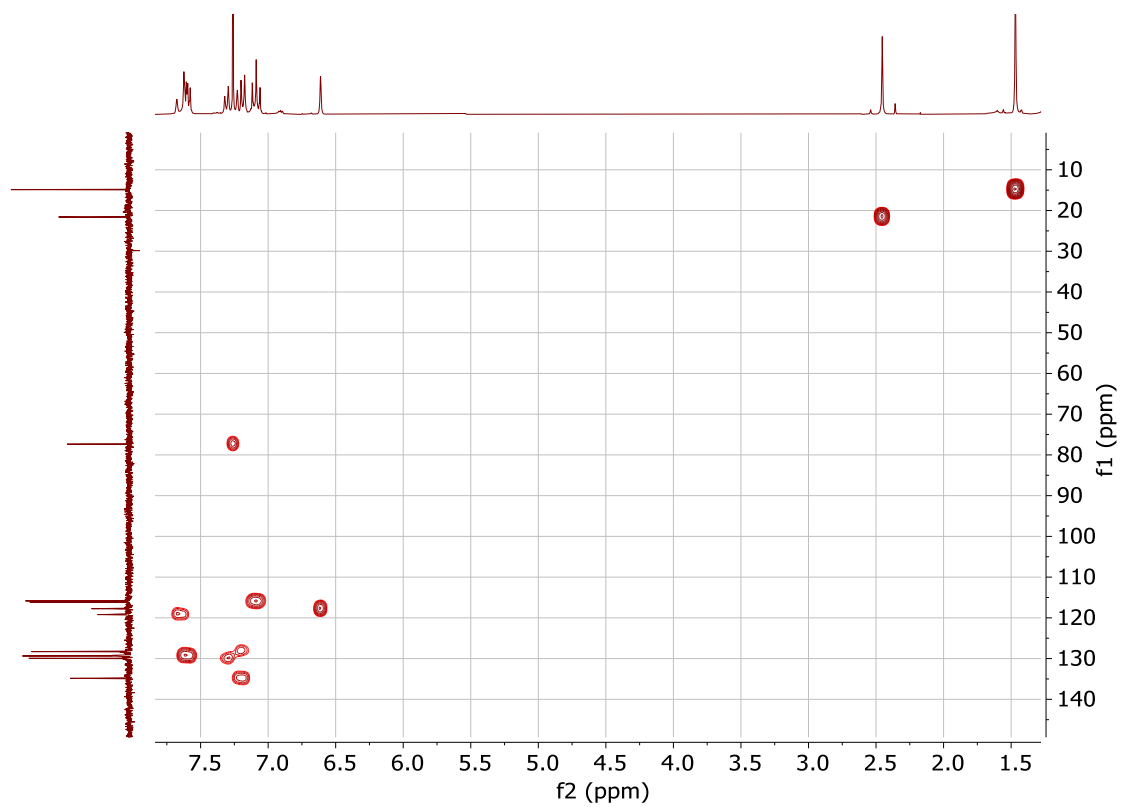
^{13}C NMR (CDCl_3 , 75 MHz) of 8



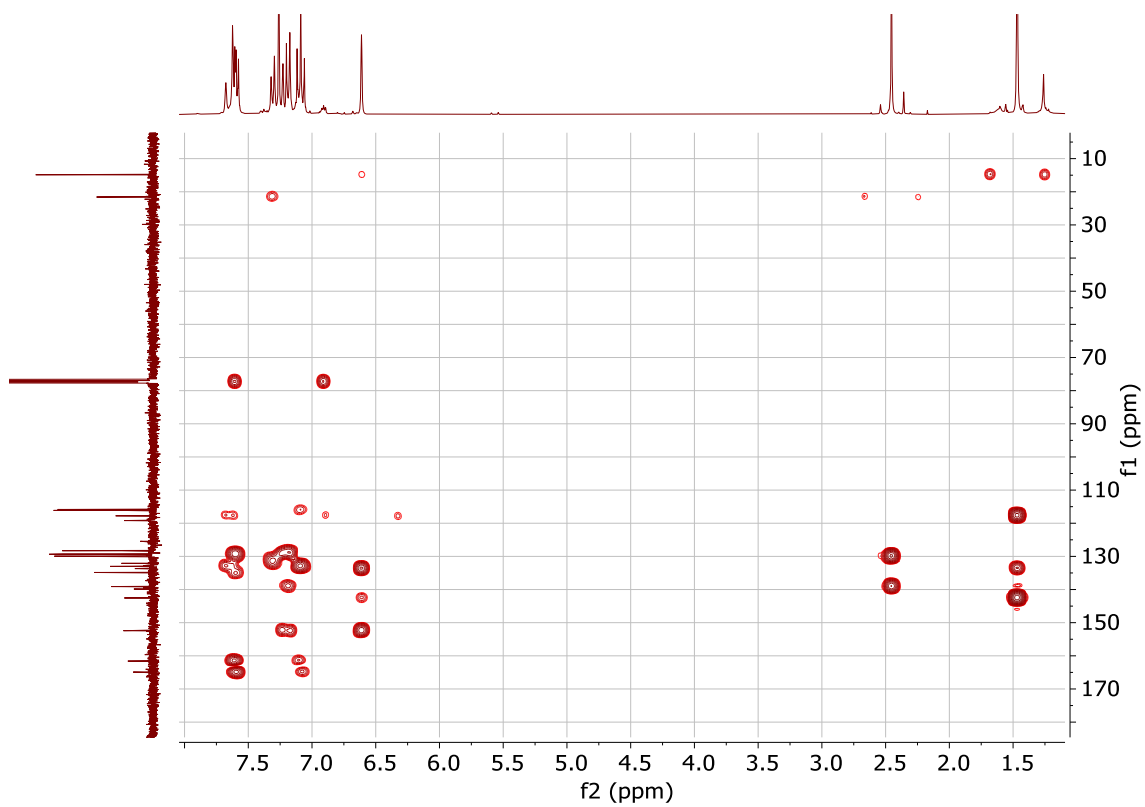
Expansion of the ^{13}C NMR spectrum of 8 (aromatic region)



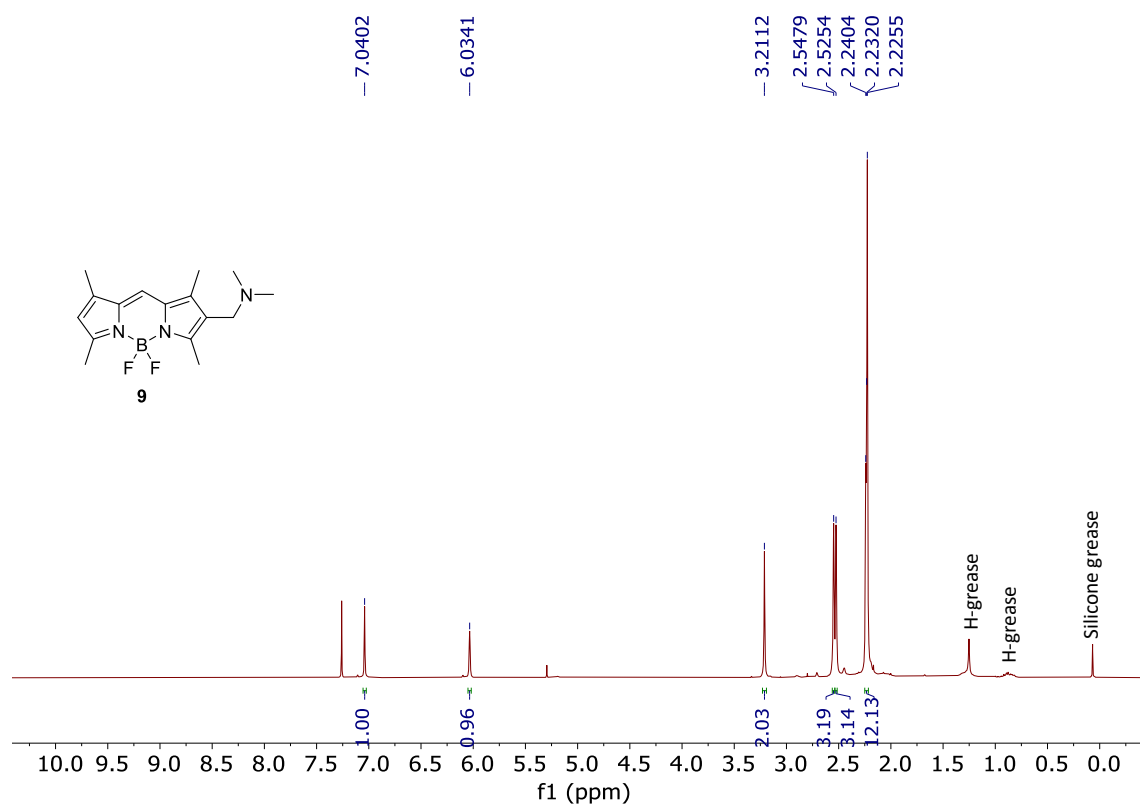
HMQC spectrum of 8



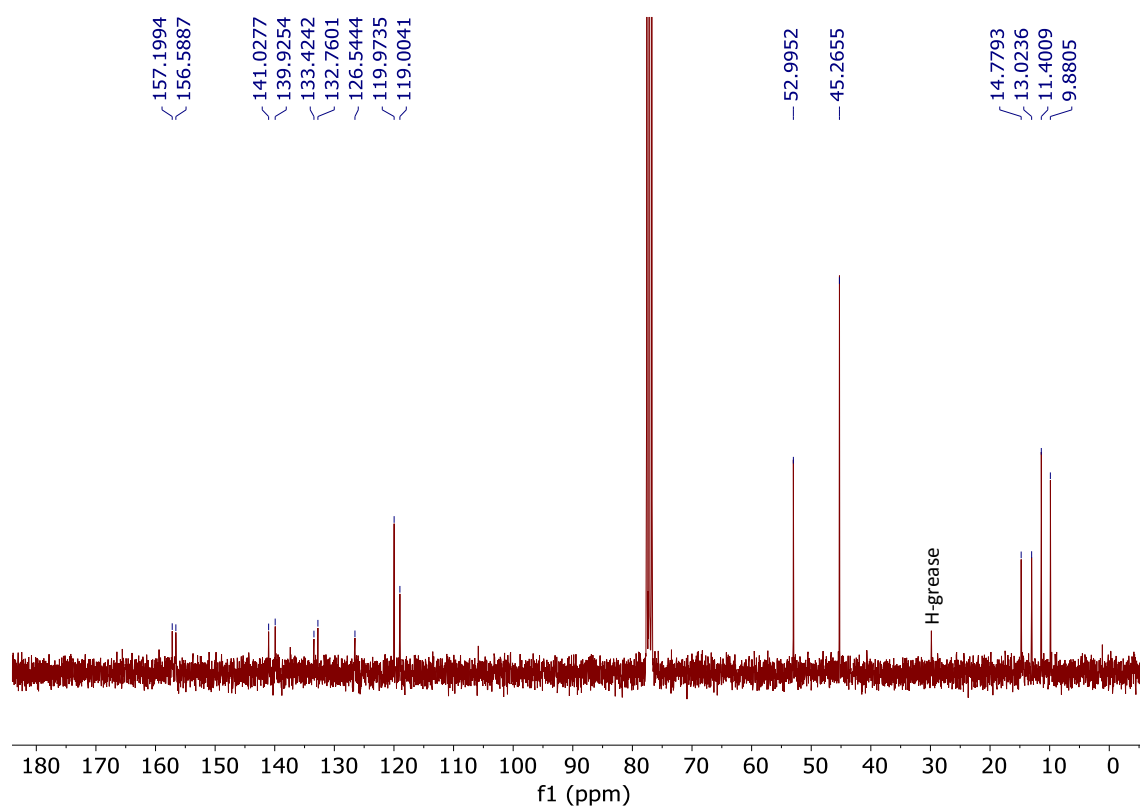
HMBC spectrum of 8



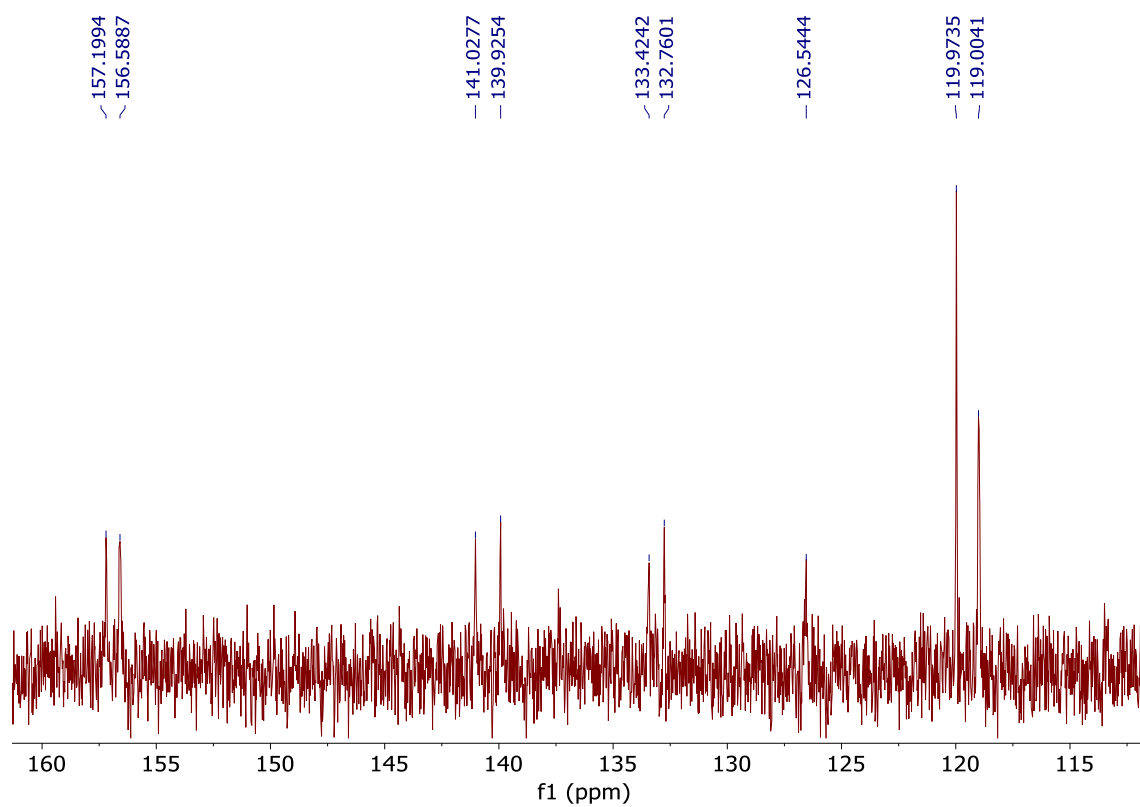
¹H NMR (CDCl₃, 300 MHz) of 9



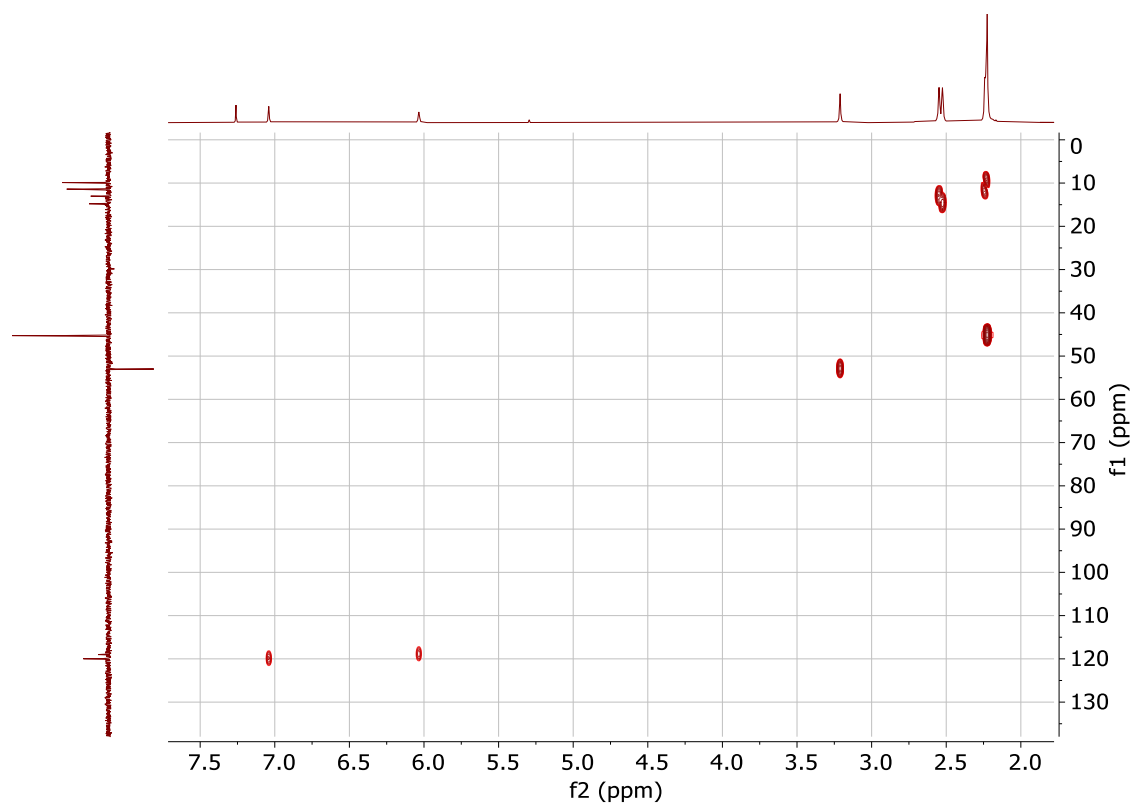
^{13}C NMR (CDCl_3 , 75 MHz) of **9**



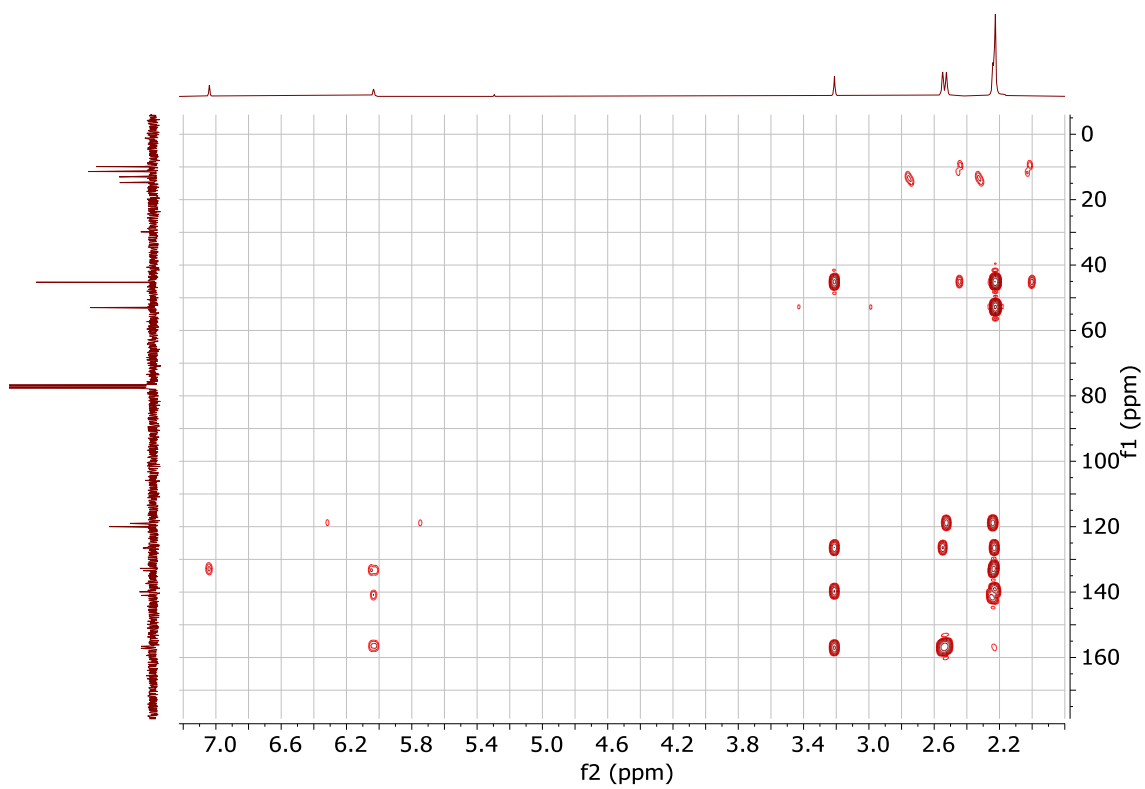
Expansion of the ^{13}C NMR spectrum of **9** (aromatic region)



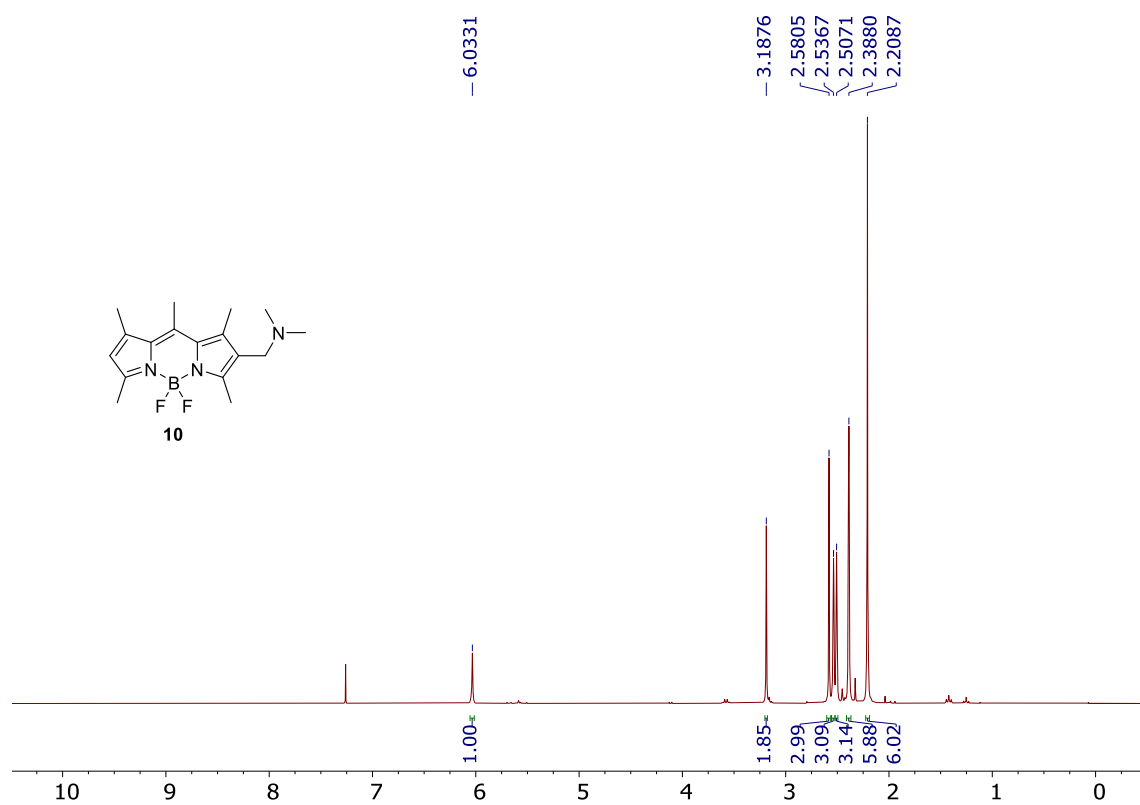
HMQC spectrum of 9



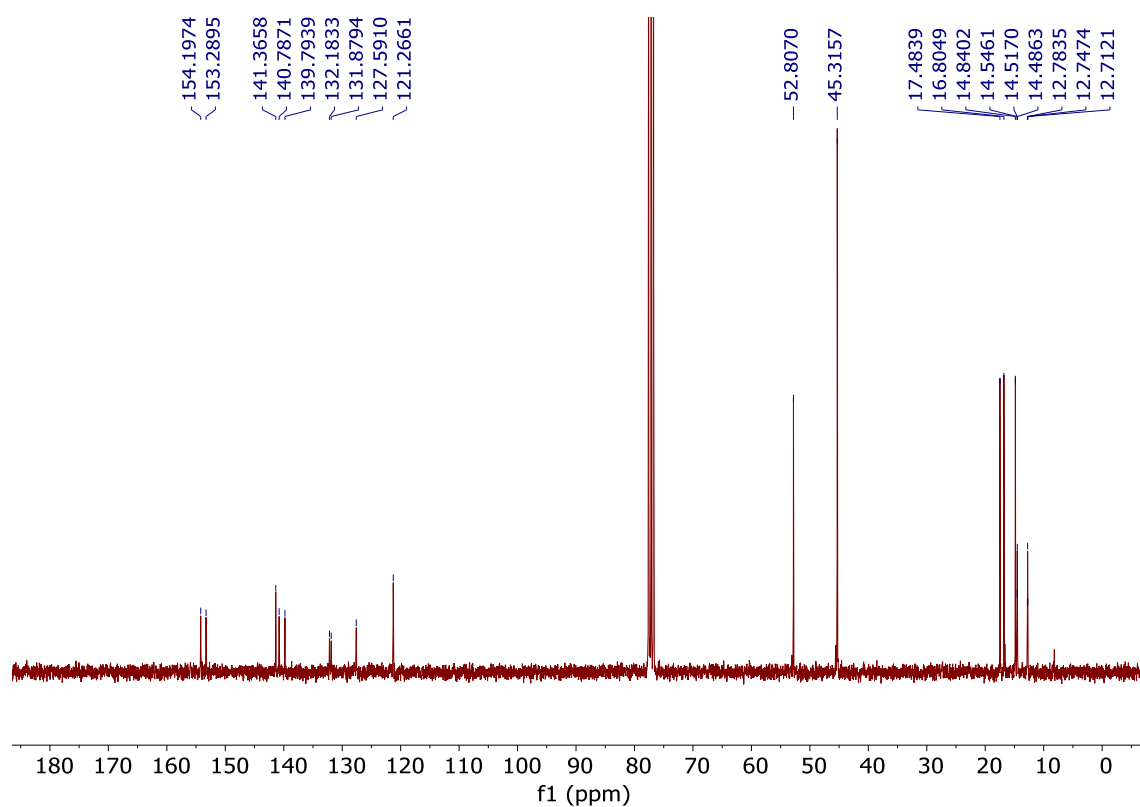
HMBC spectrum of 9



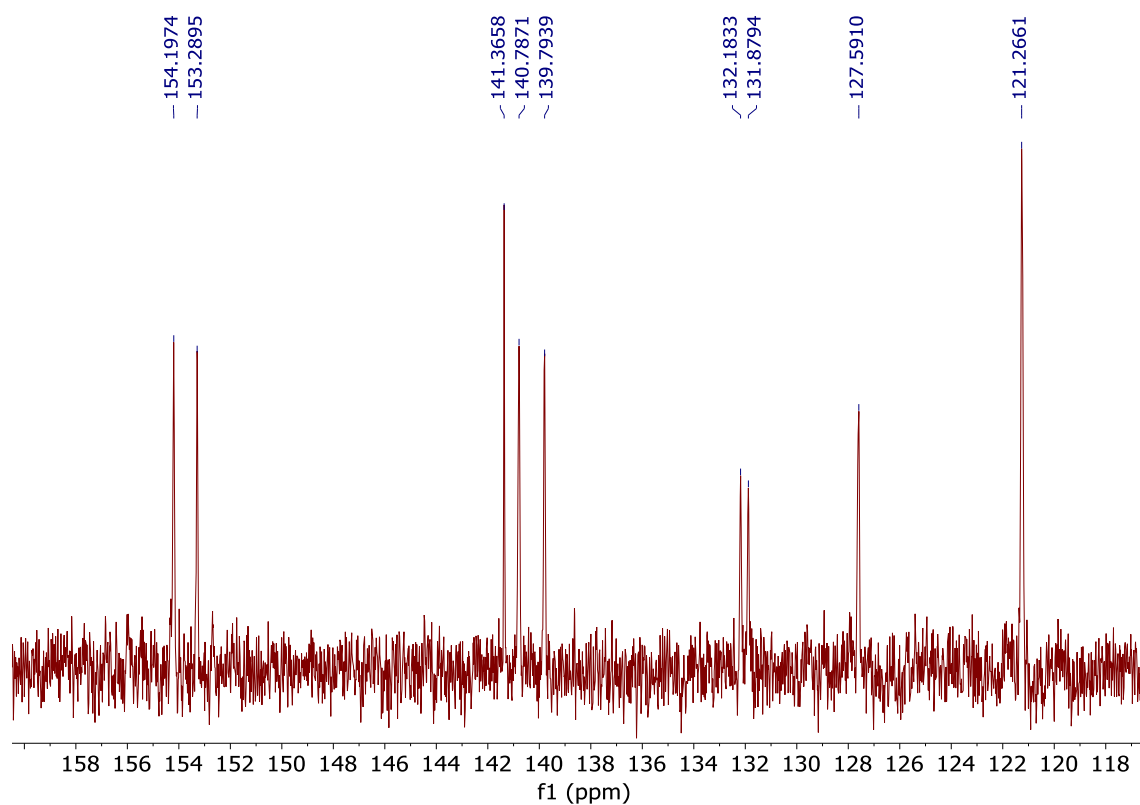
¹H NMR (CDCl₃, 300 MHz) of **10**



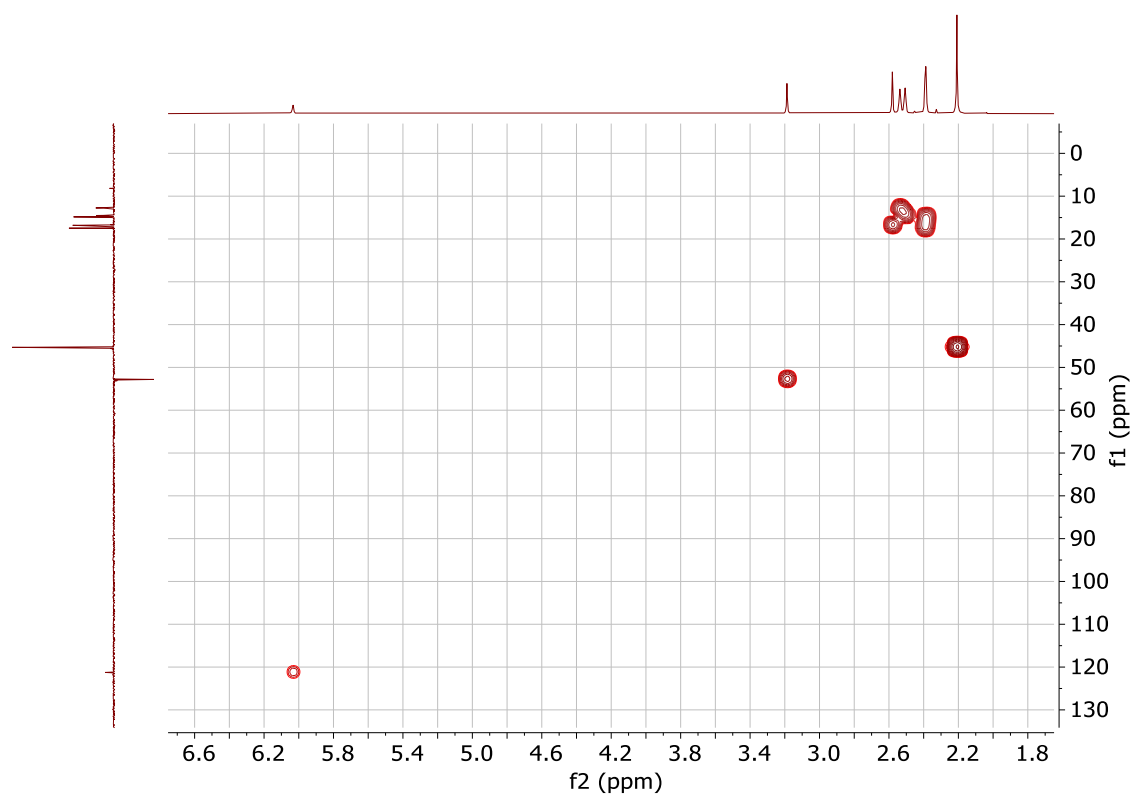
^{13}C NMR (CDCl_3 , 75 MHz) of 10



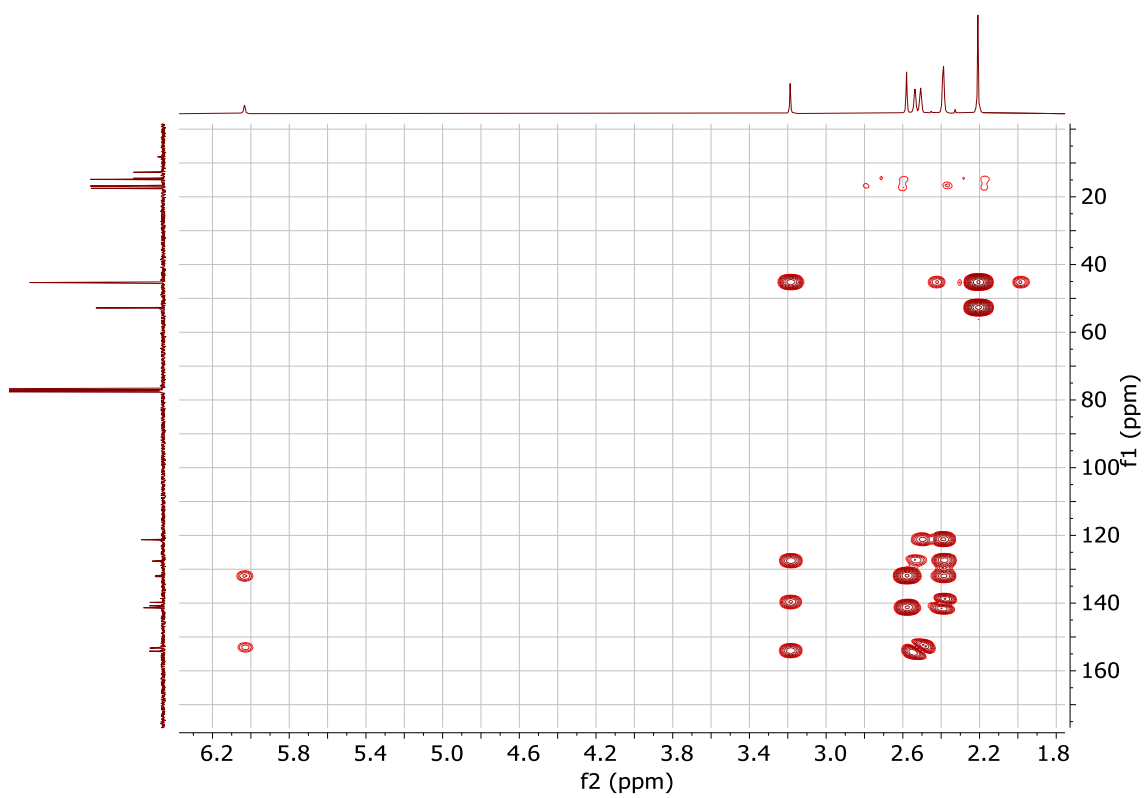
Expansion of the ^{13}C NMR spectrum of 10 (aromatic region)



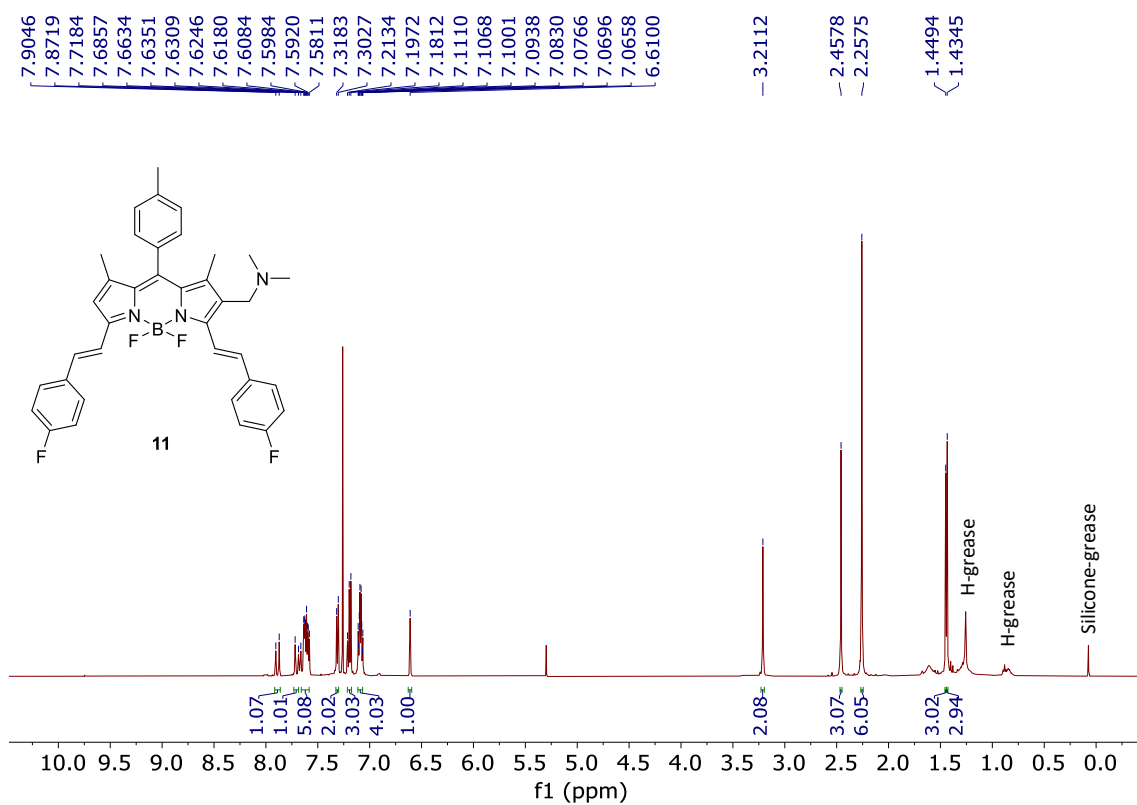
HMQC spectrum of 10



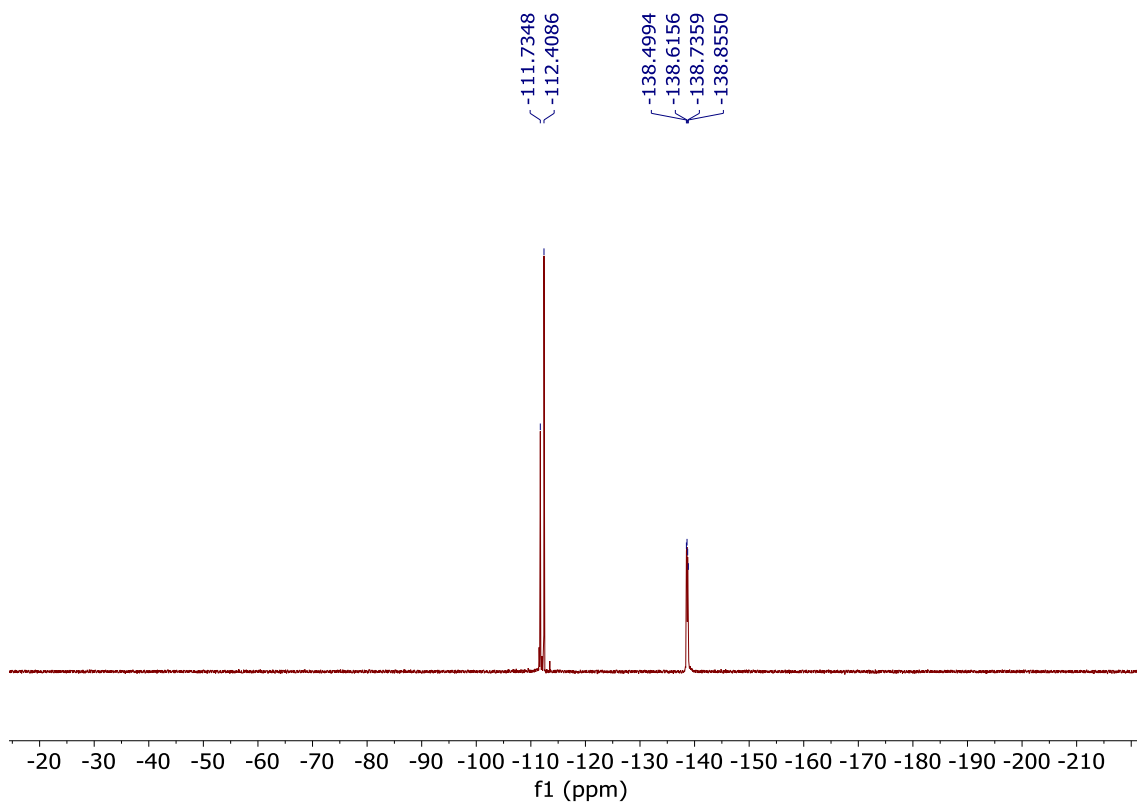
HMBC spectrum of 10



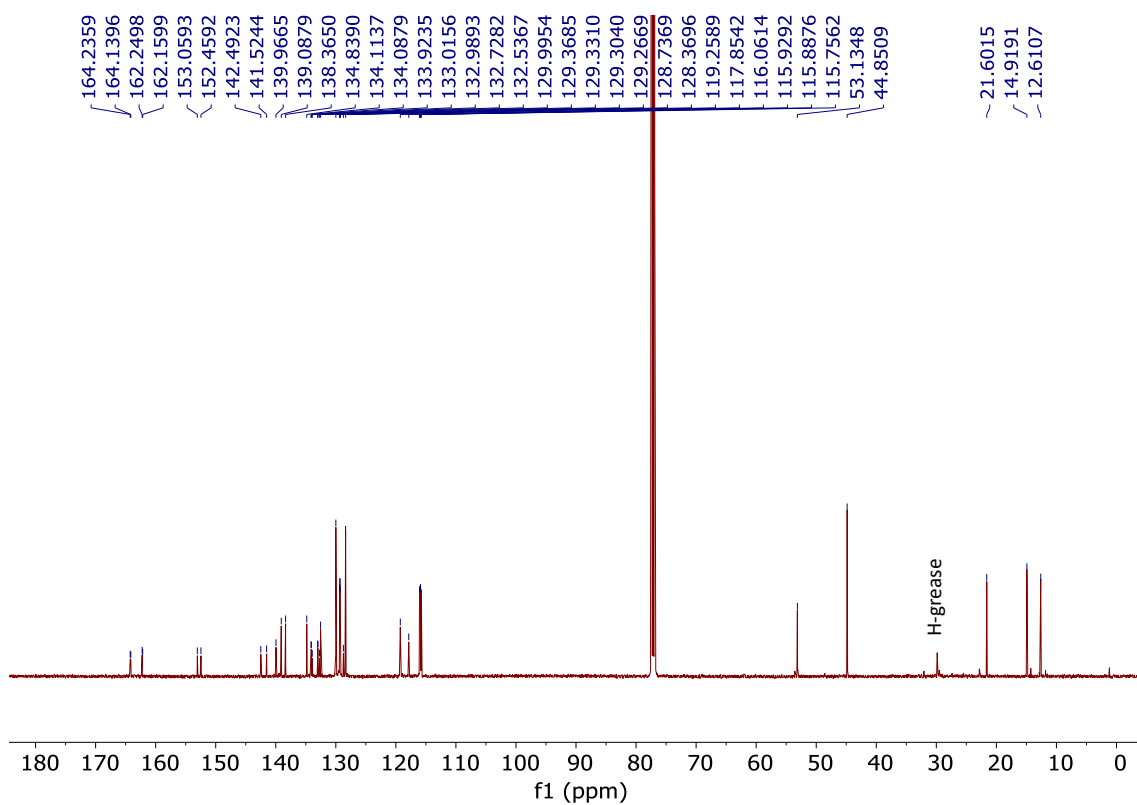
¹H NMR (CDCl₃, 500 MHz) of 11



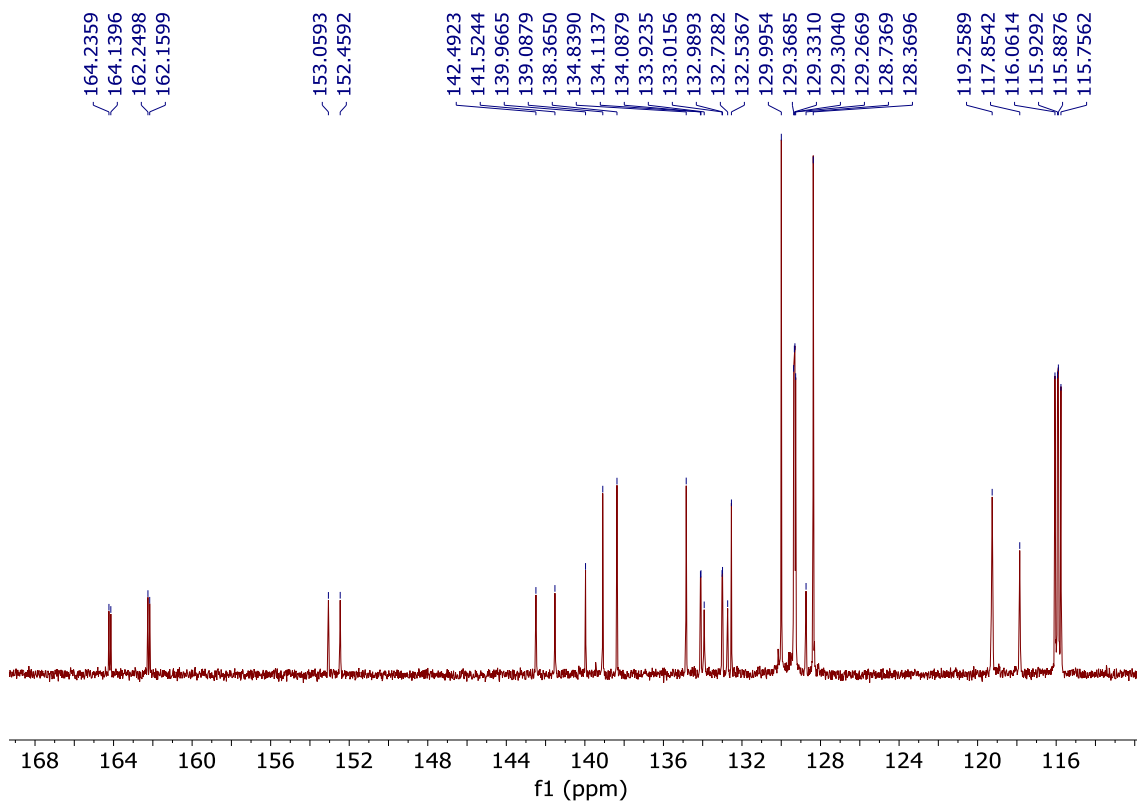
¹⁹F NMR (CDCl₃, 282 MHz) of 11



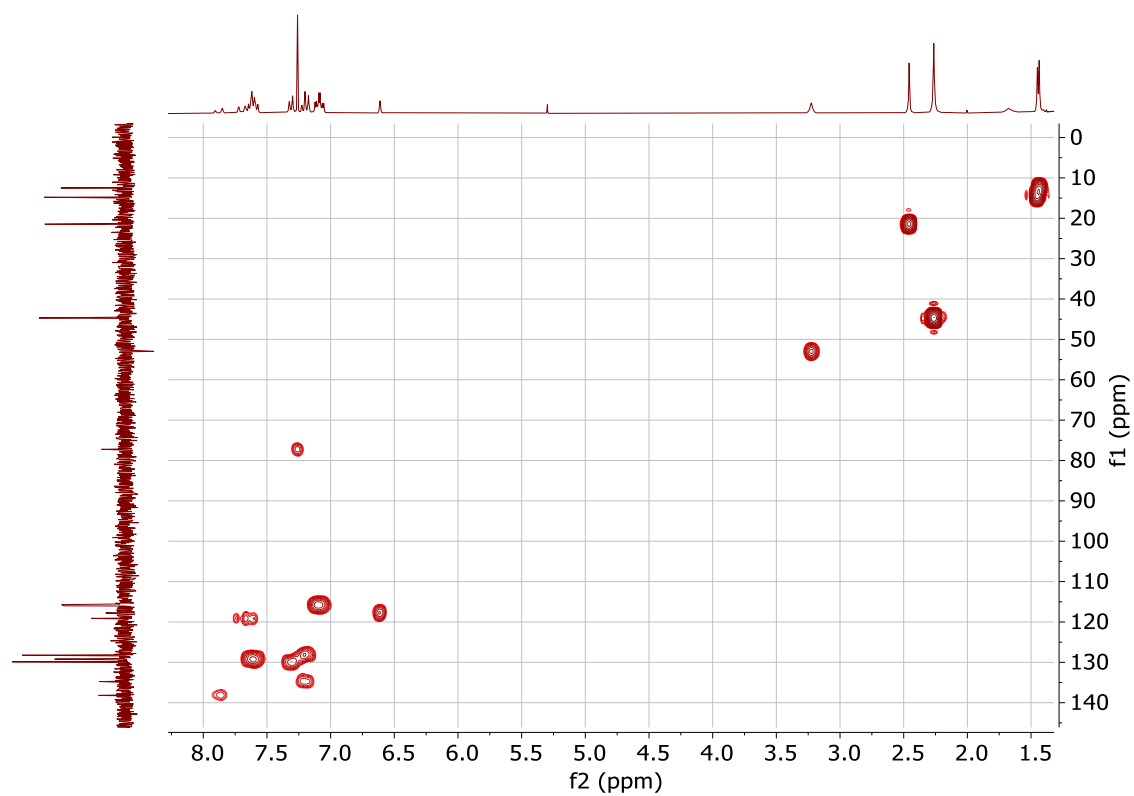
^{13}C NMR (CDCl₃, 126 MHz) of 11



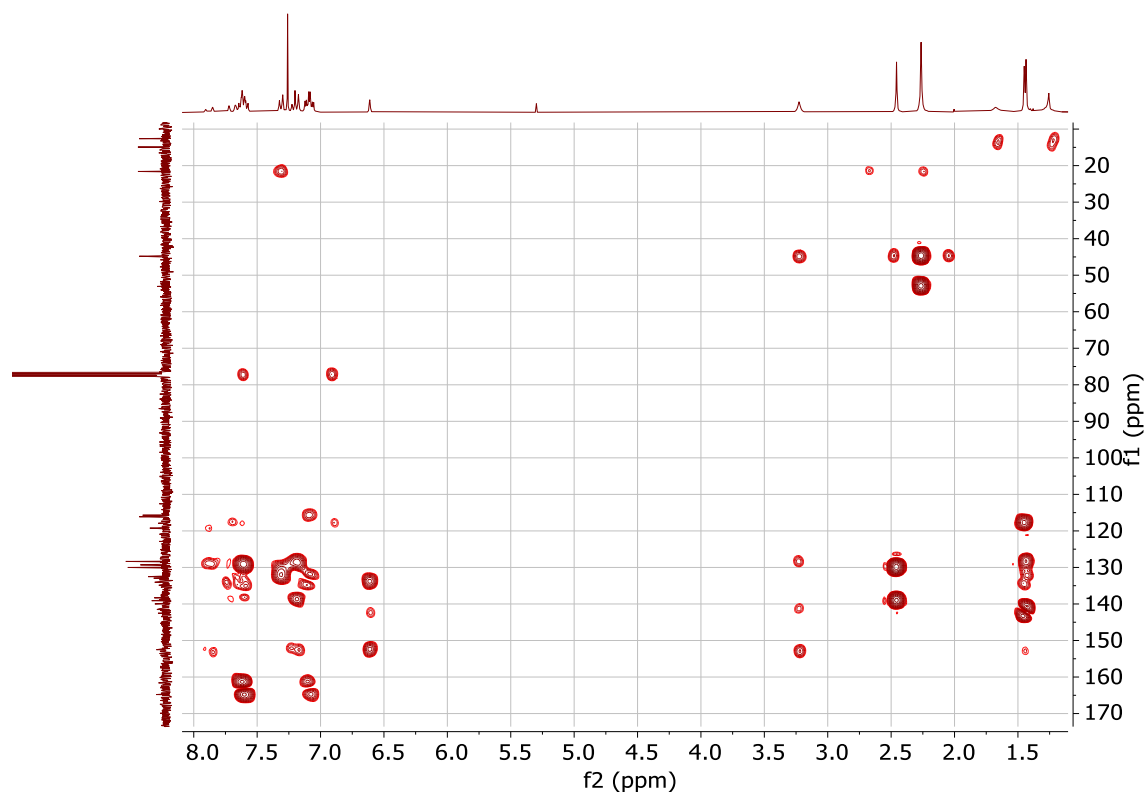
Expansion of the ^{13}C NMR spectrum of 11 (aromatic region)



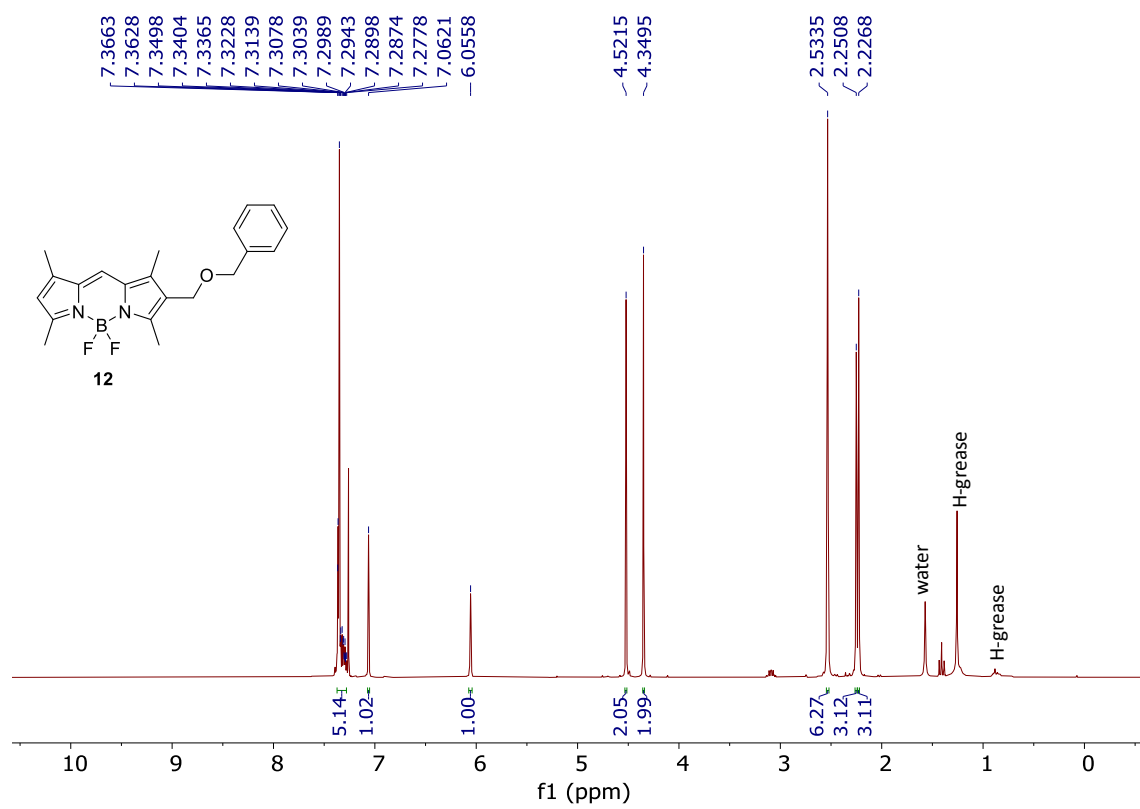
HMQC spectrum of 11



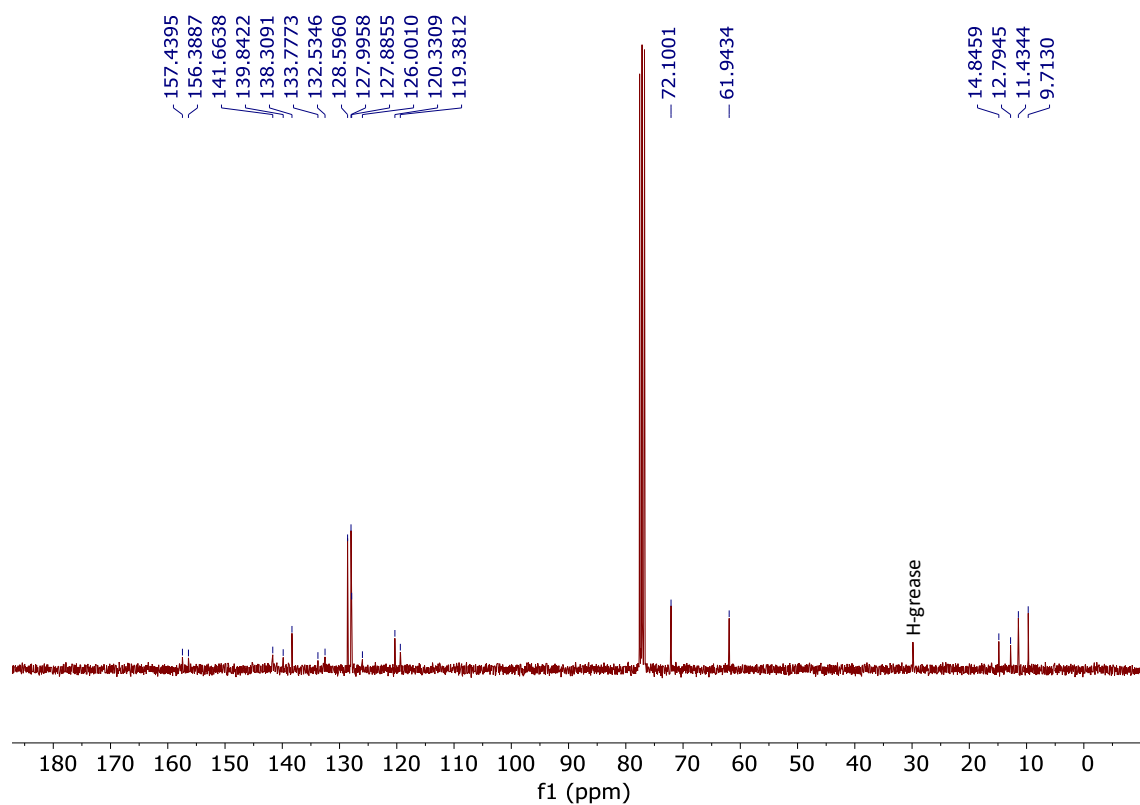
HMBC spectrum of 11



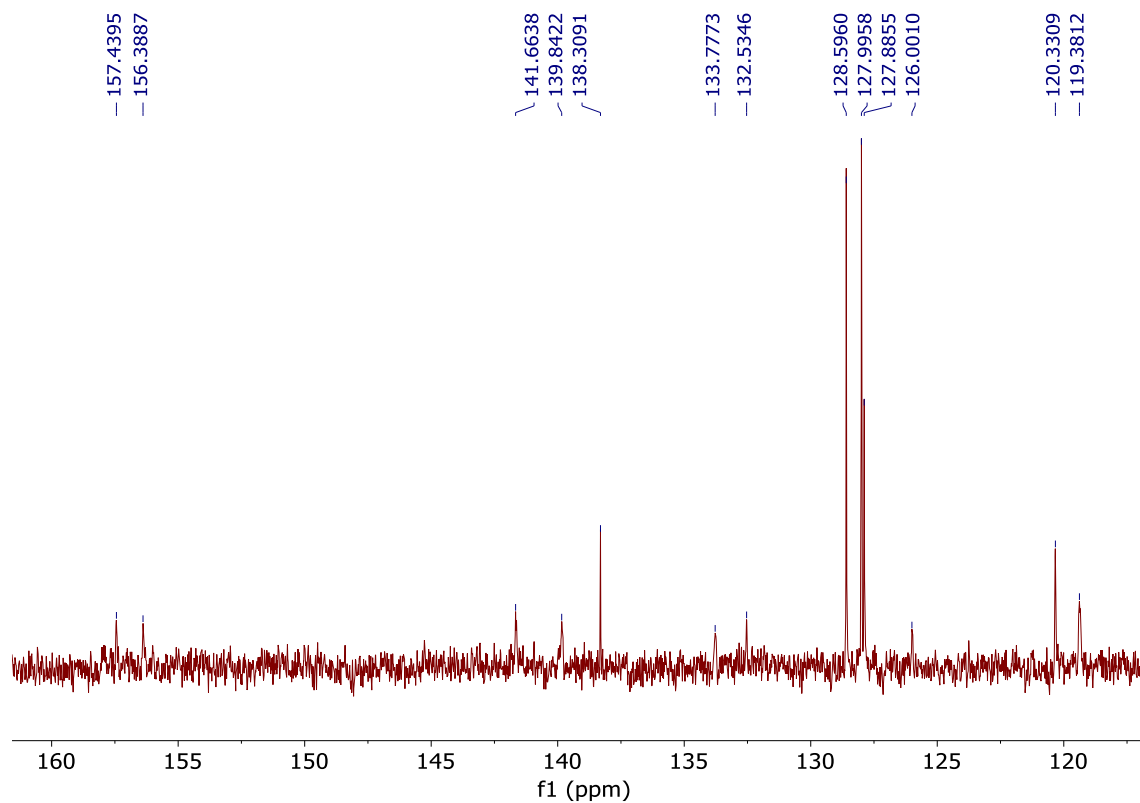
¹H NMR (CDCl₃, 300 MHz) of 12



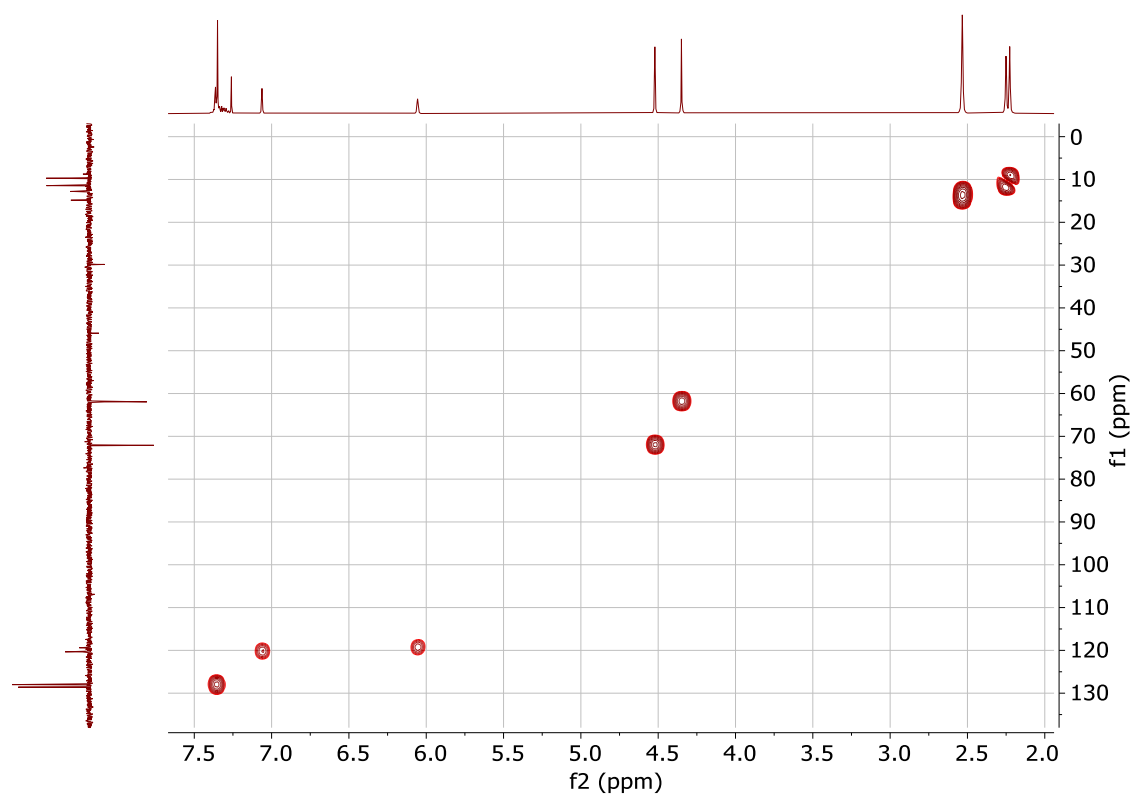
^{13}C NMR (CDCl₃, 75 MHz) of 12



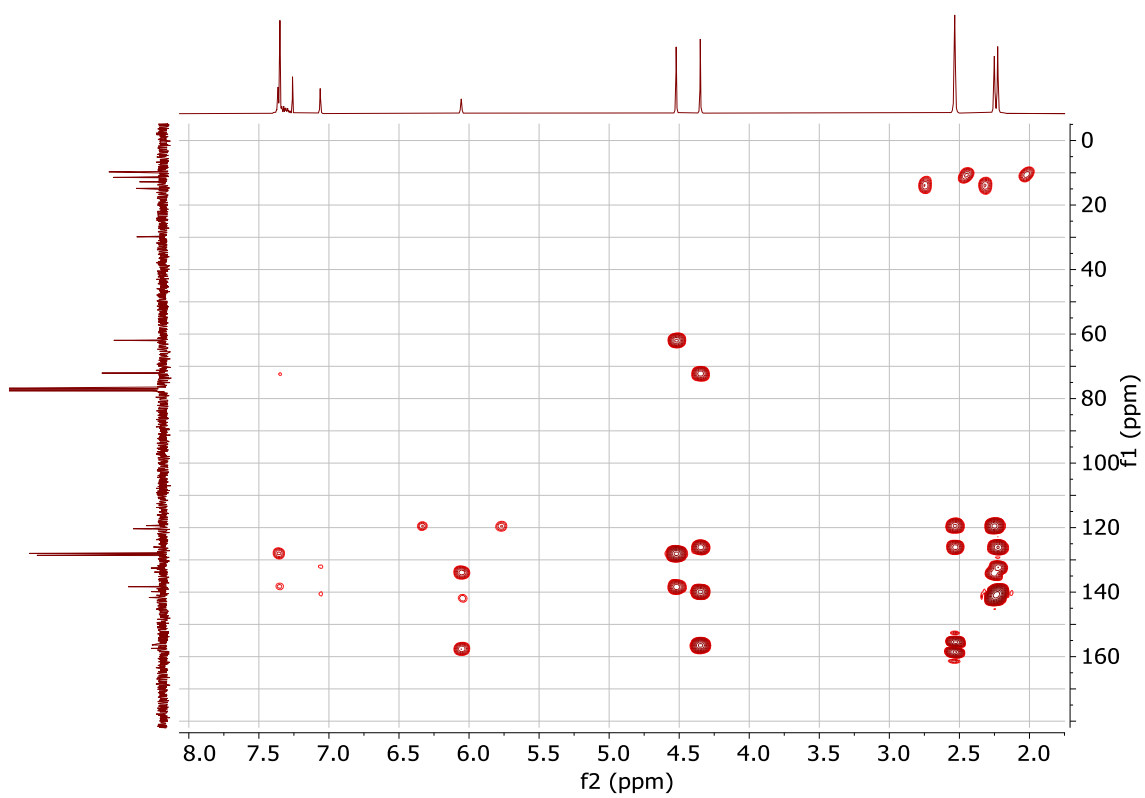
Expansion of the ^{13}C NMR spectrum of 12 (aromatic region)



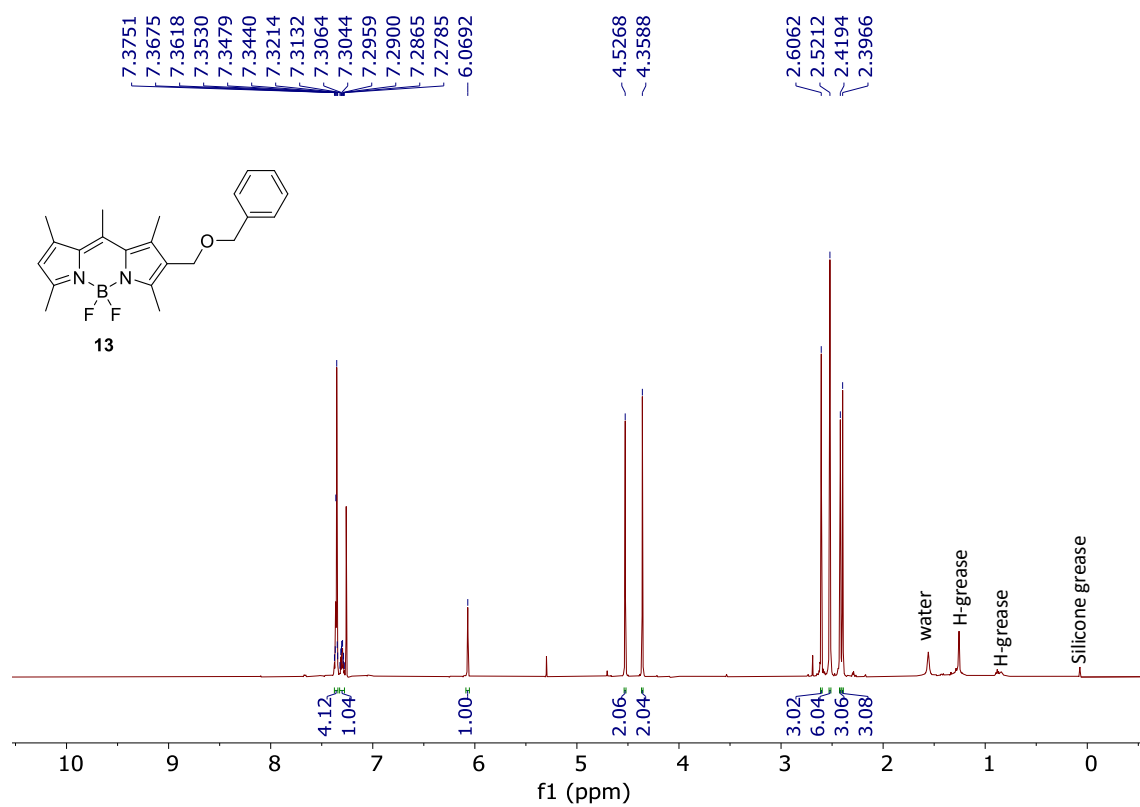
HMQC spectrum of 12



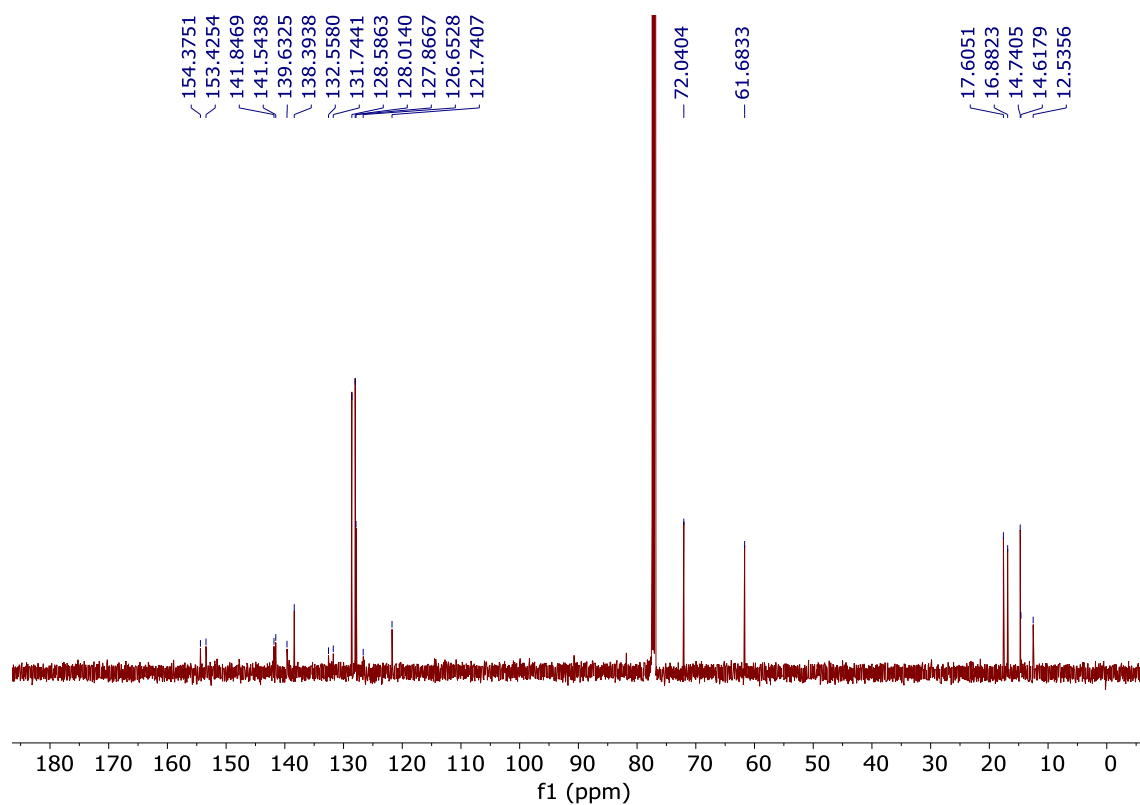
HMBC spectrum of 12



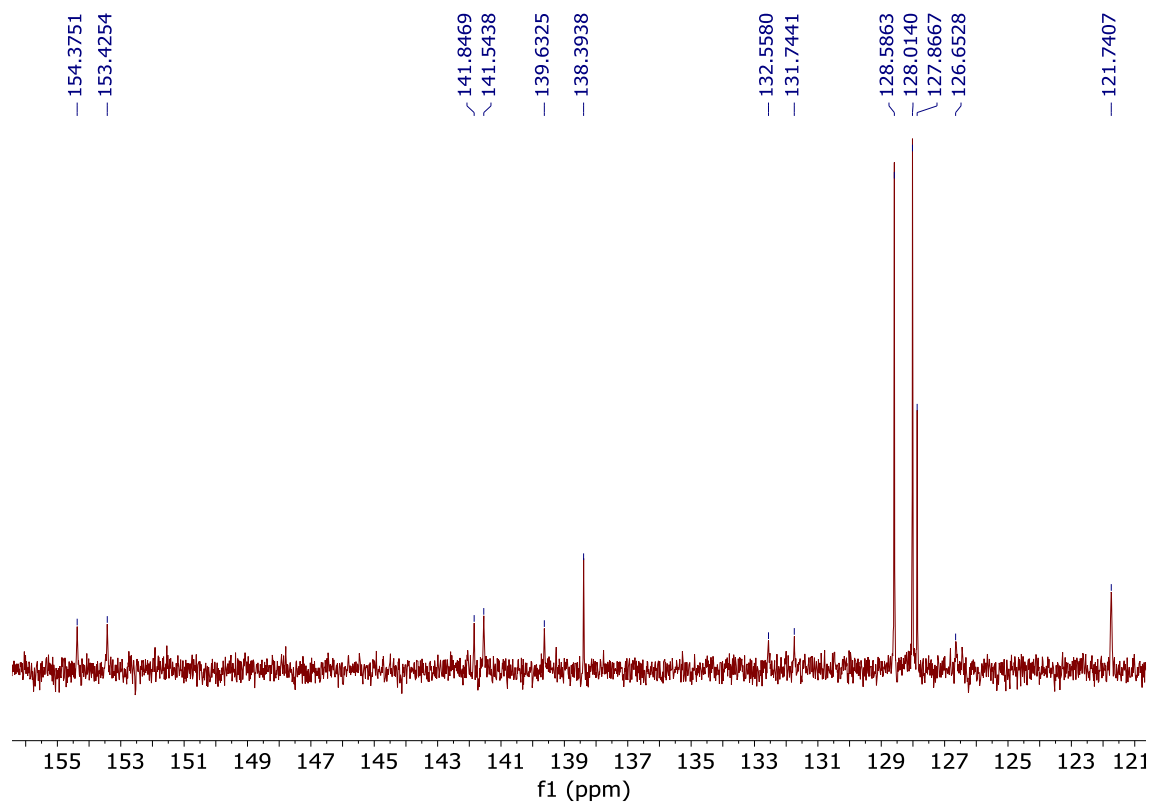
¹H NMR (CDCl₃, 500 MHz) of 13



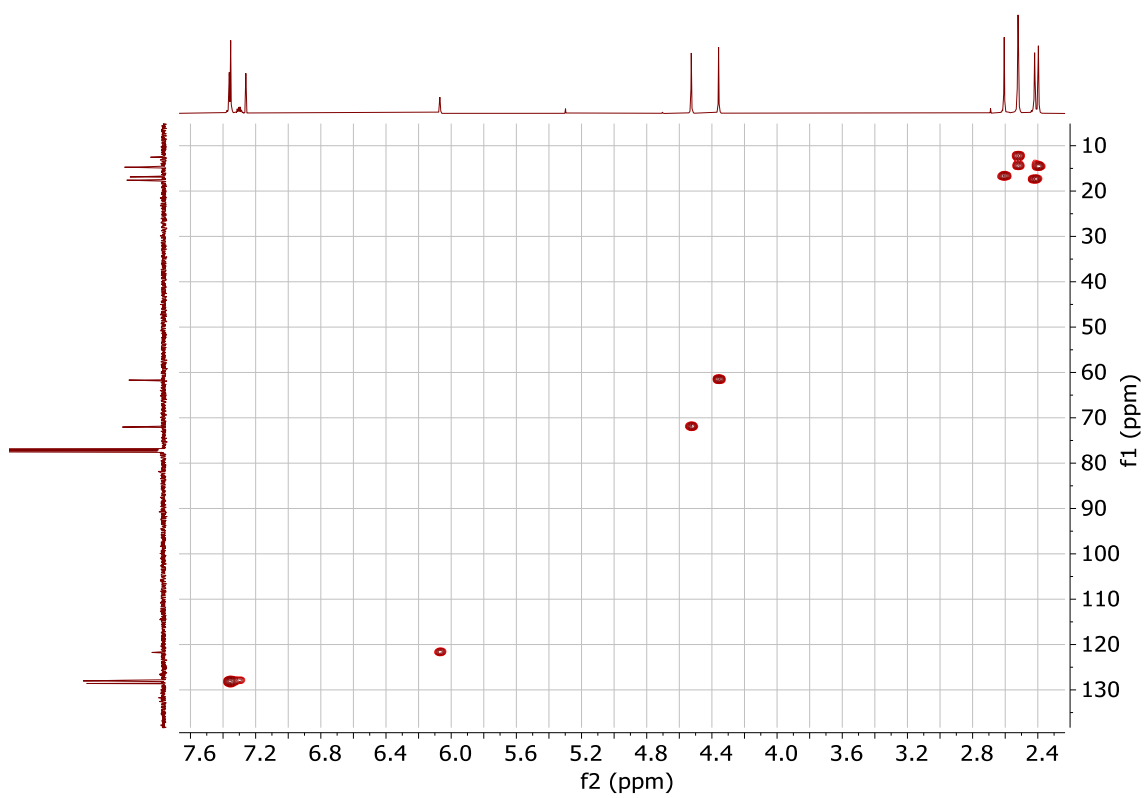
^{13}C NMR (CDCl₃, 126 MHz) of 13



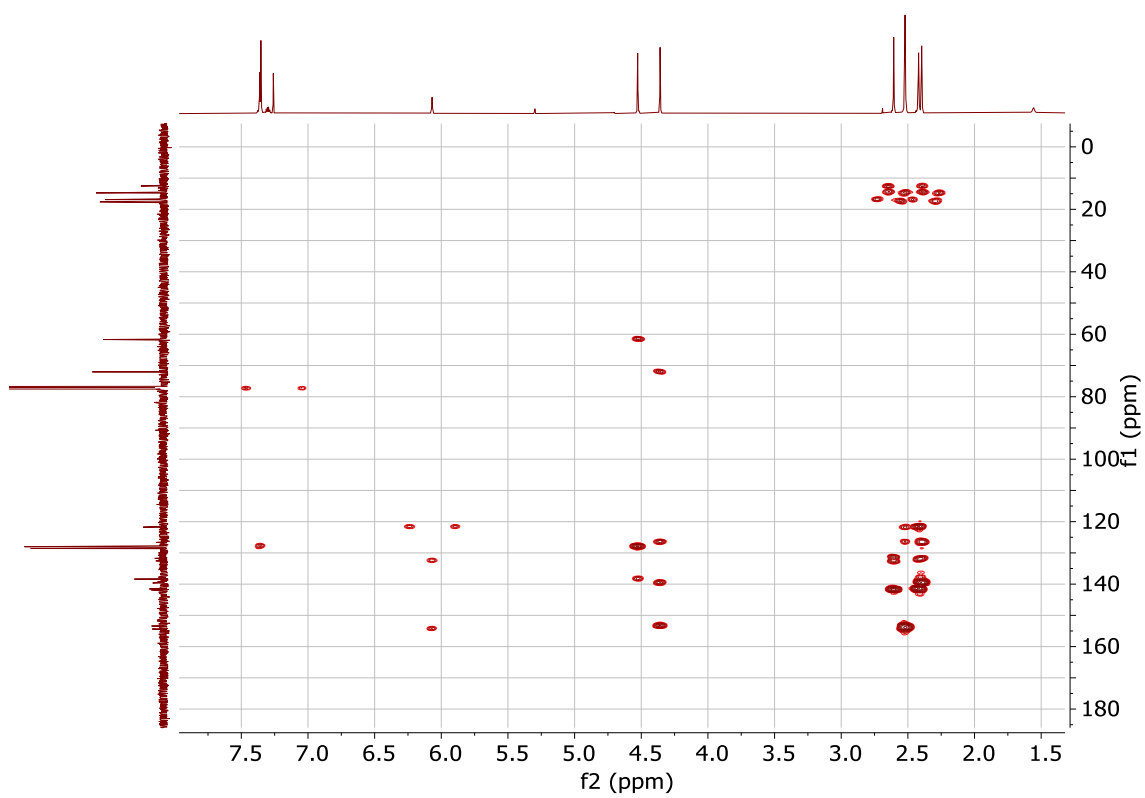
Expansion of the ^{13}C NMR spectrum of 13 (aromatic region)



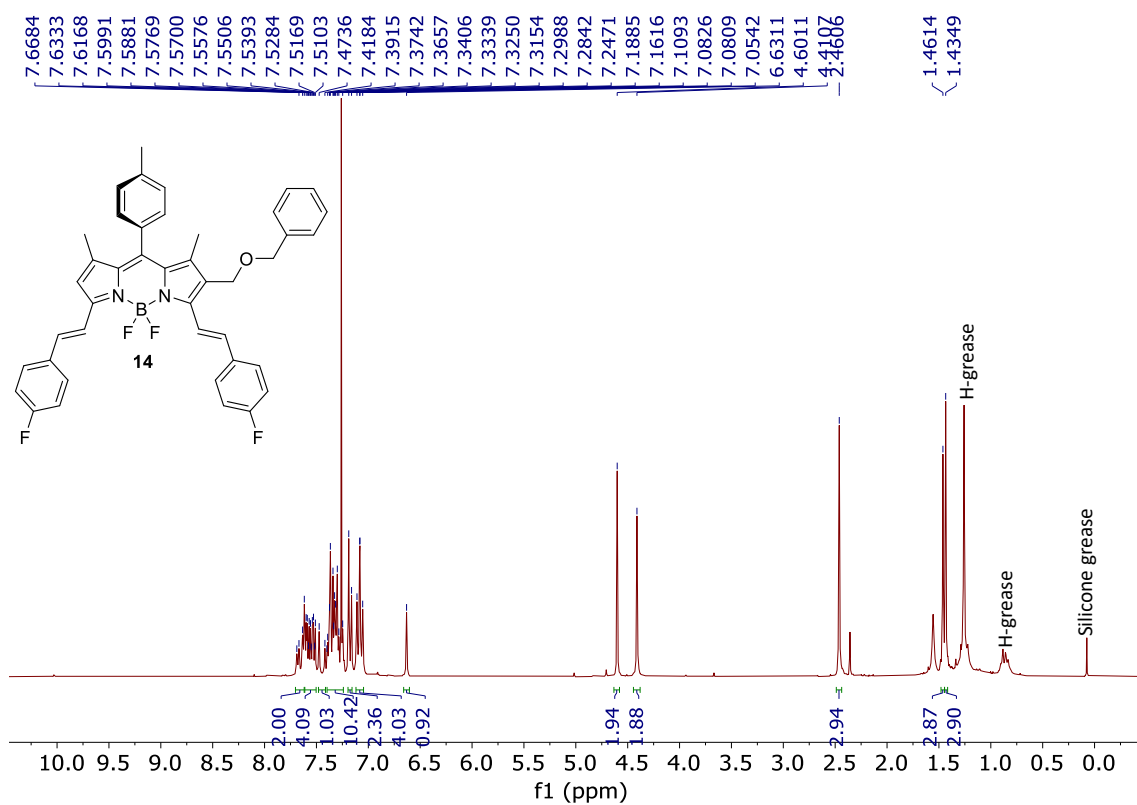
HMQC spectrum of 13



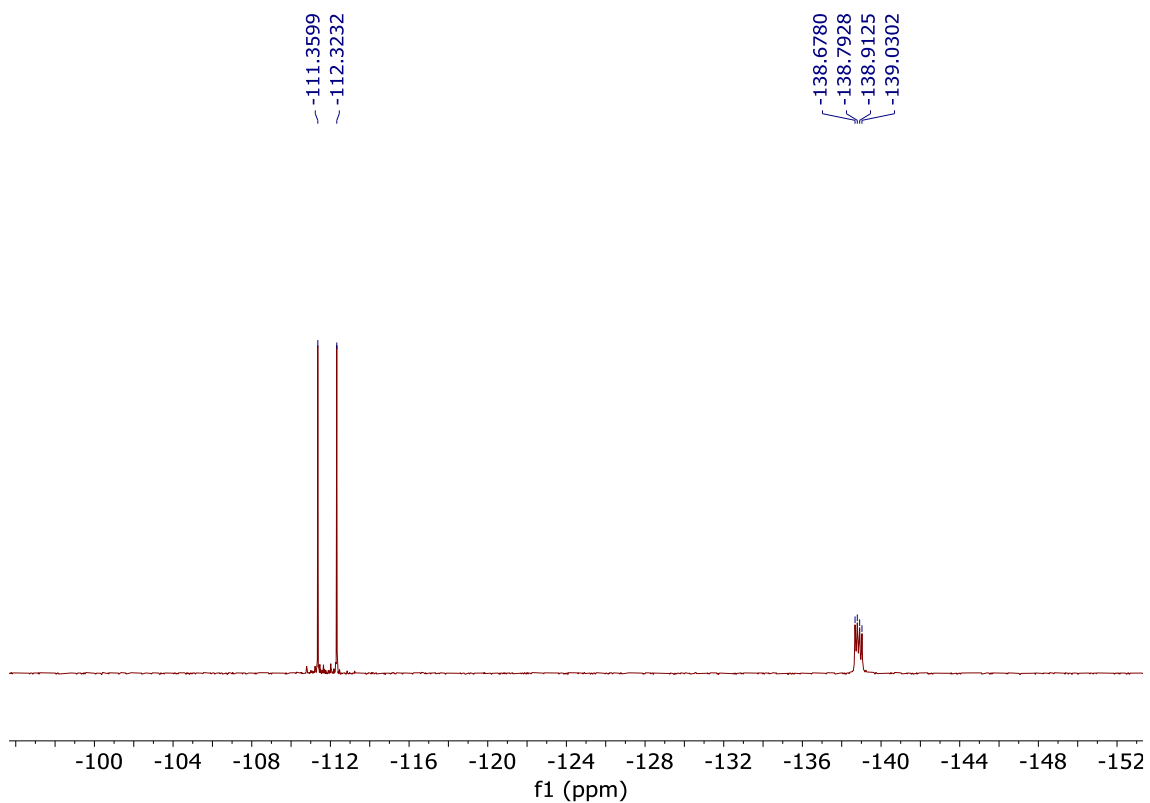
HMBC spectrum of 13



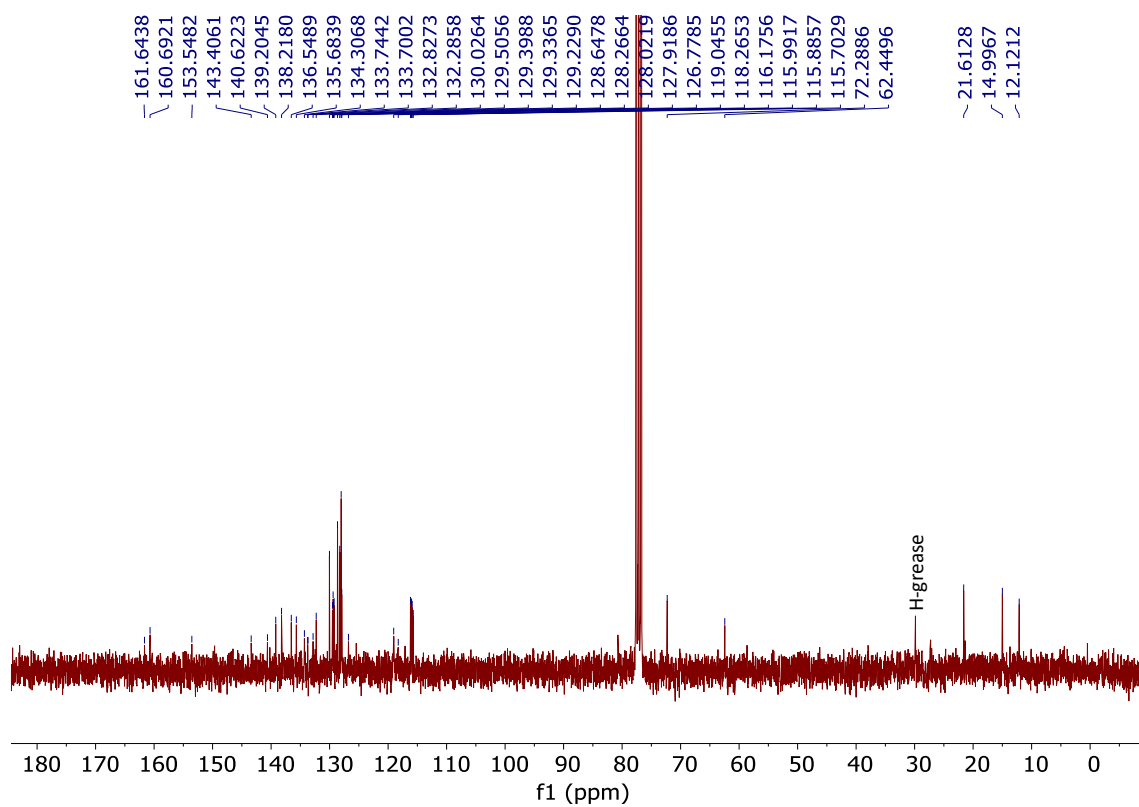
¹H NMR (CDCl₃, 300 MHz) of 14



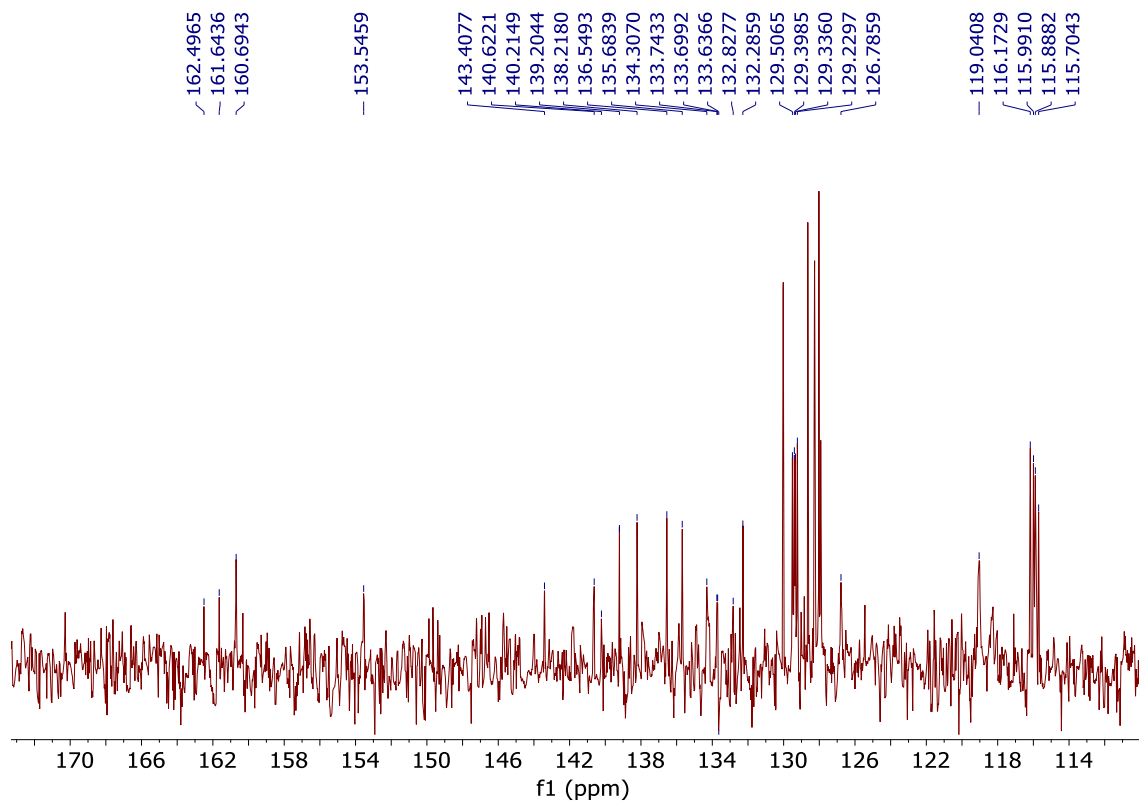
¹⁹F NMR (CDCl₃, 282 MHz) of 14



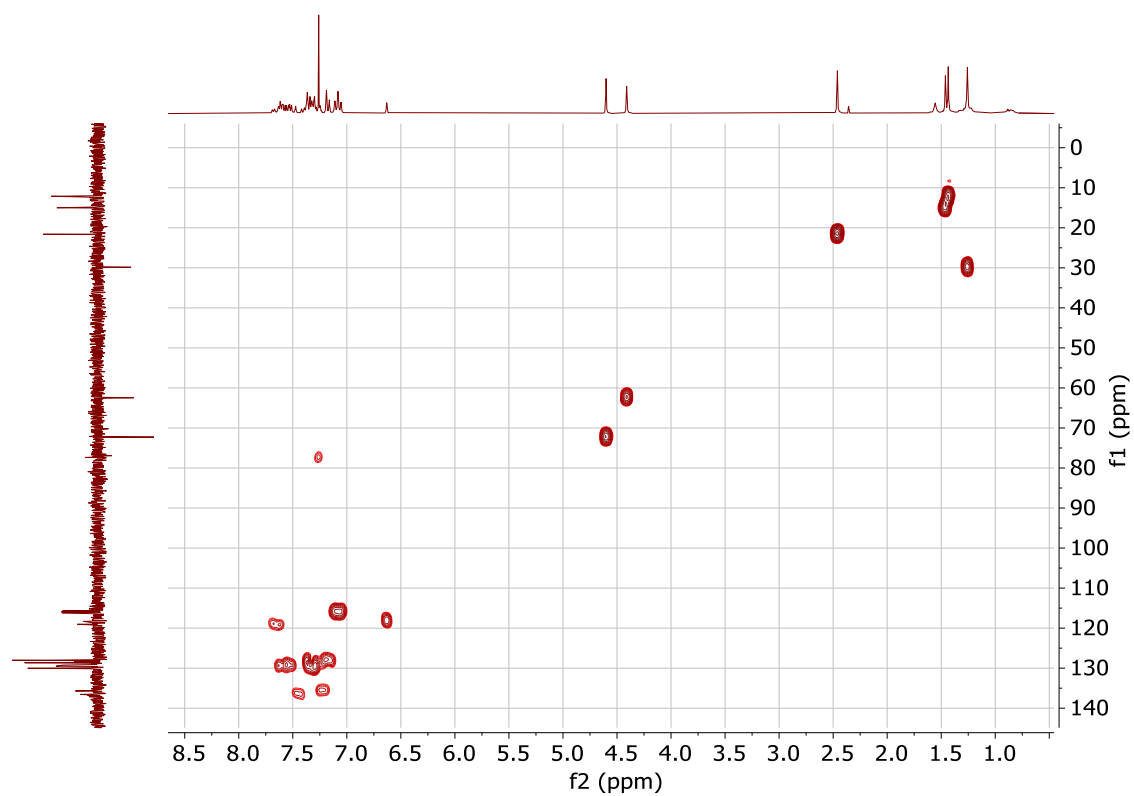
^{13}C NMR (CDCl_3 , 75 MHz) of 14



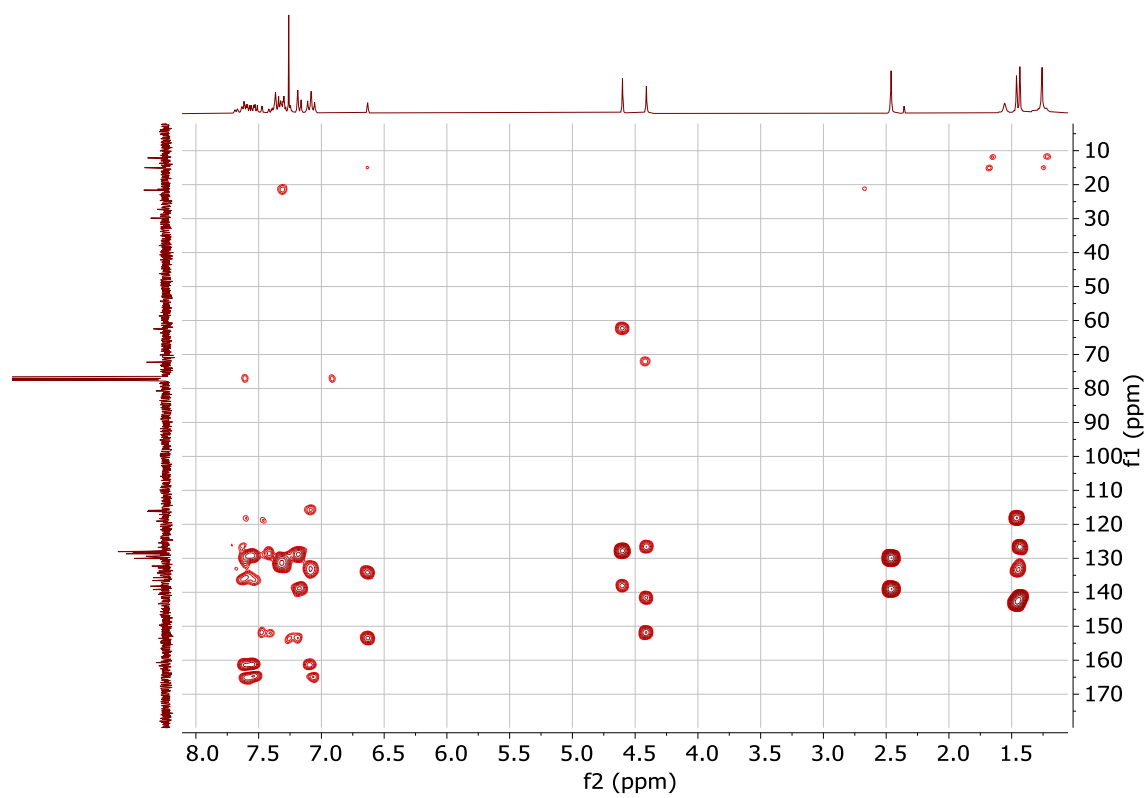
Expansion of the ^{13}C NMR spectrum of 14 (aromatic region)



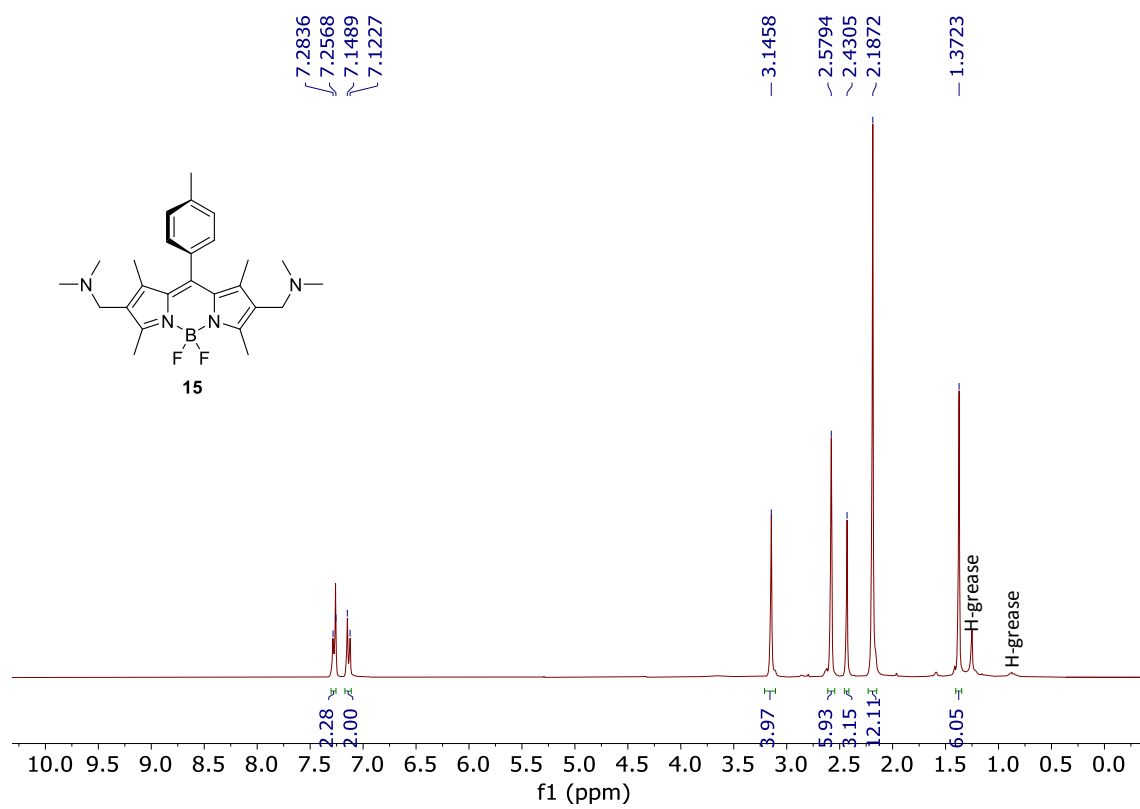
HMQC spectrum of 14



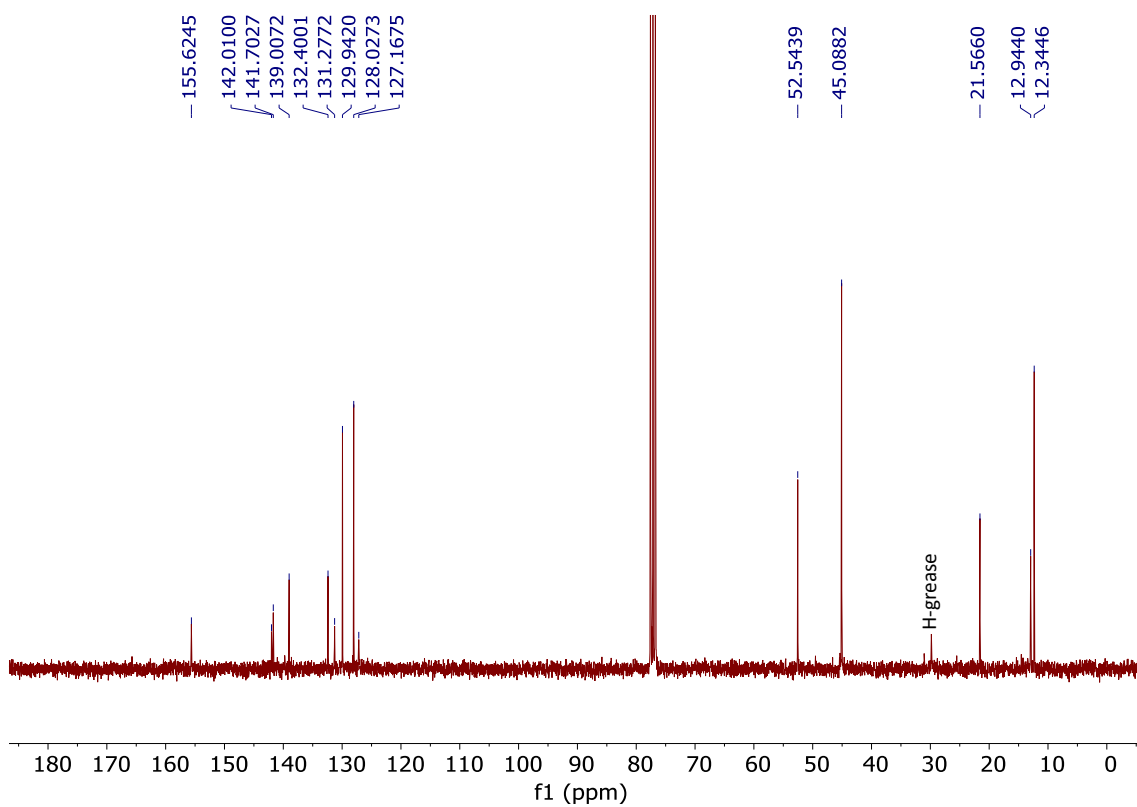
HMBC spectrum of 14



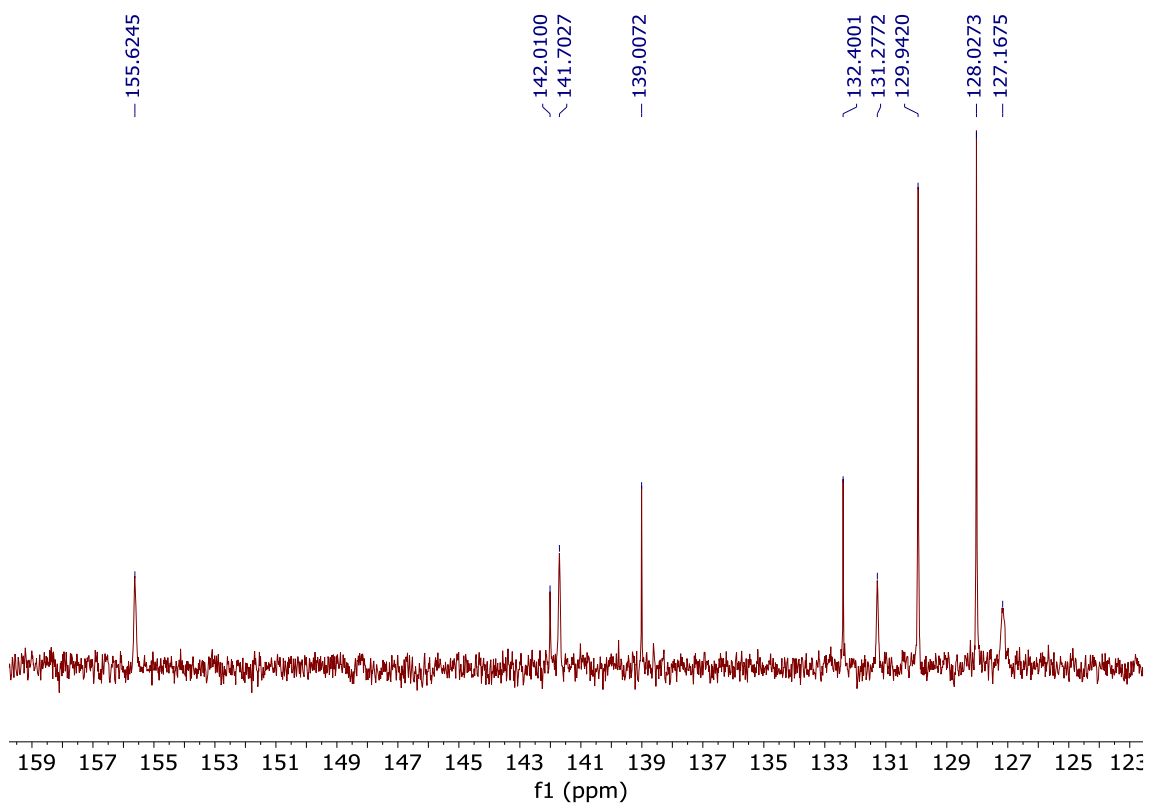
¹H NMR (CDCl₃, 300 MHz) of 15



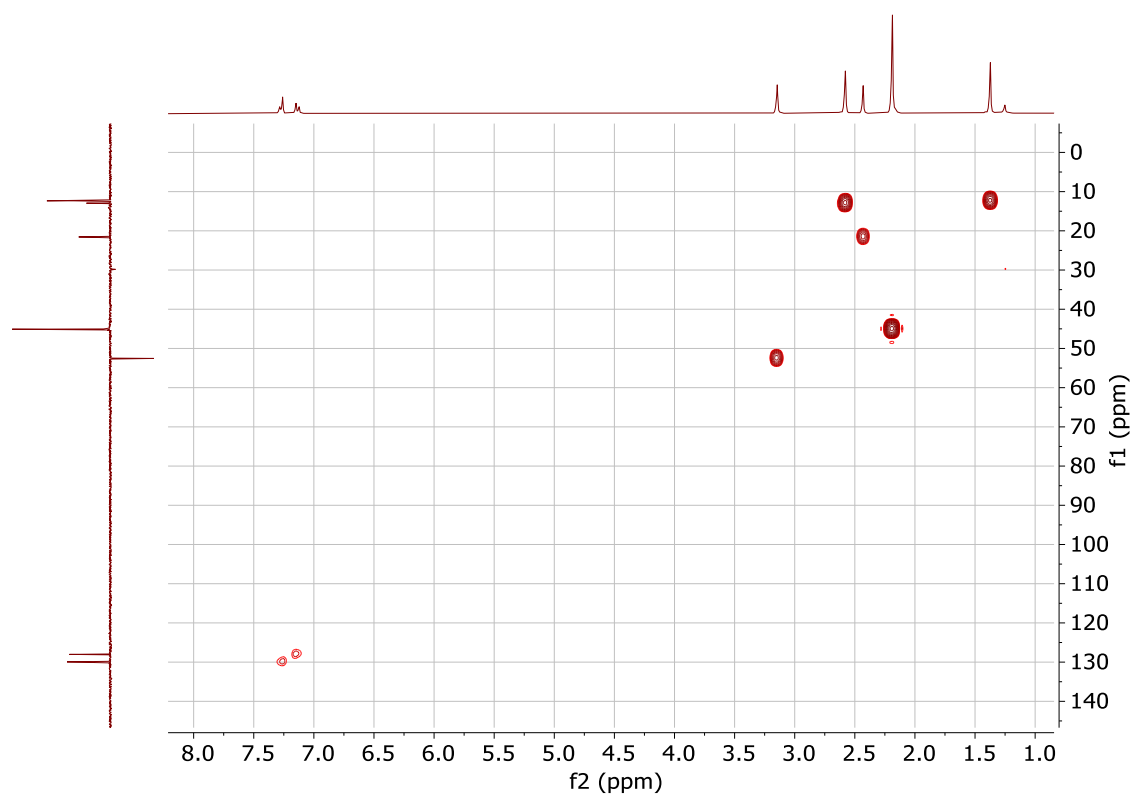
^{13}C NMR (CDCl₃, 75 MHz) of 15



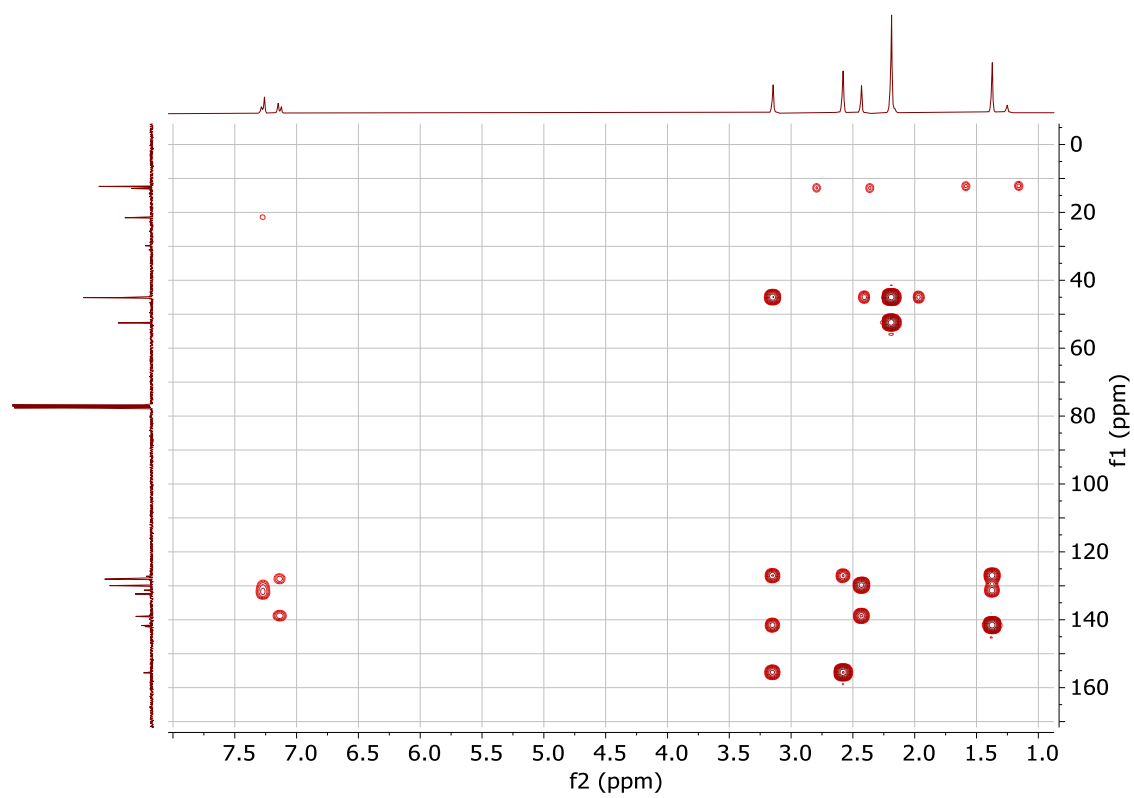
Expansion of the ^{13}C NMR spectrum of 15 (aromatic region)



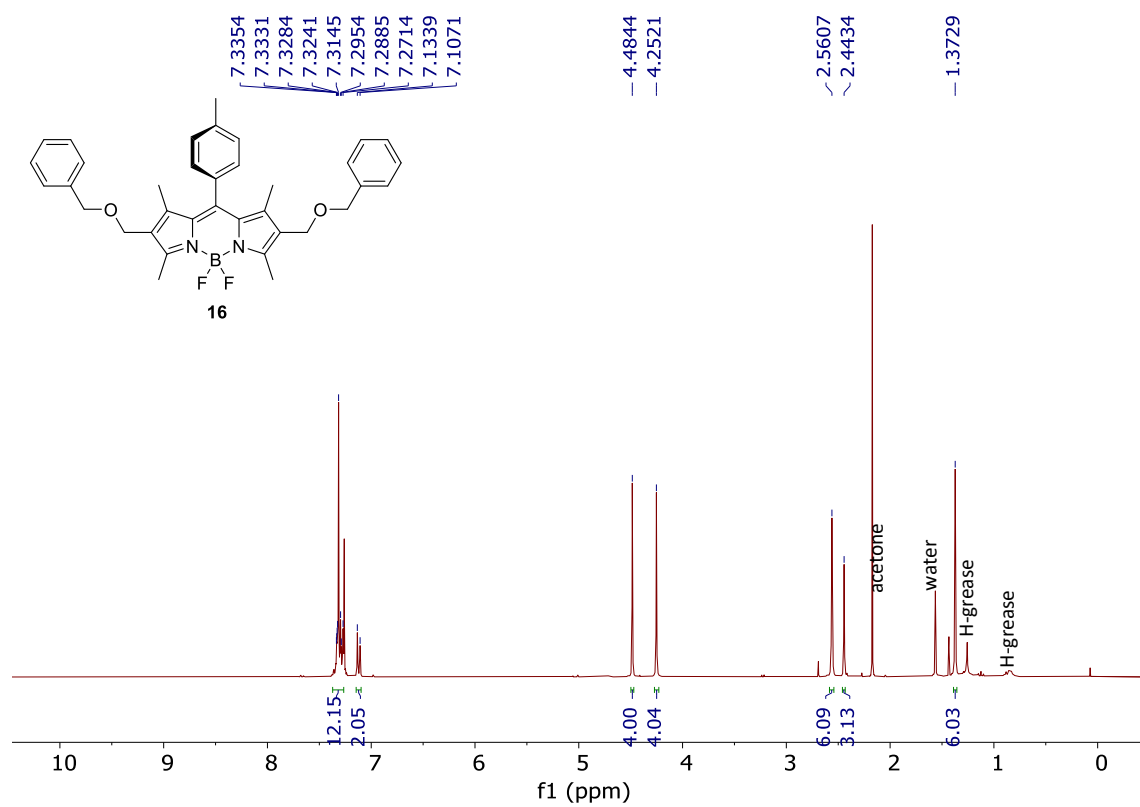
HMQC spectrum of 15



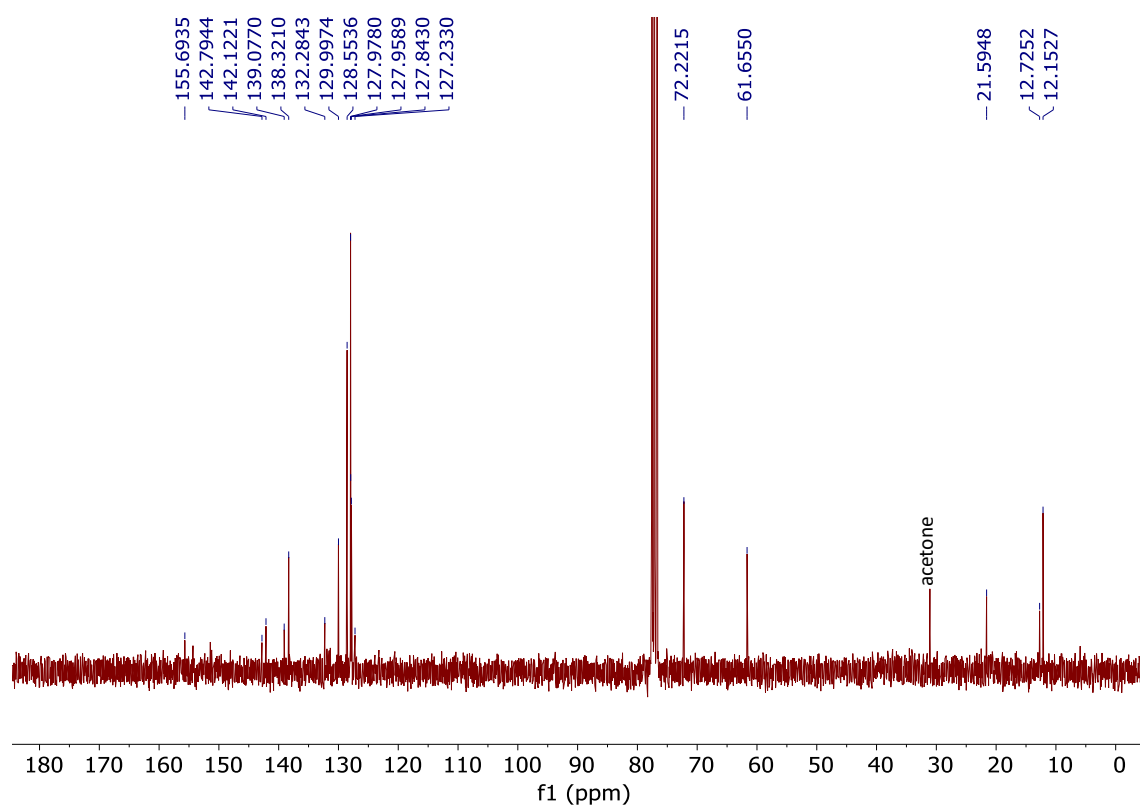
HMBC spectrum of 15



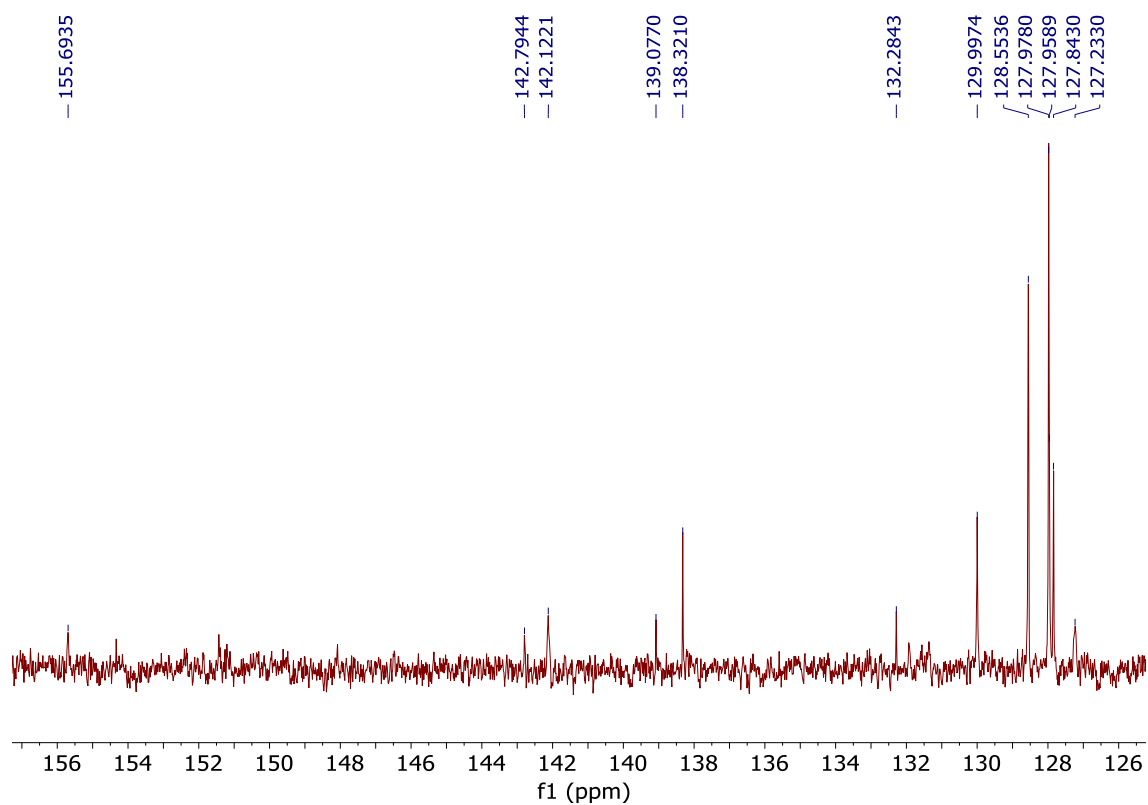
¹H NMR (CDCl₃, 300 MHz) of 16



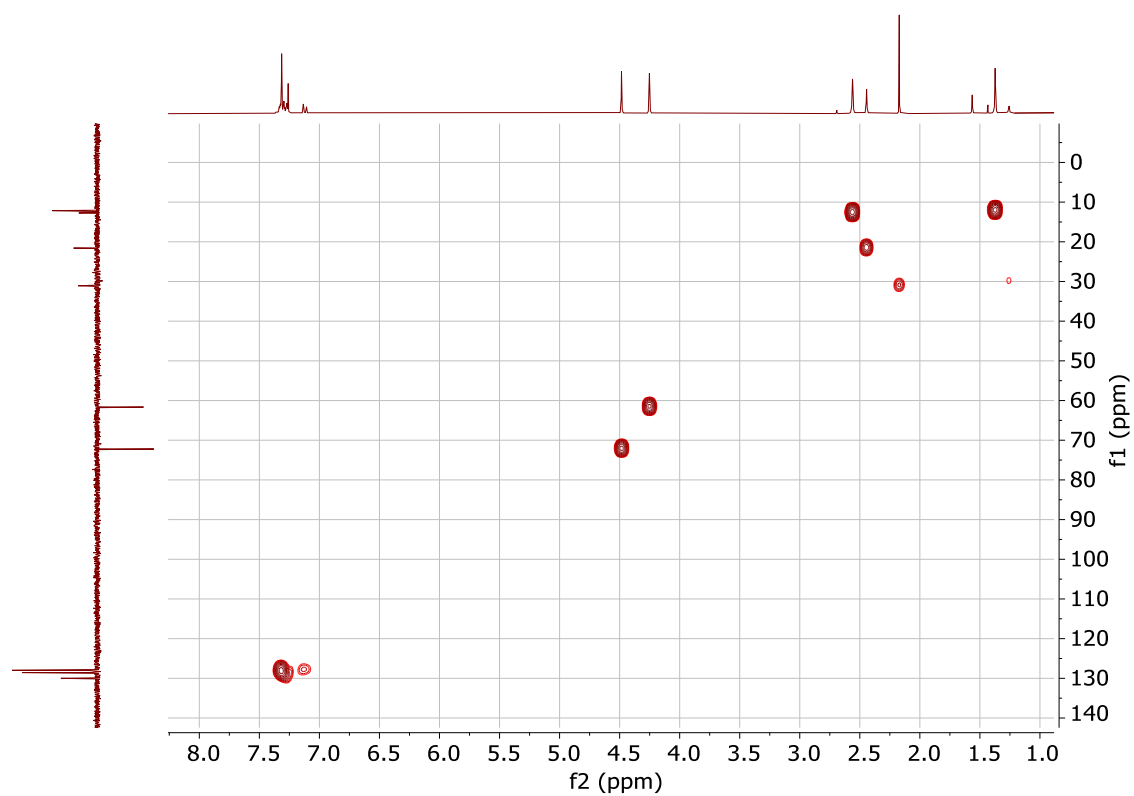
^{13}C NMR (CDCl₃, 75 MHz) of 16



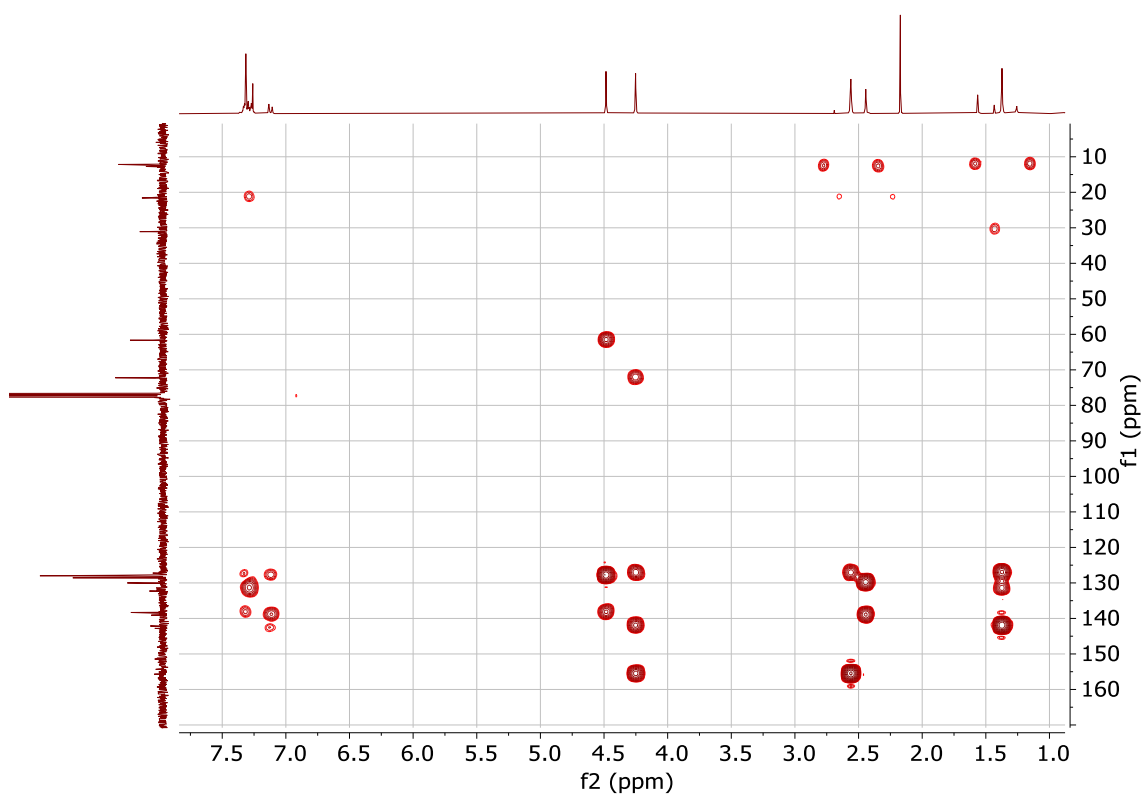
Expansion of the ^{13}C NMR spectrum of 16 (aromatic region)



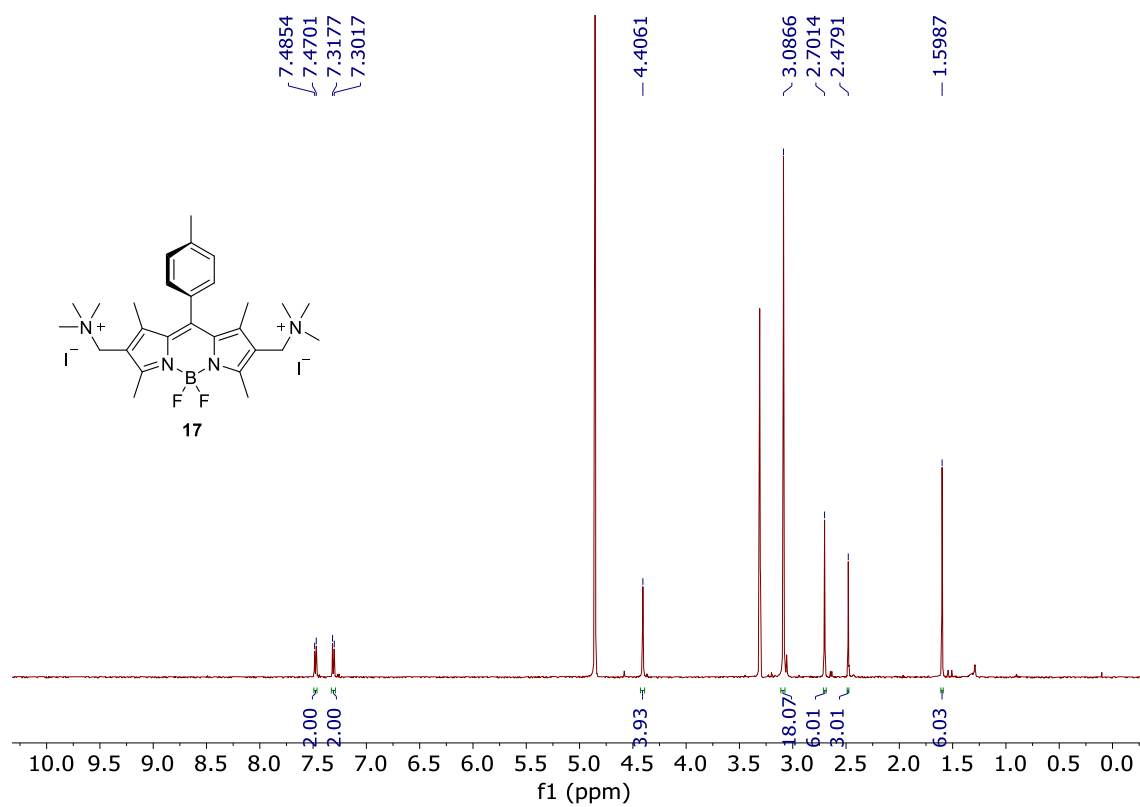
HMQC spectrum of 16



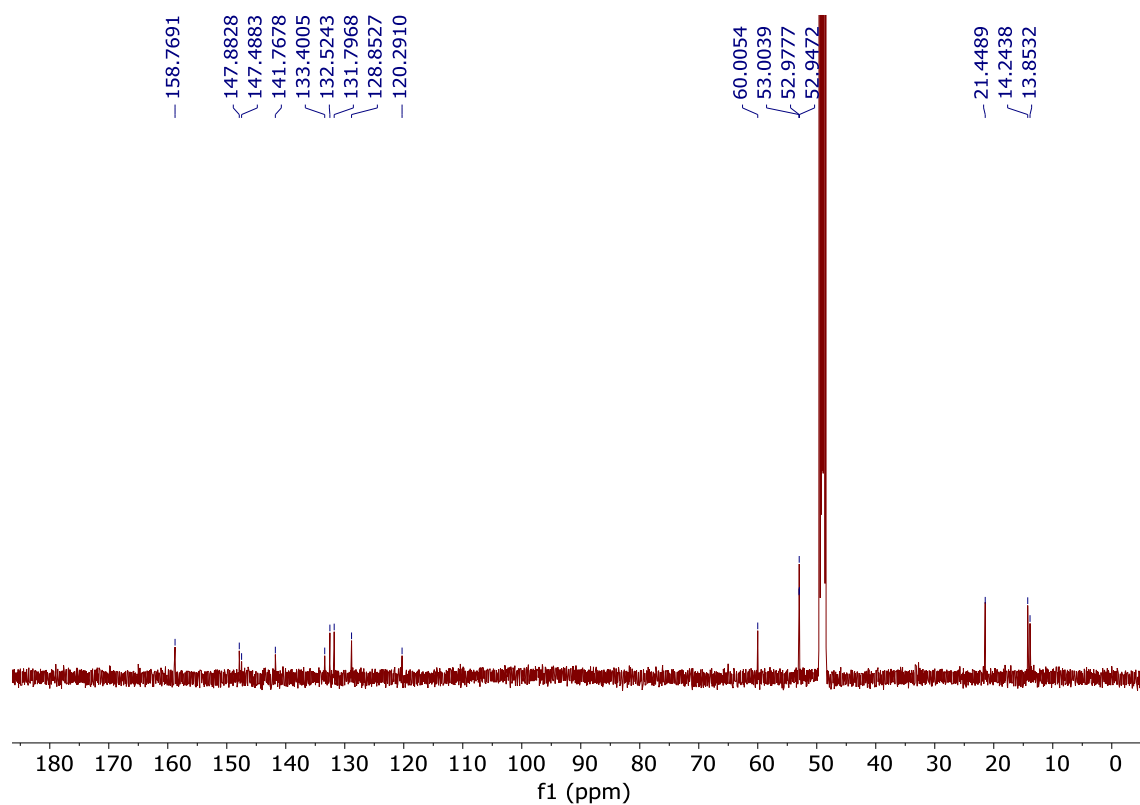
HMBC spectrum of 16



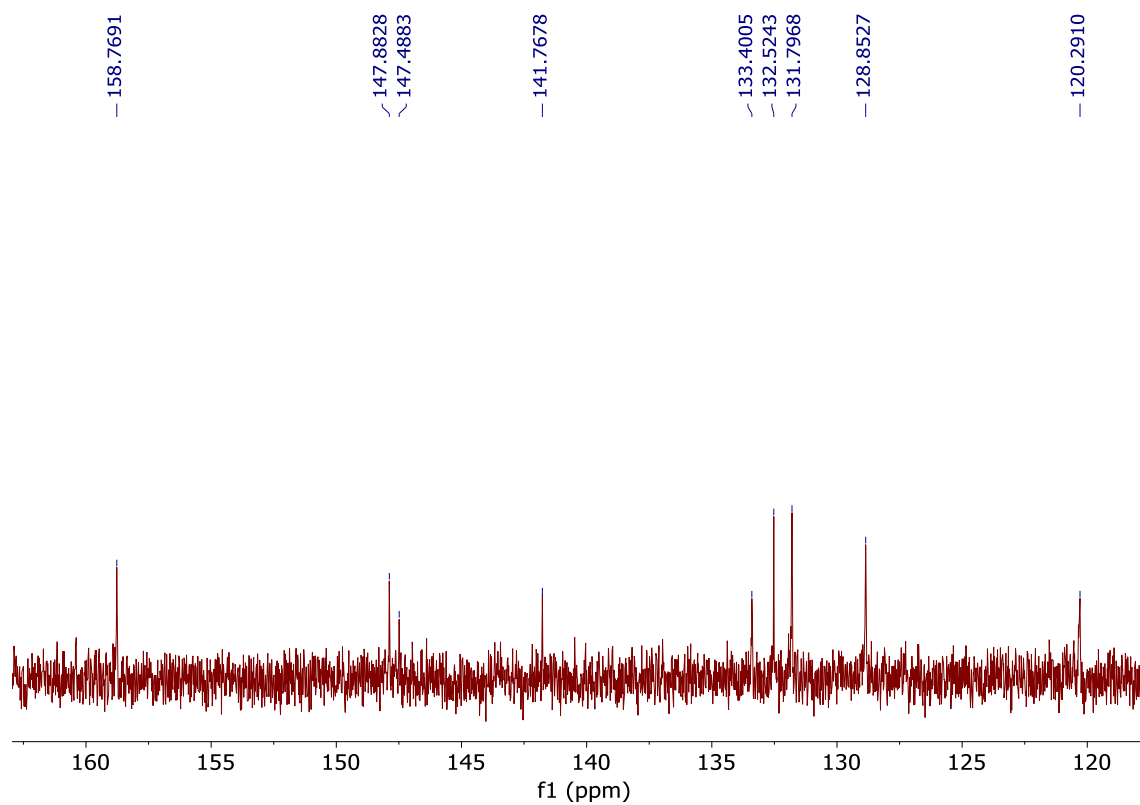
¹H NMR (MeOD, 500 MHz) of 17



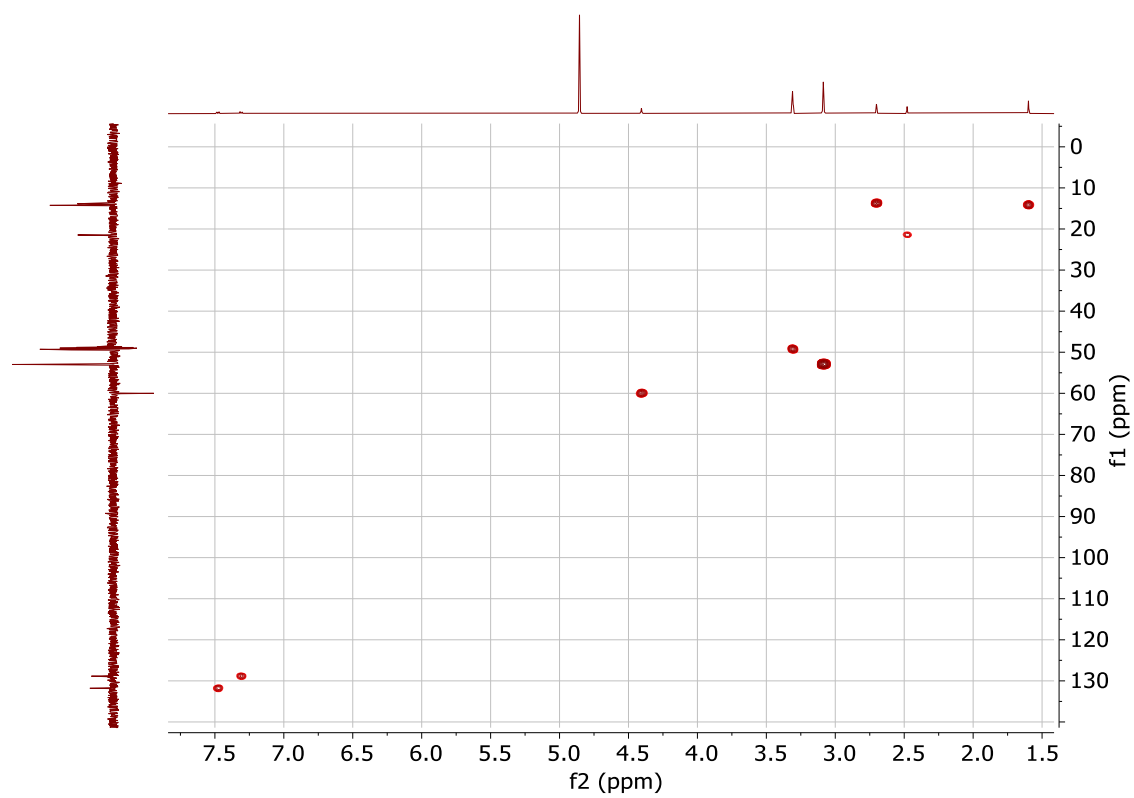
^{13}C NMR (MeOD, 126 MHz) of 17



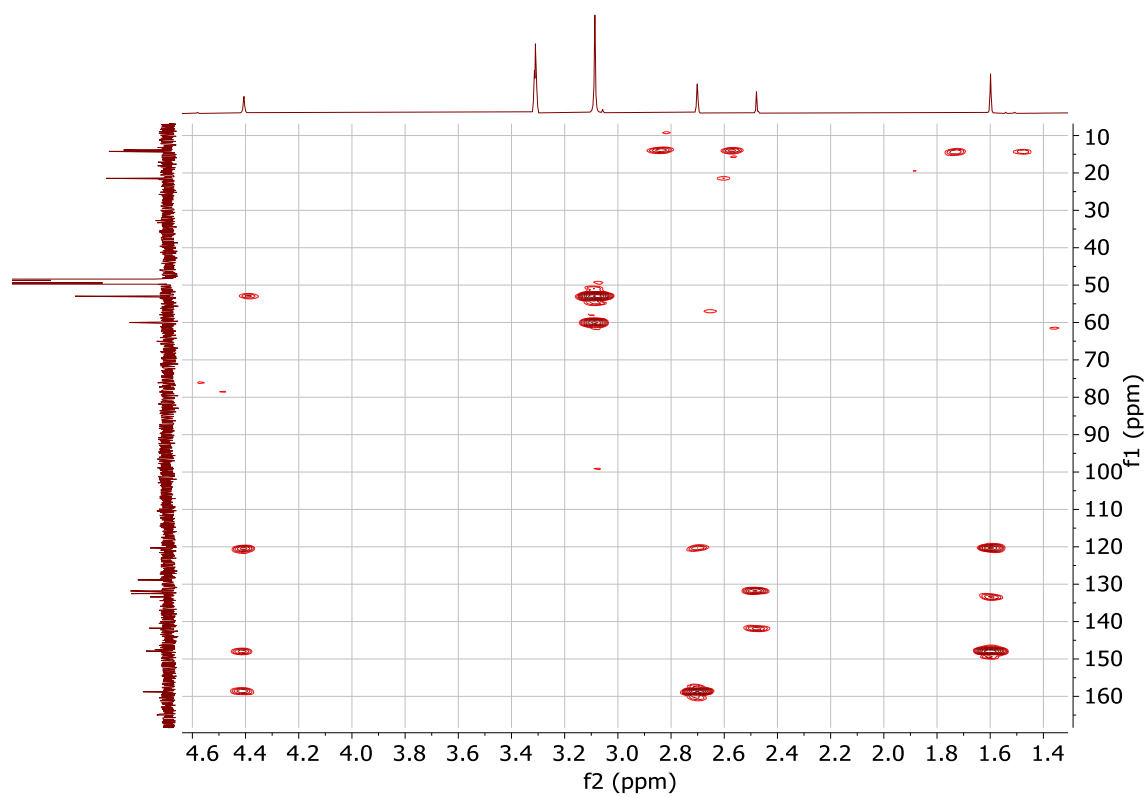
Expansion of the ^{13}C NMR spectrum of 17 (aromatic region)



HMQC spectrum of 17



HMBC spectrum of 17



4. Additional (photo)physical data

Table S1. Photophysical signatures (maximum absorption, λ_{ab} , and fluorescence, λ_{fl} , wavelengths; maximum molar absorption, ϵ_{max} ; fluorescence quantum yield, ϕ ; and lifetime, τ) of BODIPY **1**, its methylene-spaced 2-monosubstituted (**2** and **5a-j**) and 2,6-disubstituted (**15** and **16**) derivatives, featuring *N*-, *O*-, *C*- and *S*-nucleophile (Nu) moieties, in different solvents at dye concentration *ca.* 2×10^{-6} M. c-Hex: cyclohexane; ACN: acetonitrile; Tol: toluene.

Moiety type	Dye	Solvent	λ_{ab} (nm)	ϵ_{max} (M ⁻¹ cm ⁻¹)	λ_{fl} (nm)	ϕ	τ (ns)		
	1	c-Hex	503.0	78 000	511.5	0.410	2.43		
		CHCl ₃	503.0	83 000	513.5	0.600	3.57		
		ACN	498.0	77 000	507.5	0.470	3.18		
		2	Tol	510.0	92 000	522.0	0.370	2.83	
			CHCl ₃	509.0	86 000	521.0	0.130	0.77(94%)-3.37(6%)	
			ACN	504.0	83 000	515.0	0.020	0.018	
		<i>N</i> -Nu	5f	Tol	511.0	79 000	523.0	0.690	2.95
				CHCl ₃	510.0	74 000	521.0	0.090	0.10(43%)-0.47(47%)-3.32(10%)
				ACN	505.0	73 000	513.0	0.040	0.01(91%)-3.32(9%)
5g			Tol	511.0	65 000	523.0	0.650	3.71	
			CHCl ₃	510.0	77 000	522.0	0.590	3.97	
			ACN	506.0	72 000	518.0	0.230	1.12(50%)-2.20(50%)	
5h	Tol		510.0	88 000	522.0	0.007	0.01(90%)-3.35(10%)		
	CHCl ₃		509.0	92 000	521.0	0.010	0.01(95%)-3.62(5%)		
	ACN		504.0	78 000	515.0	0.006	0.03(76%)-3.49(22%)		
15	Tol	517.0	102 000	532.0	0.420	3.49			
	CHCl ₃	516.0	106 000	530.0	0.160	1.38			
	ACN	512.0	101 000	531.0	0.003	0.010			
<i>C</i> -Nu	5j	Tol	512.0	60 000	525.5	0.230	1.16(24%)-3.49(76%)		
		CHCl ₃	513.0	60 000	523.0	0.280	1.23(27%)-3.66(73%)		
		ACN	505.5	54 000	512.0	0.100	1.08(44%)-3.45(56%)		
<i>S</i> -Nu	5i	Tol	514.0	72 000	529.0	0.430	3.60		
		CHCl ₃	513.0	71 000	527.0	0.550	3.80		
		ACN	508.0	69 000	525.0	0.300	2.87		
<i>O</i> --Nu	5a	Tol	508.0	81 000	521.0	0.460	3.51		
		CHCl ₃	506.0	84 000	519.0	0.650	3.79		
		ACN	502.0	80 000	514.0	0.530	3.60		
	5b	Tol	507.0	78 000	521.0	0.650	3.50		
		CHCl ₃	506.0	75 000	517.5	0.670	3.70		
		ACN	501.0	72 000	513.0	0.440	3.43		
	5c	Tol	516.0	82 000	518.0	0.400	3.26		
		CHCl ₃	504.5	80 000	515.5	0.410	3.46		
		ACN	500.0	78 000	512.0	0.450	3.24		
	5d	Tol	506.0	90 000	518.0	0.570	3.54		
		CHCl ₃	505.0	79 000	515.0	0.610	3.61		
		ACN	500.0	77 000	511.0	0.500	3.45		
	5e	Tol	506.0	60 000	518.0	0.480	3.31		
		CHCl ₃	504.0	57 000	515.0	0.480	3.40		
		ACN	500.0	51 000	511.0	0.380	3.26		
16	Tol	516.0	52 000	526.5	0.400	3.53			
	CHCl ₃	511.0	54 000	524.0	0.510	3.81			
	ACN	507.0	47 000	519.0	0.410	3.74			

Table S2. Photophysical signatures (maximum absorption, λ_{ab} , and fluorescence, λ_{fl} , wavelengths; maximum molar absorption, ϵ_{max} ; fluorescence quantum yield, ϕ ; and lifetime, τ) of water-soluble methylene-spaced 2-(trimethylammonium)-substituted BODIPY **3**, and methylene-spaced 2,6-bis(trimethylammonium)-substituted BODIPY **17**, both derived from BODIPY **1**, in different solvents at dye concentration *ca.* 2×10^{-6} M.

Dye	Solvent	λ_{ab} (nm)	ϵ_{max} ($M^{-1}cm^{-1}$)	λ_{fl} (nm)	ϕ	τ (ns)
3	CHCl ₃	500.0	60 000	509.0	0.46	3.15
	H ₂ O	494.0	25 000	505.5	0.40	3.01
17	CHCl ₃	502.0	80 000	511.0	0.52	3.35
	H ₂ O	497.0	75 000	508.0	0.48	3.25

Table S3. Photophysical signatures (maximum absorption, λ_{ab} , and fluorescence, λ_{fl} , wavelengths; maximum molar absorption, ϵ_{max} ; fluorescence quantum yield, ϕ ; and lifetime, τ) of BODIPYs **6** and **7**, and its respective methylene-spaced 2-(dimethylamino)- (**9** and **10**) and 2-(benzyloxy)-substituted (**12** and **13**) derivatives, in different solvents at dye concentration *ca.* 2×10^{-6} M. c-Hex: cyclohexane; ACN: acetonitrile; Tol: toluene.

Dye	Solvent	λ_{ab} (nm)	ϵ_{max} ($M^{-1}cm^{-1}$)	λ_{fl} (nm)	ϕ	τ (ns)
6	c-Hex	509.0	78 000	512.0	0.99	5.40
	CHCl ₃	509.0	73 000	514.0	0.90	5.48
	ACN	501.0	65 000	508.0	0.81	5.64
9	Tol	517.0	80 000	525.5	0.54	3.15
	CHCl ₃	516.0	73 000	523.0	0.16	0.64(94%)-4.61(6%)
	ACN	509.0	72 000	515.0	0.03	0.02(99%)-4.91(1%)
12	Tol	515.0	60 000	521.5	0.40	4.60
	CHCl ₃	513.0	60 000	518.5	0.49	4.99
	ACN	505.5	54 000	513.0	0.57	5.37
7	c-Hex	499.5	97 000	512.0	0.91	5.23
	CHCl ₃	499.0	84 000	511.5	0.90	5.63
	ACN	491.0	79 000	502.0	0.83	5.39
10	Tol	507.0	72 000	522.0	0.94	4.81
	CHCl ₃	506.0	72 000	522.0	0.63	2.67(70%)-4.10(30%)
	ACN	499.0	67 000	512.5	0.03	0.03(98%)-5.16(2%)
13	Tol	505.0	60 000	521.5	0.89	5.50
	CHCl ₃	503.0	61 000	521.5	0.89	5.20
	ACN	496.0	58 000	513.0	0.78	4.81

Table S4. Photophysical signatures (maximum absorption, λ_{ab} , and fluorescence, λ_{fl} , wavelengths; maximum molar absorption, ϵ_{max} ; fluorescence quantum yield, ϕ ; and lifetime, τ) of 3,5-bis(styrylated) BODIPY **8**, and its methylene-spaced 2-(dimethylamino)-substituted (**11**) and 2-benzyloxy-substituted (**14**) derivatives, in different solvents at dye concentration *ca.* 2×10^{-6} M. c-Hex: cyclohexane; ACN: acetonitrile; Tol: toluene.

Dye	Solvent	λ_{ab} (nm)	ϵ_{max} ($10^4 M^{-1}cm^{-1}$)	λ_{fl} (nm)	ϕ	τ (ns)
8	Tol	626.0	92 000	637.0	0.83	4.56
	CHCl ₃	623.5	84 000	635.0	0.82	4.77
	ACN	614.5	83 000	626.0	0.76	5.04
11	Tol	622.5	60 000	638.0	0.77	4.29
	CHCl ₃	618.0	51 000	636.0	0.71	4.55
	MeCN	611.0	56 000	627.0	0.49	1.23(14%)-4.84(86%)
14	Tol	622.0	69 000	638.0	0.98	4.51
	CHCl ₃	618.5	64 000	636.0	0.84	4.72
	ACN	610.5	66 000	628.0	0.77	5.04

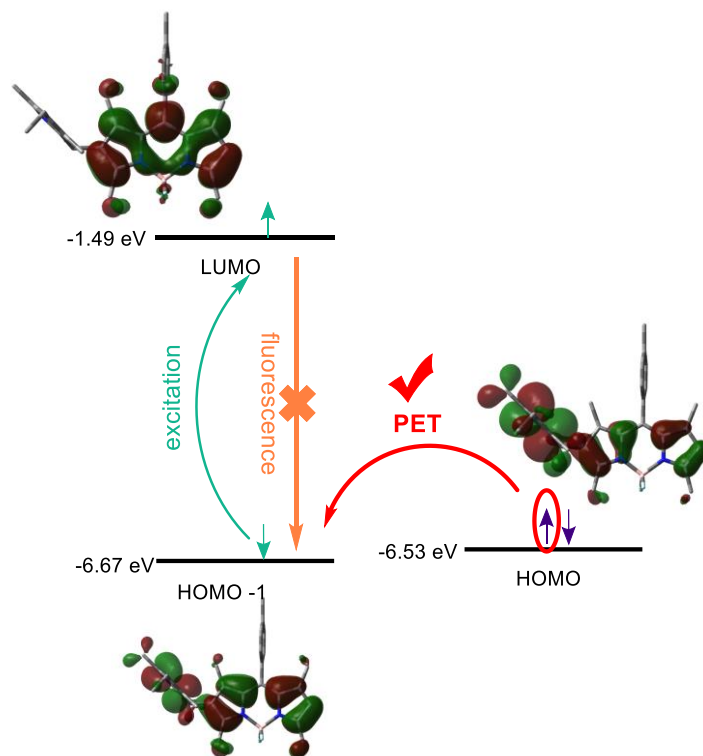


Figure S1. Computed (CAM-B3LYP/6-311g*) electronic contour maps and energy levels (in eV) of the key frontier molecular orbitals (FMOs) for methylene-spaced 2-(pyrrol-2-yl)-substituted BODIPY **5j**, supporting feasibility for fluorescence-quenching reductive PET.

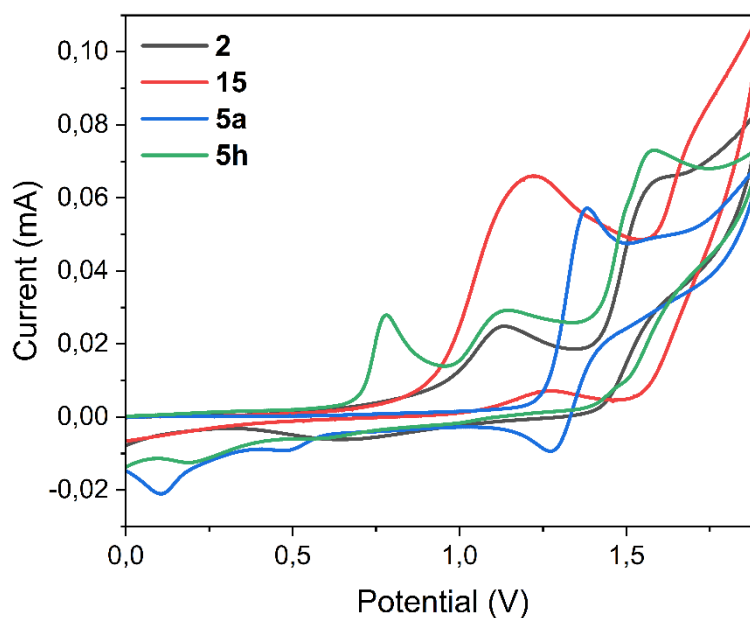


Figure S2. Anodic waves of the cyclic voltammograms for selected, representative methylene-spaced 2-(dimethylamino)- (**2**), 2-(3,5-dimethoxybenzamino)- (**5h**), 2-(benzyloxy)- (**5a**) and 2,6-bis(dimethylamino)-substituted (**15**) BODIPYs, recorded in acetonitrile (0.1 M TBAPF₆). For clarity, the cathodic wave is not displayed, as it remains nearly unaffected by the nature of the methylene-spaced substituent.

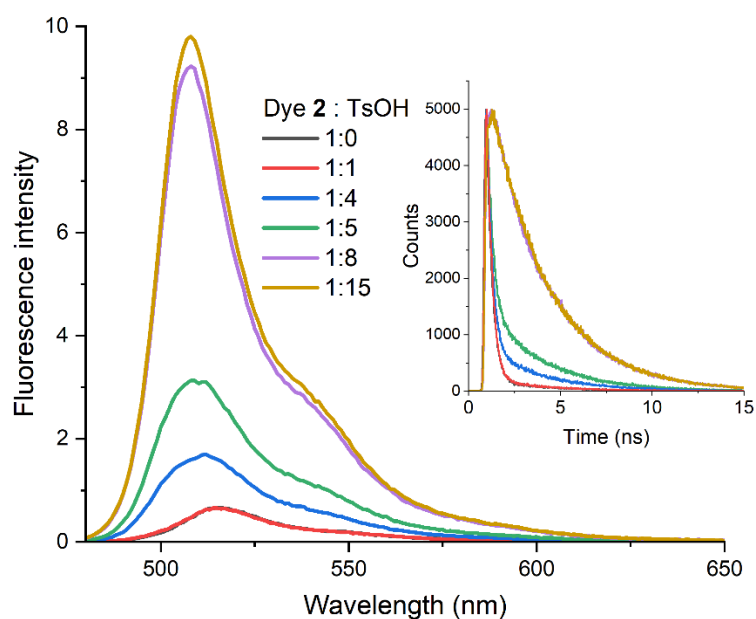


Figure S3. Variation of the fluorescence spectra (left) and fluorescence decay (right) of compound **2** (4×10^{-6} M in ethanol) upon incremental addition of *p*-toluenesulfonic acid (TsOH) (molar ratios from 1:0 to 1:15).

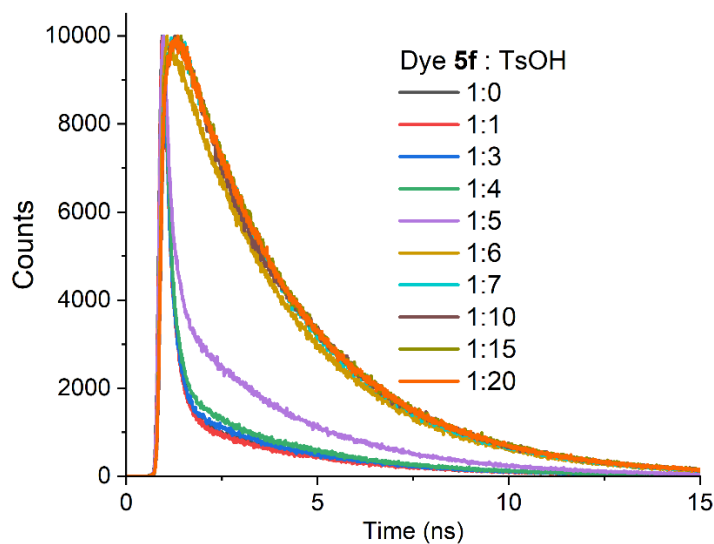


Figure S4. Variation of the fluorescence decay of compound **5f** (4×10^{-6} M in ethanol) upon incremental addition of *p*-toluenesulphonic acid (TsOH) (molar ratios from 1:0 to 1:20; fluorescence quantum yield increases from ≈ 0.04 up to ≈ 0.46).

5. Additional biophotonic data

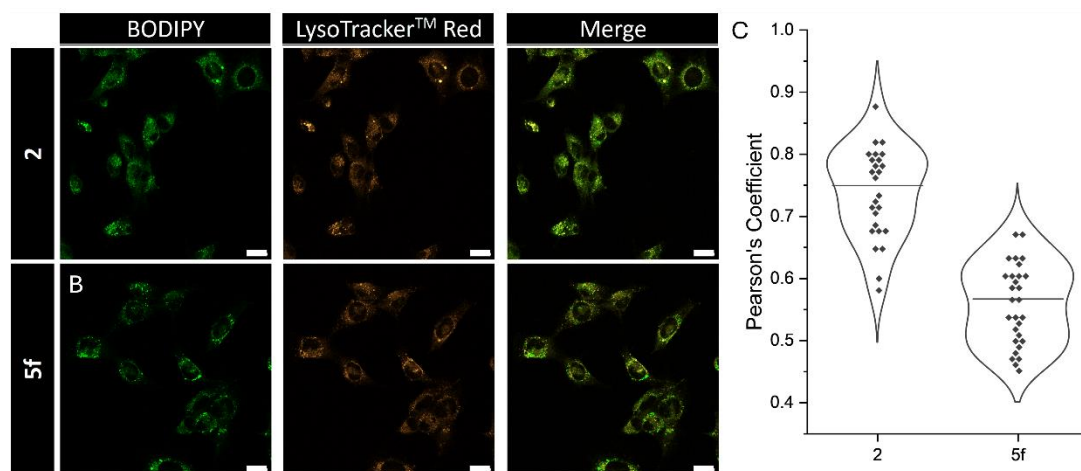


Figure S5. (A and B) Green-channel, red-channel and merged confocal laser scanning microscopy (CLSM) images of lysosomes in living MEFs co-stained with BODIPY **2** or **5f** (100 nM) and LysoTracker™ Red (100 nM). MEFs were imaged after 30 minutes of incubation. Green channel: $\lambda_{exc} = 488$ nm and $\lambda_{em} = 525 \pm 25$ nm. Red channel: $\lambda_{exc} = 561$ nm and $\lambda_{em} > 561$ nm. Scale bars are 20 μ m. (C) Violin plots of Pearson's correlation coefficients between **2** or **5f** and LysoTracker™ Red (mean \pm SD: 0.74 ± 0.07 ($n = 26$) for **2** and 0.56 ± 0.06 ($n = 29$) for **5f**).

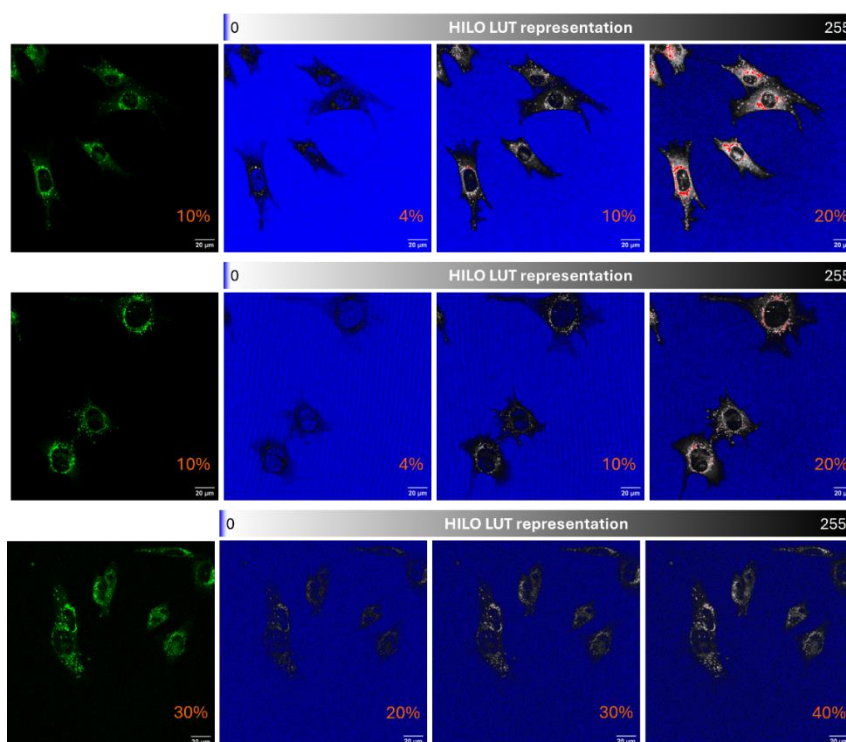


Figure S6. CLSM images of MEFs cells incubated with **2** (top), **5f** (middle) and LysoTracker™ Green (bottom). HILO LUT representation was applied to highlight the excitation power-dependent variations (in orange) in fluorescence intensity for each probe and determine the laser power for optimal imaging (software settings of 4, 10, 20, 30 and 40% laser power correspond to 12.6, 73.4, 274, 583 and 947 μ W laser power output, respectively). Scale bar = 20 μ m. MEFs were imaged after 30 minutes of incubation with probes. Final dye concentration was 100 nM.

6. References

1. C. Cobas, J. Cruces and F. J. Sardina, *MestRe-C software*, version 2.3a; Universidad de Santiago de Compostela, Spain, 2008.
2. A. Daina, O. Michielin and V. Zoete, *Sci. Rep.*, 2017, **7**, 42717.
3. A. Cui, X. Peng, J. Fan, X. Chen, Y. Wu, B. Guo, *J. Photochem. Photobiol. A.* 2007, **186**, 85–92.